

CRITICAL EVALUATION OF PARAMETERS AFFECTING  
RESILIENT MODULUS TESTS ON SUBGRADES

by

Manuel Feliberti, MSCE

Soheil Nazarian, Ph.D., P.E.

and

Thejaraj Srinivasan, BSCE

Research Project 1177

DEVELOPMENT OF ROUTINE RESILIENT MODULUS TESTING FOR USE  
WITH NEW AASHTO PAVEMENT DESIGN GUIDE

Conducted for

Texas Department of Transportation

by

Center for Geotechnical and Highway Materials Research  
The University of Texas at El Paso  
Research Report 1177-2, Volume 1

NOT INTENDED FOR CONSTRUCTION, BIDDING, OR PERMIT PURPOSES

# NOT INTENDED FOR CONSTRUCTION, BIDDING, OR PERMIT PURPOSES

The contents of this report reflect the views of the authors, who are responsible for the facts and the accuracy of the data presented herein. The contents do not necessarily reflect the official views or policies of the Federal Highway Administration. This report does not constitute a standard, specification, or regulation.

# Executive Summary

The strengths and limitations of the resilient modulus testing procedure as applied to subgrade soils have been detailed in this report. This has been a joint study between the Center for Transportation Research (CTR) and the University of Texas at El Paso (UTEP). The primary responsibilities of UTEP and the associated results are summarized here.

The overall objectives of UTEP have been:

- 1) to evaluate the accuracy of resilient modulus test procedure,
- 2) to modify the existing resilient modulus testing procedure as applied to granular materials,
- 3) to develop more rigorous constitutive models for describing the results from resilient modulus tests,
- 4) to conduct tests on limited number of soil samples from across the state, and
- 5) in more practical terms, to develop simplified relationships to be used in every day design.

To achieve these objectives, several tasks have been carried out. An extensive literature search in the areas of dynamic testing of soils as applied to transportation engineering, geotechnical engineering and earthquake engineering was carried out to obtain a list of parameters which influence the results of cyclic tests (such as the resilient modulus tests). The compliance of the testing device, sample preparation, level of deviatoric stress, and the sequence and number of loading schemes were found to be the major parameters.

This page replaces an intentionally blank page in the original.

-- CTR Library Digitization Team

# Preface

This report describes work done on Project 1177, "Development of Routine Resilient Modulus Testing for Use with the New AASHTO Pavement Design Guide", at the Center for Geotechnical and Highway Materials Research at UTEP.

Mr. Robert Mikulin was the technical Coordinator of the project. Mr. Harold Albers was of great assistance in providing samples.

This project has been a joint effort amongst UTEP, the Center for Transportation Research (CTR) at The University of Texas at Austin and The Texas Transportation Institute (TTI). The authors enjoyed interaction with these groups.

Ms. Cindy Edgar has been the technical editor of this report.

# **Implementation Statement**

The results of this study may be of great value in terms of implementation. The proposed testing sequence for granular materials may result in a more reliable testing procedure. Also, the new models proposed may be of great help if utilized in the reduction of data.

# Abstract

This report contains a critical evaluation of the resilient modulus testing procedure based on more than 200 tests. The state-of-the-art for obtaining and interpreting resilient modulus data is reviewed. The initial testing procedures proposed by AASHTO and modified by SHRP were evaluated. A new testing procedure for granular materials is proposed and evaluated. It was found that the AASHTO procedure for resilient modulus testing is inadequate. The SHRP protocol for testing cohesive soils is adequate. However, the SHRP protocol for testing granular soils induces sample disturbance during the first level of confining pressure. The new procedure proposed here minimizes sample disturbances and degradation.

The existing constitutive models were studied also. It was found that these models may not be adequate for all sands and clays. Two alternative models were then proposed. These models are more appropriate for describing the behavior of the materials tested.

Finally, simplified relationships for determining the constitutive models as a function of clay content and water content were proposed.

This page replaces an intentionally blank page in the original.

-- CTR Library Digitization Team

# Table of Contents

|   |      |
|---|------|
| Executive Summary . . . . .                             | iii  |
| Preface . . . . .                                       | v    |
| Implementation Statement . . . . .                      | vi   |
| Abstract . . . . .                                      | vii  |
| List of Tables . . . . .                                | xiii |
| List of Figures . . . . .                               | xv   |
| 1 Introduction . . . . .                                | 1    |
| 1.1 Problem Statement . . . . .                         | 1    |
| 1.2 Objectives . . . . .                                | 1    |
| 1.3 Organization . . . . .                              | 2    |
| 2 Background . . . . .                                  | 3    |
| 2.1 Introduction . . . . .                              | 3    |
| 2.2 Development of Resilient Modulus Test . . . . .     | 6    |
| 2.3 Factors Affecting Resilient Modulus . . . . .       | 7    |
| 2.3.1 Compaction . . . . .                              | 9    |
| 2.3.2 Stress State . . . . .                            | 11   |
| 2.3.3 Index Soil Properties . . . . .                   | 11   |
| 2.3.4 Soil Gradation . . . . .                          | 11   |
| 2.4 Correlations . . . . .                              | 11   |
| 2.5 Problems With Resilient Modulus . . . . .           | 12   |
| 2.6 Constitutive Models For Resilient Modulus . . . . . | 14   |

|         |  |    |
|---------|--|----|
| 3       | Equipment                              | 19 |
| 3.1     | Introduction                           | 19 |
| 3.2     | Equipment                              | 19 |
| 3.2.1   | Load Unit                              | 19 |
| 3.2.2   | Controller                             | 22 |
| 3.2.3   | Hydraulic Power Supply                 | 26 |
| 4       | Testing Procedures                     | 27 |
| 4.1     | Introduction                           | 27 |
| 4.2     | Definition of Soil Types               | 27 |
| 4.2.1   | AASHTO Definitions                     | 27 |
| 4.2.2   | SHRP Definitions                       | 28 |
| 4.3     | Sample Preparation                     | 28 |
| 4.3.1   | Granular Soils                         | 28 |
| 4.3.2   | Cohesive Soils                         | 31 |
| 4.4     | Testing Procedures                     | 32 |
| 4.4.1   | Granular Soils                         | 32 |
| 4.4.1.1 | AASHTO Procedures                      | 32 |
| 4.4.1.2 | SHRP Procedure                         | 32 |
| 4.4.1.3 | UTEP Procedure                         | 37 |
| 4.4.2   | Cohesive Soils                         | 37 |
| 4.4.2.1 | AASHTO Procedure                       | 37 |
| 4.4.2.2 | SHRP Procedure                         | 37 |
| 4.5     | Testing Procedure For One Loading Step | 41 |
| 4.6     | Post Testing Steps                     | 42 |
| 4.7     | Reduction of Data                      | 42 |
| 5       | Synthetic Specimens                    | 43 |
| 5.1     | Introduction                           | 43 |
| 5.2     | Properties of Synthetic Samples        | 43 |
| 5.3     | Testing Matrix                         | 48 |
| 5.4     | Presentation of Results                | 48 |
| 5.5     | Discussion of Results                  | 51 |
| 5.6     | Variability in Results                 | 60 |
| 5.7     | Effects of Utilizing Grouting Agent    | 60 |
| 6       | Clay Specimens                         | 63 |
| 6.1     | Introduction                           | 63 |
| 6.2     | Index Properties                       | 63 |
| 6.3     | Testing Matrix                         | 64 |
| 6.4     | Presentation of Results                | 64 |
| 7       | Sand Specimens                         | 73 |
| 7.1     | Introduction                           | 73 |
| 7.2     | Index Properties                       | 73 |
| 7.3     | Testing Matrix                         | 74 |

|       |                                  |     |
|-------|----------------------------------|-----|
| 7.4   | Presentation of Results          | 74  |
| 8     | Specimens of Clay-Sand Mixes     | 83  |
| 8.1   | Introduction                     | 83  |
| 8.2   | Index Properties                 | 83  |
| 8.3   | Testing Matrix                   | 87  |
| 8.4   | Presentation of Results          | 87  |
| 9     | Constitutive Models              | 97  |
| 9.1   | Introduction                     | 97  |
| 9.2   | Evaluation of Existing Models    | 97  |
| 9.3   | Proposed New Models              | 98  |
| 9.4   | Effects of Clay Content          | 106 |
| 9.4.1 | AASHTO/SHRP Cohesive Model       | 106 |
| 9.4.2 | AASHTO/SHRP Granular Model       | 106 |
| 9.4.3 | UTEP Models                      | 114 |
| 9.5   | Evaluation of Accuracy of Models | 114 |
| 10    | Testing of Subgrade Soils        | 133 |
| 10.1  | Introduction                     | 133 |
| 10.2  | Index Properties                 | 133 |
| 10.3  | Testing Matrix                   | 139 |
| 10.4  | Presentation of Results          | 139 |
| 11    | Conclusions and Recommendations  | 147 |
| 11.1  | Summary                          | 147 |
| 11.2  | Conclusions                      | 147 |

This page replaces an intentionally blank page in the original.

-- CTR Library Digitization Team

# List of Tables

|     |   |     |
|-----|---|-----|
| 2.1 | Parameters Affecting Modulus (from Hardin & Drnevich, 1972) . . . . .           | 8   |
| 4.1 | AASHTO's Guide to Selection of Compaction Method . . . . .                      | 29  |
| 4.2 | Loading Sequence Proposed by AASHTO for Granular Soils . . . . .                | 34  |
| 4.3 | Loading Sequence Proposed by SHRP for Type 1 Soils . . . . .                    | 36  |
| 4.4 | Loading Sequence Proposed by UTEP for Type 1 Soils . . . . .                    | 38  |
| 4.5 | Loading Sequence Proposed by AASHTO for Cohesive Soils . . . . .                | 39  |
| 4.6 | Loading Sequence Proposed by SHRP for Type 2 Soils . . . . .                    | 40  |
| 5.1 | Summary of the Results for TU-700 . . . . .                                     | 56  |
| 5.2 | Summary of the Results for TU-900 . . . . .                                     | 57  |
| 5.3 | Summary of the Results for TU-960 . . . . .                                     | 58  |
| 5.4 | Minimum and Maximum Moduli for Synthetic Samples . . . . .                      | 59  |
| 8.1 | Liquid Limit, Plastic Limit, Classification and Plasticity Index for Mixtures . | 84  |
| 8.2 | Maximum Dry Density and Optimum Moisture Content . . . . .                      | 85  |
| 9.1 | Regression Constants for AASHTO/SHRP Models for Cohesive (Type 2) Soils .       | 108 |
| 9.2 | Regression Constants for AASHTO/SHRP Models for Granular (Type 1) Soils .       | 108 |
| 9.3 | Regression Constants for UTEP Model One . . . . .                               | 121 |

9.4 Regression Constants for UTEP Model Two . . . . . 122

9.5 Typical Differences between Measured and Calculated Moduli from Three Models  
(Granular Soils) . . . . . 130

9.6 Typical Differences between Measured and Calculated Moduli from Three Models  
(Cohesive Soils) . . . . . 132

10.1 Index Properties of Soils from El Paso, Midland, & Hardeman County . . . . . 134

10.2 Proctor Density Relation and AASHTO/USCS Classification . . . . . 134

10.3 Percent Passing for Soils from El Paso, Midland, & Hardeman County . . . . . 138

# List of Figures

|  |    |
|--|----|
| Figure 2.1 - Stress Distribution Under a Wheel Load . . . . .  | 4  |
| Figure 2.2 - Schematic of Load and Displacement Time Histories from a Resilient Modulus Test . . . . .   | 5  |
| Figure 2.3 - Soil Behavior and Associated Strain Ranges.(from Stokoe et al, 1988) . . . . .  | 10 |
| Figure 2.4 - Correlations of Resilient Modulus of Roadbed Soils with Laboratory Tests (from AASHTO, 1986) . . . . .  | 13 |
| Figure 3.1 - Overall Picture of Testing System . . . . .   | 20 |
| Figure 3.2 - Components of Load Unit . . . . .   | 21 |
| Figure 3.3 - Triaxial Testing Cell . . . . .   | 23 |
| Figure 3.4 - Components of Upper Load Platen of Triaxial Cell . . . . .  | 24 |
| Figure 3.5 - Components of Controller . . . . .  | 25 |
| Figure 4.1 - Equipment for Preparing Specimens for Granular (Type 1) Materials . . . . .   | 30 |
| Figure 4.2 - Equipment for Preparing Specimens for Cohesive (Type 2) Materials . . . . .   | 33 |
| Figure 5.1 - Comparison of Axial Strains Generated in MR Testing with those Generated in Calibrating the Synthetics Specimens (from Stokoe et al, 1990) . . . . .  | 45 |
| Figure 5.2 - Variation in Young's Modulus with Axial Strain Amplitude and Loading Frequency as Determined by Cyclic Torsional and Resonant Column Tests at Zero Confining Pressure (from Stokoe et al, 1990) . . . . . | 46 |

|              |  |    |
|--------------|--|----|
| Figure 5.3 - | Variation in Normalized Young's Modulus with Loading Frequency<br>as Determined by Cyclic Torsional Tests (from Stokoe et al, 1990) . . . . .  | 47 |
| Figure 5.4 - | Variation in Young's Modulus with Temperature for Specimen TU-900<br>Tested at Various Loading Frequencies (from Stokoe et al, 1990) . . . . . | 49 |
| Figure 5.5 - | Variation in Resilient Modulus with Deviatoric Stress for Sample TU-900<br>using AASHTO Cohesive Procedure and Hydrostone . . . . .            | 50 |
| Figure 5.6 - | Variation in Resilient Modulus with Deviatoric Stress for Sample TU-900<br>using SHRP Type 2 Procedure and Hydrostone . . . . .                | 52 |
| Figure 5.7 - | Variation in Resilient Modulus with Deviatoric Stress for Sample TU-900<br>using AASHTO Granular Procedure and Hydrostone . . . . .            | 53 |
| Figure 5.8 - | Variation in Resilient Modulus with Deviatoric Stress for Sample TU-900<br>using SHRP Type 1 Procedure and Hydrostone . . . . .                | 54 |
| Figure 5.9 - | Variation in Resilient Modulus with Deviatoric Stress for Sample TU-900<br>using UTEP Type 1 Procedure and Hydrostone . . . . .                | 55 |
| Figure 6.1 - | Grain Size Distribution for Clay Soil . . . . .  | 65 |
| Figure 6.2 - | Variation of Dry Unit Weight with Moisture Content for Pure Clay . . . . .   | 66 |
| Figure 6.3 - | Variation in Resilient Modulus with Deviatoric Stress for a Clay Sample<br>at Optimum Water Content Following AASHTO Procedure . . . . .       | 67 |
| Figure 6.4 - | Variation in Resilient Modulus with Deviatoric Stress for a Clay Sample<br>at 17.4 Percent Water Content Following SHRP Procedure . . . . .    | 68 |
| Figure 6.5 - | Variation in Resilient Modulus with Deviatoric Stress for a Clay Sample<br>at 17.2 Percent Water Content Following SHRP Procedure . . . . .    | 69 |
| Figure 6.6 - | Variation in Resilient Modulus with Deviatoric Stress for a Clay Sample<br>at 19.3 Percent Water Content Following SHRP Procedure . . . . .    | 70 |
| Figure 6.7 - | Variation in Resilient Modulus with Deviatoric Stress for a Clay Sample<br>at 15.0 Percent Water Content Following SHRP Procedure . . . . .    | 71 |
| Figure 7.1 - | Variation of Relative Density with Dial Reading for Sand . . . . .   | 75 |
| Figure 7.2 - | Variation in Resilient Modulus with Bulk Stress for a Sand Sample at a<br>Relative Density of 100 Percent Following SHRP Procedure . . . . .   | 76 |

|  |     |
|--|-----|
| Figure 7.3 - Variation in Resilient Modulus with Bulk Stress for a Sand Sample at a Relative Density of 100 Percent Following UTEP Procedure . . . . .                     | 78  |
| Figure 7.4 - Variation in Resilient Modulus with Bulk Stress for a Sand Sample at a Relative Density of 100 Percent Following UTEP Procedure . . . . .                     | 79  |
| Figure 7.5 - Variation in Resilient Modulus with Bulk Stress for a Sand Sample at a Relative Density of 100 Percent Following UTEP Procedure . . . . .                     | 80  |
| Figure 7.6 - Variation in Resilient Modulus with Bulk Stress for a Sand Sample at a Relative Density of 70 Percent Following UTEP Procedure . . . . .                      | 81  |
| Figure 8.1 - Variation in Water Content with Clay Content for Mixtures . . . . .   | 86  |
| Figure 8.2 - Variation in Maximum Dry Density with Clay Content for Mixtures . . . . .   | 88  |
| Figure 8.3 - Variation in Optimum Moisture Content with Percent Clay for Mixtures . . . . .  | 89  |
| Figure 8.4 - Variation in Resilient Modulus with Deviatoric Stress for 90% Clay-10% Sand Specimen at a Moisture Content of 20.6 Percent Following SHRP Procedure . . . . . | 90  |
| Figure 8.5 - Variation in Resilient Modulus with Bulk Stress for 10% Clay-90% Sand Specimen at a Moisture Content of 10.4 Percent Following UTEP Procedure . . . . .       | 91  |
| Figure 8.6 - Variation in Resilient Modulus with Deviatoric Stress for 10% Clay-90% Sand Specimen at a Moisture Content of 10.4 Percent Following UTEP Procedure . . . . . | 92  |
| Figure 8.7 - Variation in Resilient Modulus with Clay Content at Optimum Water Content for 6 psi Confining Pressure and 6 psi Deviatoric Stress . . . . .                  | 94  |
| Figure 8.8 - Variation in Resilient Modulus with Clay Content at Wet of Optimum Water Content for 6 psi Confining Pressure and 6 psi Deviatoric Stress . . . . .           | 95  |
| Figure 8.9 - Variation in Resilient Modulus with Clay Content at Dry of Optimum Water Content for 6 psi Confining Pressure and 6 psi Deviatoric Stress . . . . .           | 96  |
| Figure 9.1 - Typical Variation in Percent Difference Between Measured and Modelled Moduli Using AASHTO/SHRP Model on a Sand Specimen . . . . .                             | 100 |
| Figure 9.2 - Typical Variation in Percent Difference Between Measured and Modelled Moduli Using Model One on a Sand Specimen . . . . .                                     | 101 |

|  |     |
|--|-----|
| Figure 9.3 - Typical Variation in Percent Difference Between Measured and Modelled Moduli Using Model Two on a Sand Specimen . . . . .         | 102 |
| Figure 9.4 - Typical Variation in Percent Difference Between Measured and Modelled Moduli Using AASHTO/SHRP Model on a Clay Specimen . . . . . | 103 |
| Figure 9.5 - Typical Variation in Percent Difference Between Measured and Modelled Moduli Using Model One on a Clay Specimen . . . . .         | 104 |
| Figure 9.6 - Typical Variation in Percent Difference Between Measured and Modelled Moduli Using Model Two on a Clay Specimen . . . . .         | 105 |
| Figure 9.7 - Variation in Constant $k_1$ from AASHTO/SHRP Model with Clay Content at Optimum Water Content for Cohesive Soil . . . . .         | 107 |
| Figure 9.8 - Variation in Constant $k_1$ from AASHTO/SHRP Model with Clay Content at Wet of Optimum Water Content for Cohesive Soil . . . . .  | 109 |
| Figure 9.9 - Variation in Constant $k_1$ from AASHTO/SHRP Model with Clay Content at Dry of Optimum Water Content for Cohesive Soil . . . . .  | 110 |
| Figure 9.10 - Variation in Constant $k_2$ from AASHTO/SHRP Model with Clay Content at Optimum Water Content for Cohesive Soil . . . . .        | 111 |
| Figure 9.11 - Variation in Constant $k_2$ from AASHTO/SHRP Model with Clay Content at Wet of Optimum Water Content for Cohesive Soil . . . . . | 112 |
| Figure 9.12 - Variation in Constant $k_2$ from AASHTO/SHRP Model with Clay Content at Dry of Optimum Water Content for Cohesive Soil . . . . . | 113 |
| Figure 9.13 - Variation in Constant $k_1$ from AASHTO/SHRP Model with Clay Content at Optimum Water Content for Granular Soil . . . . .        | 115 |
| Figure 9.14 - Variation in Constant $k_1$ from AASHTO/SHRP Model with Clay Content at Wet of Optimum Water Content for Granular Soil . . . . . | 116 |
| Figure 9.15 - Variation in Constant $k_1$ from AASHTO/SHRP Model with Clay Content at Dry of Optimum Water Content for Granular Soil . . . . . | 117 |
| Figure 9.16 - Variation in Constant $k_2$ from AASHTO/SHRP Model with Clay Content at Optimum Water Content for Granular Soil . . . . .        | 118 |
| Figure 9.17 - Variation in Constant $k_2$ from AASHTO/SHRP Model with Clay Content at Wet of Optimum Water Content for Granular Soil . . . . . | 119 |

Figure 9.18 - Variation in Constant  $k_2$  from AASHTO/SHRP Model with Clay Content at Dry of Optimum Water Content for Granular Soil . . . . . 120

Figure 9.19 - Typical Variation in Percent Difference Between Measured and Modelled Moduli Using Simplified Relationship for Regression Constants of AASHTO/SHRP Model . . . . . 124

Figure 9.20 - Typical Variation in Percent Difference Between Measured and Modelled Moduli Using Simplified Relationship for Regression Constants of Model One . . . . . 125

Figure 9.21 - Typical Variation in Percent Difference Between Measured and Modelled Moduli Using Simplified Relationship for Regression Constants of Model Two . . . . . 126

Figure 9.22 - Typical Variation in Percent Difference Between Measured and Modelled Moduli Using Simplified Relationship for Regression Constants of AASHTO/SHRP Model . . . . . 127

Figure 9.23 - Typical Variation in Percent Difference Between Measured and Modelled Moduli Using Simplified Relationship for Regression Constants of Model One . . . . . 128

Figure 9.24 - Typical Variation in Percent Difference Between Measured and Modelled Moduli Using Simplified Relationship for Regression Constants of Model Two . . . . . 129

Figure 10.1 - Grain Size Distribution Curve for Hardeman County Soil . . . . . 135

Figure 10.2 - Grain Size Distribution Curve for Midland County Soil . . . . . 136

Figure 10.3 - Grain Size Distribution Curve for El Paso County Soil . . . . . 137

Figure 10.4 - Typical Variation in Resilient Modulus with Deviatoric Stress for Hardemen County Specimen at Optimum Water Content . . . . . 140

Figure 10.5 - Typical Variation in Resilient Modulus with Bulk Stress for Midland County Specimen at Optimum Water Content . . . . . 141

Figure 10.6 - Typical Variation in Resilient Modulus with Bulk Stress for El Paso County Specimen at Optimum Water Content . . . . . 142

Figure 10.7 - Variation in Resilient Modulus with Moisture Content for Hardeman County Soil . . . . . 144

Figure 10.8 - Variation in Resilient Modulus with Moisture Content for  
Midland County Soil . . . . . 145

Figure 10.9 - Variation in Resilient Modulus with Moisture Content for  
El Paso County Soil . . . . . 146

# **Chapter 1**

## **Introduction**

### **1.1 Problem Statement**

In recent years, resilient modulus testing has gained tremendous popularity. This increased interest has been attributed to the new AASHTO design procedure adopted in 1986. In the new design procedure, the resilient modulus of subgrade soil is considered as one of the most important input parameters.

Since 1986, numerous research projects have focused on improving the laboratory procedure involved in conducting resilient modulus tests. A workshop was held at the University of Oregon in 1989 to summarize the state of practice in resilient modulus testing. The major conclusions of the workshop were straightforward. The employment of the resilient modulus as a design parameter would significantly improve the design procedures. The available testing procedures were found to be inadequate and illogical, the resilient modulus testing devices were determined to be improper, and the constitutive models proposed were found to be incomplete. The Strategic Highway Research Program (SHRP) has developed improved testing procedures. However, more improvements are still necessary. In addition, more reliable and sophisticated testing procedures require more advanced constitutive models. Unfortunately, such models have not been suggested by SHRP.

### **1.2 Objectives**

This report addresses some of the inadequacies related to laboratory testing and modelling of the resilient modulus tests. Extensive laboratory tests were conducted to study the limitations of the existing methods proposed by SHRP and AASHTO. An improved testing procedure was proposed for the granular samples which will induce the least amount of degradation and

disturbance to the sample. In addition, two improved constitutive models were proposed for the granular and cohesive soils. Three synthetic samples were extensively tested to determine the limitations of the device used in this study. It was found that the UTEP system can adequately determine the modulus of the synthetic samples. Extensive tests were carried out on a sand and a clay common to El Paso, Texas. These two materials were thoroughly characterized and their constitutive models were determined. In addition, the two soils were mixed at nine different proportions. The effects of clay content on the resilient modulus of these materials at optimum water content, 2 percent wet of optimum water content and 2 percent dry of optimum water content were determined. Simplified relationships for determining the resilient modulus as a function of clay content, water content, deviatoric stress and confining pressure were presented.

### **1.3 Organization**

This report consists of ten chapters. Chapter 2 contains a comprehensive literature review. In Chapter 3, the components of the UTEP resilient testing device are described. The approach taken in testing different soils is described in Chapter 4. A detailed description of a preferred approach for testing granular materials is proposed in this chapter as well. In Chapter 5, the versatility of the UTEP device is established by testing a synthetic sample. The laboratory results are presented. In Chapters 6, 7 and 8, the properties of a sand, a clay, and the mixture of the two are respectively described. Existing constitutive models are evaluated in Chapter 9. Also included in chapter 9 are two new proposed models. Chapter 10 is the closure which contains a summary of the report, conclusions and recommendations for future studies. The results and relationships are comprehensively documented in eight appendices.

# Chapter 2

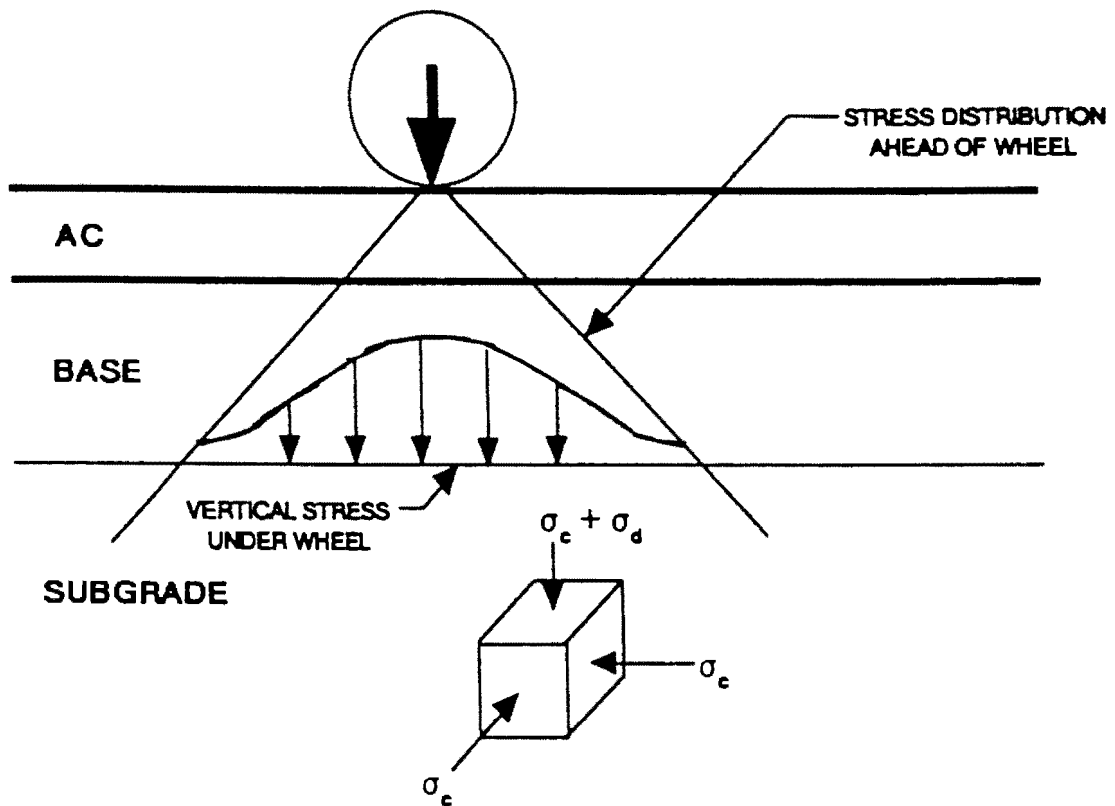
## Background

### 2.1 Introduction

The resilient modulus test is used to determine the response of paving materials to repeated loading similar to loads applied to a pavement from vehicular traffic. Figure 2.1 illustrates the stress distribution in the subgrade due to a moving wheel load. Initially, an element of soil in the subgrade is subjected only to overburden pressure. Due to the approaching load, stress levels on the element increase. The maximum stress is reached when the load is directly above the soil element. Stresses in the element then decrease gradually to the initial overburden stresses. This variation in stress can be idealized as a half-sine wave. Such a loading regime can be reproduced in the laboratory.

The typical load applied in a resilient modulus test is shown in Figure 2.2. Initially, the specimen is subjected to an overall load. This load is marked as SL in the figure. A periodic half-sine load is applied on top of the overall load. This load is marked as DL. The loading period, LP, can be varied to simulate different vehicular speeds. A rest period, RP, is imposed between the end of one cycle of load and the beginning of the next to simulate traffic conditions.

Due to the deviatoric load, DL, the specimen will undergo a total deformation of TD. Depending on the intensity of the load applied, this deformation may or may not be fully recoverable. The unrecoverable portion of the deformation is termed permanent deformation, PD. For an elastic material, PD should be equal to zero. This is also true for small levels of load PL. The recoverable deformation can be divided into two parts: elastic deformation, ED, and viscoelastic deflection, VD. As shown in Figure 2.2, for a viscoelastic material, the duration of the displacement with time-history record will not be identical to the loading period, PD. The elastic deformation is determined by subtracting the deformation at the time equal to loading



$\sigma_c$  = confining pressure  
 $\sigma_d$  = deviator stress =  $\sigma_v$   
 $\sigma_v$  = vertical stress applied by wheel

Figure 2.1 - Stress Distribution Under a Wheel Load.

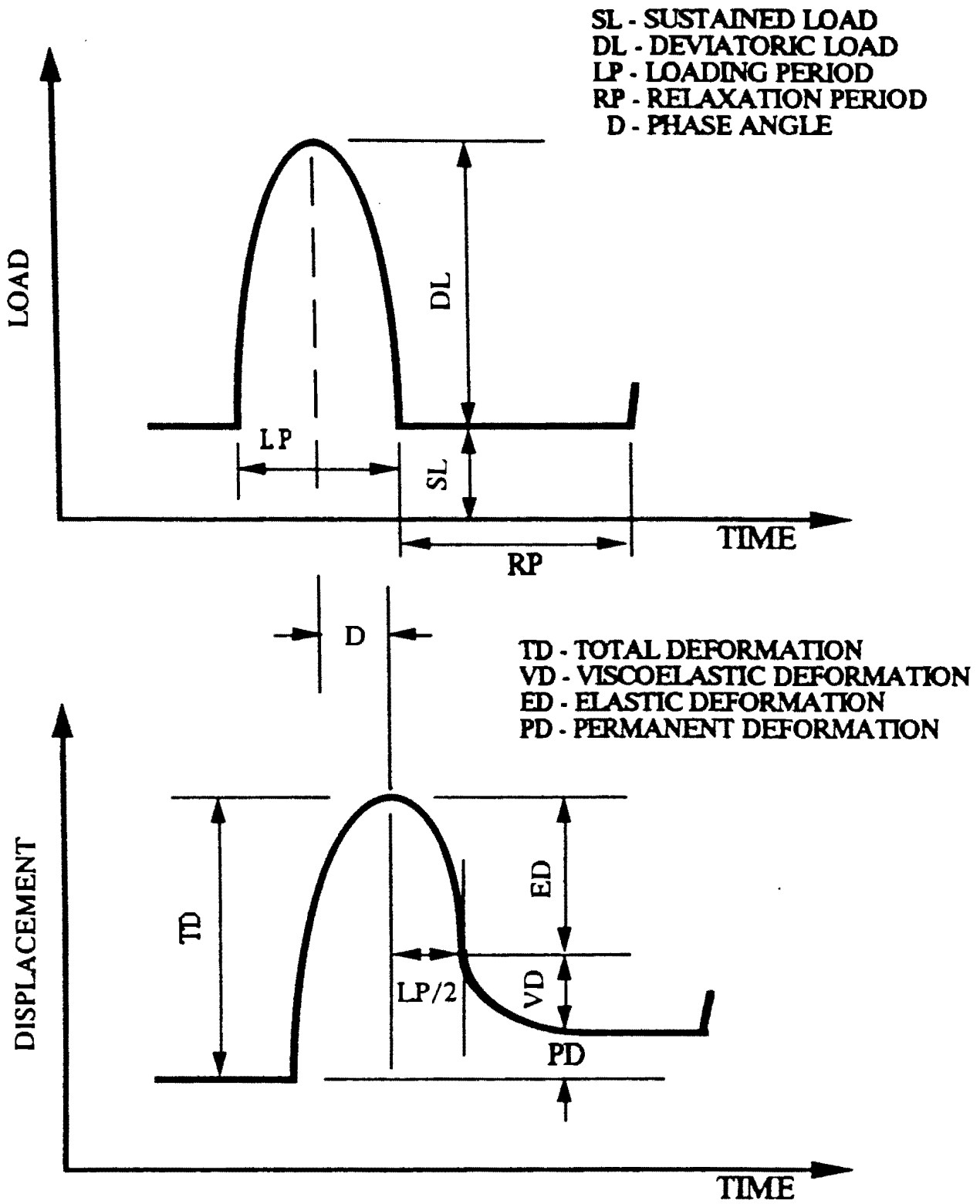


Figure 2.2 - Schematic of Load and Displacement Time Histories from a Resilient Modulus Test.

period from the total deformation. The difference between the recoverable deformation and the elastic deformation is termed the viscoelastic deformation. For small load levels, the viscoelastic deformation is negligible.

Typically, the peak load and the peak deformation are not concurrent. This shift in the peaks, denoted as D in Figure 2.2, is representative of energy absorbing (damping) properties of the soil. In practice, resilient modulus,  $M_R$ , is defined as:

$$M_R = \frac{\sigma_d}{\epsilon_r} \quad (2.1)$$

where:

|              |   |                          |
|--------------|---|--------------------------|
| $\sigma_d$   | = | $\frac{DL}{A_i}$         |
| $\epsilon_r$ | = | $\frac{RD}{L_i}$         |
| $\sigma_d$   | = | deviatoric stress        |
| $\epsilon_r$ | = | resilient strain         |
| $A_i$        | = | initial area of specimen |
| $L_i$        | = | initial specimen length  |
| RD           | = | recoverable deformation. |

The resilient modulus test has several advantages. According to Baladi (1989), the test is nondestructive so that one sample can be used for several tests. The test frequency and relaxation period may be varied to simulate various vehicular speeds, axle configurations and load transmitted. The test provides an indication of the permanent deformations of the material that will aid an engineer in determining when a pavement has fatigued. Brown (1989) also added that the resilient modulus is an engineering property and the test contains a wealth of information. There are several parameters that can be determined from one test. Finally, the test may yield some indication of the viscoelastic properties of materials.

Several highway agencies have been incorporating the resilient modulus in their design process. Dhamrait (1989), Kim (1989), Allen (1989), Baladi (1989), Monismith (1989), and Mahoney (1989) have shown examples of pavement design using the resilient modulus.

## 2.2 Development of Resilient Modulus Test

Investigators like Mitry (1964), Seed (1955), Hicks (1971), Kasianchuk (1968) were involved in the early development of the resilient modulus test. A large difference in the modulus is obtained from a static loading as compared to a dynamic loading (Vinson, 1989 and Thompson, 1989). Usually, a static loading produces much higher deflections than a comparable dynamic

loading. Since the dynamic loading represents traffic conditions better than static loading, it is more logical to assume that the dynamic modulus is more representative.

After World War II, several researchers studied the effects of repeated loads on pavement sections (Vinson, 1989). In the 1950's and 1960's, several investigations were carried out on asphaltic concrete materials using repeated loading. Previously, the repeated load tests were performed with in situ plate load tests that were costly and involved a considerable amount of time. In the 1960's, the development of laboratory resilient modulus testing procedure for subgrade materials was initiated. It was noted that the resilient modulus test was simple and inexpensive compared to the previous repeated loading test.

Seed (1967), Thompson (1969), Hicks and Monismith (1971), Rada and Witczak (1981), Thompson (1989), Jackson (1989), and Huddleston and Zhou (1989), found that for a given fine-grained specimen, the resilient modulus when plotted against deviatoric stress remained relatively constant. Conversely, for coarse-grained soils, a weak relationship between resilient modulus and the bulk stress existed. It was concluded that the relationships developed for the fine-grained soils were more reliable than the coarse-grained soils. Hicks and Monismith (1971) stated that, for granular soils, 50 to 100 axial stress repetitions should be applied in order to obtain reasonable estimates of the resilient modulus. Huddleston and Zhou (1989) stated that there was great variability in modulus of granular soils while there was little variability in modulus of cohesive soils.

## **2.3 Factors Affecting Resilient Modulus**

Many factors affect the resilient modulus of the subgrade. Resilient modulus is equivalent to dynamic modulus measured for geotechnical earthquake engineering projects. Cyclic triaxial tests (Silver et al, 1976) and resonant column tests (Drnevich, 1985 and Isenhower et al, 1987) are two examples of tests typically used for this purpose. Dynamic modulus is the most important parameter utilized in this field. Naturally, a wealth of information is available which cannot and should not be ignored. This information is summarized first and then related to resilient modulus.

Based upon numerous laboratory tests, Hardin and Drnevich (1972) proposed many parameters that affect the moduli of soils. These parameters, along with their degree of importance in affecting moduli, are summarized in Table 2.1. They suggested that state of stress, void ratio and strain amplitude are the main parameters affecting moduli measured in the laboratory. For cohesive soils, degree of saturation is also a very important parameter.

Basically, as void ratio decreases, the dynamic modulus of soil increases (Richart, 1977; Iwasaki and Tatsuoka, 1977; Hardin, 1978; Kokusho, 1980). One of the most important factors which affects the dynamic modulus of soils is the applied confining pressure. Dubby and Mindlin (1957), Hardin and Richart (1963), Hardin and Black (1966) and Hardin and Drnevich (1972) concluded that a linear logarithmic relationship exists between modulus and applied confining pressure.

Table 2.1 Parameters Affecting Modulus (from Hardin & Drnevich, 1972)

| Parameter                         | Importance <sup>1</sup> |                |
|-----------------------------------|-------------------------|----------------|
|                                   | Clean Sands             | Cohesive Soils |
| Strain Amplitude                  | V                       | V              |
| Effective Mean Principle Stress   | V                       | V              |
| Void Ratio                        | V                       | V              |
| Degree of Saturation              | R <sup>2</sup>          | T              |
| Overconsolidation Ratio           | R                       | V              |
| Effective Strength Envelop        | R                       | L              |
| Octahedral Shear Stress           | L                       | L              |
| Frequency of Loading              | L                       | L              |
| Other Time Effects (Thixotropy)   | R                       | R              |
| Grain Characteristics             | R                       | L              |
| Soil Structures                   | R                       | R              |
| Volume Change Due to Shear Strain | V                       | R              |

- 1) V means Very Important, L means Less Important, R means Relatively Unimportant, and U means importance is not known at the time.
- 2) Except for saturated clean sand where the number of cycles of loading is a less Important Parameter.

The strain level has a significant effect on the dynamic modulus. Stokoe et al (1988) identified four ranges of strain amplitude. The thresholds are shown in Figure 2.3. The strain can be divided into four categories as illustrated in Figure 2.3:

1. Small strains - also called elastic or low-amplitude strains at which linear behavior occurs.
2. Medium Strains - where nonlinear elastic behavior dominates this strain range.
3. Large Strains - significant plastic deformation occurs but failure is not reached.
4. Failure Strains - all greater than large strains.

Two other threshold strains shown in the figure are the boundaries where the number of cycles of loads (denoted as strain repetition threshold) and strain rate of the load applied (denoted as strain rate threshold) become important in soils. The strain rate threshold roughly coincides with the limit of the small strains and the strain repetition is located within medium strain level. As soon as the strain repetition threshold has passed, progressive failure will be imminent.

In pavement design, the strain levels are typically within ranges of small strains and medium strains. Simply higher strains will cause instantaneous rutting or fatigue cracking of the pavement.

In pavement engineering, factors affecting resilient modulus are usually considered less comprehensively and are divided into two major categories: level of compaction and stress state. These factors along with several others of less importance are discussed next.

### **2.3.1 Compaction**

The primary factor affecting the resilient modulus is compaction. The degree of compaction is related to moisture content, degree of saturation and relative density (or void ratio). Rada and Witczak (1981) showed that an increase in compaction increased the resilient modulus for fine-grained soils. Thompson (1989) stated that there was a strong correlation between resilient modulus and the degree of saturation. He concluded that higher degree of compaction provided a higher resilient modulus for a given degree of saturation. Thompson and Robnett (1989) mentioned that soils wet of the optimum moisture content had a low resilient modulus regardless of compaction. Also, they mentioned that the difference in resilient modulus for 100 percent and 95 percent compaction efforts decrease with an increase in the degree of compaction. Thompson (1969), Hicks and Monismith (1971), Thompson (1989), Huddleston and Zhou (1989), and Cochran (1989) concluded that an increase in the dry density also provided an increase in the resilient modulus but moisture content above the optimum resulted in a decrease in the resilient modulus. Seim (1989) studied the effects of different compaction methods on the resilient modulus.

Three different compacting methods were compared: static, kneading and Proctor. The results were the following: 1) due to static compaction the highest but the most variable resilient modulus was obtained; 2) kneading compaction yields the lowest values but were the most consistent; and 3) results from the proctor method fell in between those of the static and kneading but were usually closer to that of kneading compaction.

| STRAIN            | SMALL          | MEDIUM               | LARGE           | FAILURE |
|-------------------|----------------|----------------------|-----------------|---------|
|                   | $10^{-6}$      | $10^{-4}$            | $10^{-2}$       | $10^0$  |
| LINEAR ELASTIC    |                |                      |                 |         |
| NONLINEAR ELASTIC |                |                      |                 |         |
| ELASTIC-PLASTIC   |                |                      |                 |         |
| FAILURE           |                |                      |                 |         |
| STRAIN REPETITION |                |                      |                 |         |
| STRAIN RATE       |                |                      |                 |         |
| SOIL MODEL        | LINEAR ELASTIC | QUASI-LINEAR ELASTIC | ELASTIC-PLASTIC |         |

Figure 2.3 - Soil Behavior and Associated Strain Ranges (from Stokoe, et al, 1988).

This page was missing from the print copy.  
-- CTR Library Digitization Team

resistance to deform expressed in the ratio of transmitted lateral pressure to the applied vertical pressure (Mahoney et al, 1988). For R-values equal to or less than 20, he found the following expression:

$$M_R = A + B (R\text{-value}) \quad (2.3)$$

The A and B values range from 772 to 1155 and from 369 to 555, respectively. However, the A value is usually taken as 1000 while the B value is taken as 555.

Several other correlations have been suggested which are summarized in Figure 2.4.

## 2.5 Problems With Resilient Modulus

Brickman (1989), Fager and Valencia (1989), Ho (1989), Moses (1989), Seim (1989) and Thompson (1989) have discussed equipment set-up for the resilient modulus tests. They all agree that the load actuator should be mounted above the triaxial cell on a rigid beam. Seim (1989) and Brickman (1989) discussed in detail problems associated with different components of the resilient modulus device. Seim (1989) stated that AASHTO prefers the load cell to be mounted on the inside of the triaxial cell between the specimen and the loading ram. In contrast, if the load cell is mounted on the outside of the triaxial cell then friction has to be accounted for. He also stated that LVDT's should be clamped directly to the specimen if the modulus of the specimen exceeded 15000 psi or clamped on the outside of the triaxial cell if the modulus of the specimen was less than 15000 psi. In addition, two LVDT's mounted 180° opposed and connected to produce an average signal would be the most accurate method. The confining fluid may be either air or water.

Several investigators discovered numerous problems associated with the resilient modulus testing, especially AASHTO T-274-82 procedures. Jackson (1989) and Ho (1989) stated that the stress states suggested by AASHTO were too severe for their specimens. Several of their specimens failed during testing. Seim (1989) said that the test procedure was too vague; there was no clear distinction between the fine and granular materials. Jackson (1989) and Seim (1989) found that the accuracy of the results strongly depended on the experience of the technician performing the test.

Several investigators encountered problems with low deviatoric stress loading conditions (i.e. 1 psi and 2 psi). Seim (1989) and Ho (1989) suggested that these two loading steps be eliminated from test procedure. They stated that 1 and 2 psi deviatoric stress did not produce large enough strains to be accurately measured with LVDT's.

Brickman (1989) listed several developments that should be implemented: 1) method for testing be simplified, 2) cost of testing be decreased, 3) calculated numbers from the test be more accurate, and 4) machinery be more dependable, more rugged and easier to operate.

In summary, the resilient modulus tests require major new developments to be incorporated as a direct input for future designs of pavements. Claros et al (1990) and Pezo et al (1991) stated

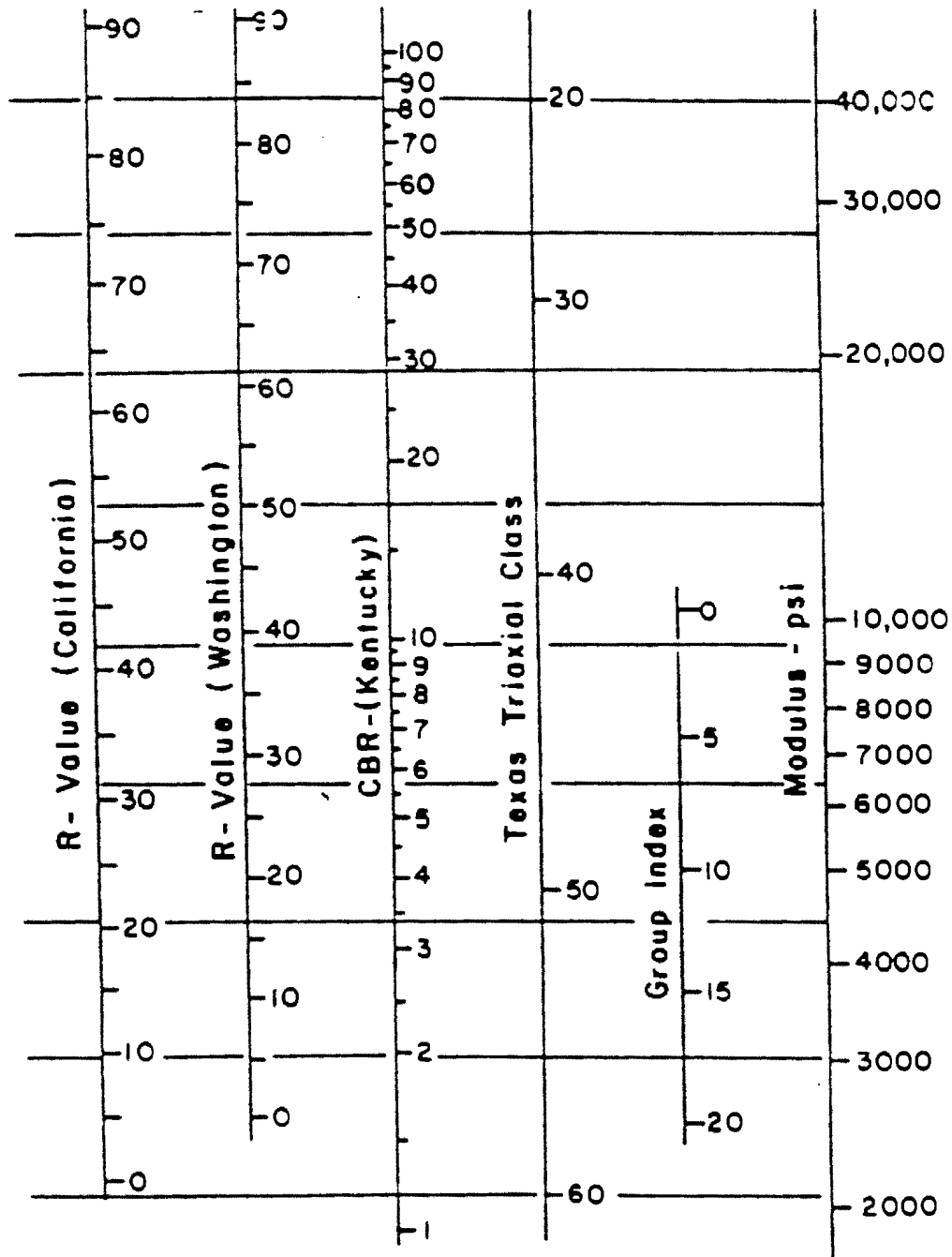


Figure 2.4 - Correlations of Resilient Modulus of Roadbed Soils with Laboratory Tests (from AASHTO, 1986).

that synthetic samples are an excellent medium to calibrate resilient modulus testing equipment. Three samples, composed of polyurethane elastomers, of different stiffness, should be used. Pezo et al (1991) also stated that good contact between the sample and load platens is essential to obtain reliable resilient modulus values.

## 2.6 Constitutive Models For Resilient Modulus

Several constitutive models have been proposed for describing the results of resilient modulus tests. For base coarse and granular (cohesionless) soils, Biarez (1962) established the following relationship:

$$M_R = k\theta_m^n \quad (2.4)$$

where:

k and n = constants  
 $\theta_m$  = mean normal stress = 1/3 bulk stress.

A more widely-used variation to this formula is:

$$M_R = k_1\theta^{k_2} \quad (2.5)$$

where:

$k_1$  and  $k_2$  = constants  
 $\theta$  = bulk stress =  $3\sigma_c + \sigma_d$   
 $\sigma_c$  = confining pressure  
 $\sigma_d$  = deviatoric stress.

This relationship is used extensively for granular materials and is adopted by AASHTO. Uzan (1985) modified this relationship. He suggested that:

$$M_R = k_1 \sigma_d^{k_2} \quad (2.6)$$

Uzan indicated that his relationship is more representative of the behavior of granular soils.

For subgrade materials and cohesive soils, Equation 2.6 is commonly used. This relationship has been adapted by AASHTO.

Several more advanced relationships have been developed in the geotechnical earthquake

engineering area. These relationships are normally developed for shear modulus but they can easily transformed to resilient modulus using

$$M_R = 2(1 + \nu)G \quad (2.7)$$

where:

- $\nu$  = Poisson's ratio
- G = shear modulus.

In these studies the elastic modulus is first determined and then converted to nonlinear moduli. Hardin and Black (1966) studied extensively the effect of isotropic confining pressure. They concluded that the elastic modulus was dependent only on the octahedral normal stress and was essentially independent of the deviatoric component of the initial state of stress. They indicated that a functional relationship for the modulus can be formulated as:

$$G = f(\sigma'_o, e, H, S_r, \tau_o, C_g, A_p, F, T, O, K_T) \quad (2.8)$$

where:

- $\sigma'_o$  = effective octahedral normal stress
- e = void ratio
- H = ambient stress and vibration history
- $S_r$  = degree of saturation
- $\tau_o$  = octahedral shear stress
- $C_g$  = grain characteristics, grain shape, grain size, grading and mineralogy
- $A_p$  = amplitude of vibration
- F = frequency of vibration
- T = secondary effects that are a function of time
- O = soil structure
- $K_T$  = temperature including freezing.

Based on numerous tests on different soils, Hardin and Black (1966 and 1968) suggested an empirical equation for clay and clean sands. This equation is given as:

$$G_{max} = 1230 F(e) OCR^K \sigma'_o{}^{0.5} \quad (2.9)$$

where:

- $G_{max}$  = elastic shear modulus
- F(e) =  $(2.973 - e)^2 / (1 + e)$
- OCR = overconsolidation ratio
- K = overconsolidation adjustment factor.

Several other researchers (Richart, 1977; Iwasaki and Tatsuoka, 1977; Hardin, 1978) proposed similar relationships for finding elastic modulus. These empirical relationships are shown in Equations 2.10 through 2.12. Hardin (1978) recommended:

$$G_{\max} = \frac{A(OCR)}{F(e)} \sigma'_o P_a^{(1-n)} \quad (2.10)$$

where:

$$\begin{aligned} F(e) &= 0.3 + 0.7e^2 \\ A &= 625 \\ n &= 0.5 \\ P_a &= \text{atmospheric pressure (in same units as } G_{\max} \text{ and so)}. \end{aligned}$$

Richart (1977), based upon tests on round-grained sands and angular-grained crushed quartz, suggested:

$$G_{\max} = A \frac{(B-e)^2}{(1+e)} \sigma'_o{}^{0.5} \quad (2.11)$$

where:

$$\begin{aligned} A &= 2630 \text{ (for round sands) and } 1230 \text{ (for angular sands)} \\ B &= 2.17 \text{ (for round sands) and } 2.97 \text{ (for angular sands)}. \end{aligned}$$

Iwasaki and Tatsuoka (1977) studied the effects of grain size and gradation on dynamic moduli. They suggested the following relationship:

$$G_{\max} = A(\gamma) B F(e) \sigma'_o{}^{m(\gamma)} \quad (2.12)$$

The term  $A(\gamma)$  is a function of  $\gamma$ , the strain amplitudes, and varies from 900 at  $\gamma = 0.0001\%$  to 700 at  $\gamma = 0.01\%$ . The value of  $m(\gamma)$  is also a function of  $\gamma$  and varies from 0.4 at  $\gamma = 0.0001\%$  to 0.5 at  $\gamma = 0.01\%$ . The parameter,  $B$ , is about 1 for uniform clean sands for a wide range of grain sizes. The function  $F(e)$  equals  $(2.17 - e)^2 / (1 + e)$ .  $G_{\max}$  and  $\sigma'_o$  are in  $\text{kg/cm}^2$  in Equation 2.13.

Several investigators have proposed relationships to calculate nonlinear modulus from the elastic modulus. The Ramberg-Osgood model (1963) is the most widely used and is discussed below.

Ramberg-Osgood (1943) suggested a mathematical expression to represent the nonlinear stress-strain behavior. They suggested that:

$$\gamma = \frac{G_\gamma}{G_{\max}} + C \left[ \frac{G_\gamma}{G_{\max}} \gamma \right]^R \quad (2.13)$$

where:

$G_\gamma$  = modulus at strain level  $\gamma$   
 $G_{\max}$  = elastic modulus  
C and R = constants.

This relationship can be simplified as:

$$Lg[\gamma[1 - \frac{G_\gamma}{G_{\max}}]] - LgC + RLg[\frac{G_\gamma}{G_{\max}}\gamma] \quad (2.14)$$

This equation is a linear equation of the form:  $y = K + Rx$ . These relationships can be easily utilized in studying resilient modulus tests for more rigorous constitutive relationships.

This page replaces an intentionally blank page in the original.

-- CTR Library Digitization Team

# Chapter 3

## Equipment

### 3.1 Introduction

The resilient modulus test is used to study the elasticity of a soil under repeated loading. The test involves several loading sequences, which require changing the deviatoric stress and the confining pressure. This is explained in detail in Chapter 4. The resilient modulus tests are load-controlled tests; that is a pre-determined load is applied to the specimen and the corresponding deformation is measured. A description of the equipment used is included in this chapter.

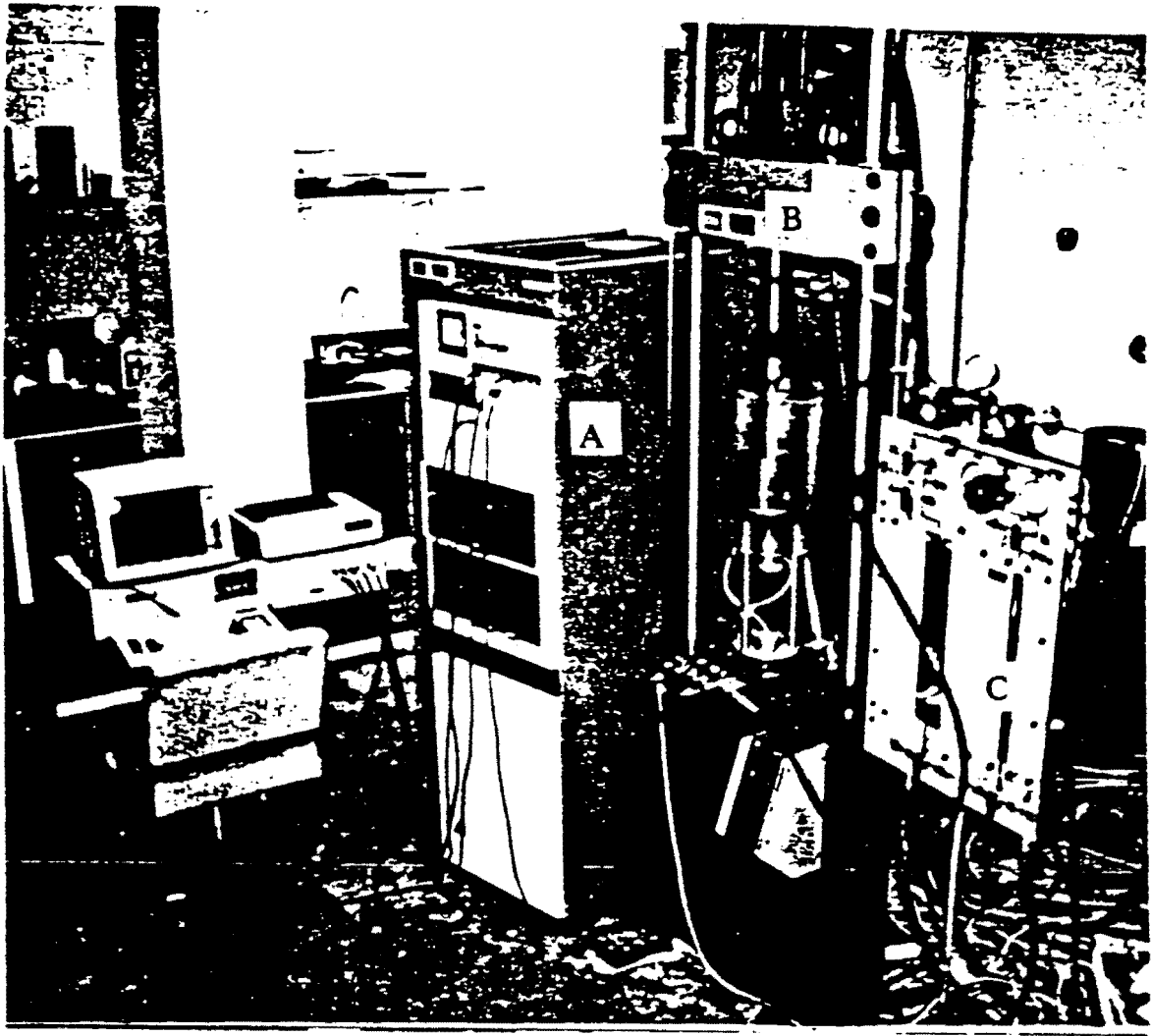
### 3.2 Equipment

In this study, resilient modulus tests were performed with a closed-loop servo-valve system manufactured by MTS, Inc. The system consists of several interacting units, that can be grouped into three main components: 1) load unit, 2) controller, and 3) hydraulic power supply (not shown in the figure). These components are shown in Figure 3.1. A brief description of each component follows.

#### 3.2.1 Load Unit

The load unit is shown in Figure 3.2 and consists of two smooth vertical columns that join two stiff structural members; i.e., a movable crosshead and a fixed platen. The crosshead is vertically adjustable to accommodate specimens of varying lengths. A vertical load can be applied to the specimen using a hydraulic actuator which is mounted on the crosshead.

The load unit is provided with a triaxial cell, so that soil samples can be tested with an all around confining pressure. The triaxial cell consists of lower and upper support plates. A push rod extends



- A - Controller
- B - Load Unit
- C - Service Manifold

Figure 3.1 - Overall Picture of Testing System.

This page replaces an intentionally blank page in the original.

-- CTR Library Digitization Team

through the upper support plate and is attached to the upper load platen to apply an axial load to the specimen. A shut-off valve manifold at the base of the triaxial cell provides control over specimen saturation, pore pressure measurement and removal of entrapped air in the platen. The upper platen is connected to the shut-off valve manifold with flexible tubing.

Figure 3.3 shows a close-up of the triaxial cell. The load platens and the support plates are enclosed by a translucent cylindrical shell that acts as a sealed confining chamber and allows observation of the specimen. Access clamps on the upper support plate restrain the shell during testing. Specimen mountings and removals are accomplished by unlocking the access clamps and raising the shell. Such a design is ideal for a cell because its stiff nature minimizes the problems with equipment compliances.

The triaxial cell push-rod is rigidly mounted to the actuator by way of a load cell. The position of the push-rod is monitored by a linear variable differential transformer (LVDT). The triaxial cell is also equipped with two transducers: one to measure cell pressure, and the other to monitor pore pressure within the sample.

There are two different methods for applying the confining pressure. Either a hydraulic actuator mounted at the base of the load frame can be utilized, or confining pressure can be applied pneumatically to the specimen through the pressure ports in the upper support plate. Generally, for short term testing at low confining pressures, the first option is used. For saturation of the sample and long-term tests at high confining pressures, the second option is used.

The upper load platen consists of two steel parts as shown in Figure 3.4. The upper part always remains attached to the push-rod, while the second part rests on the sample. The two parts are held together by means of a vacuum applied between them. The vacuum is applied through a port in the shut-off valve manifold at the base of the triaxial cell. (see Figure 3.3)

An additional service manifold is attached to the load frame to accommodate reservoirs for the confining fluid and the pore fluid. Compressed air (obtained from an external air compressor), applied on the water in the pore fluid reservoir, causes water to flow into the specimen under pressure. A valve and a pressure gage are provided to control the pore pressure.

### **3.2.2 Controller**

The MicroConsole controls and monitors the operation of the load unit. It also contains jacks on the rear panel for transducers, servovalves, hydraulic service manifolds, etc.

A picture of the controller is included in Figure 3.5. Three plug-in modules are provided: an AC Controller, a DC Controller, and an Auxiliary span-control. The Auxiliary span-control was not used during these tests, and will not be discussed herein. Either the AC Controller or the DC Controller can be used to operate the actuator mounted at the top of the load frame. The AC Controller and the DC Controller control the movement of and the load applied by the actuator rod, respectively. Depending on the selected active controller, the test can be run in strain- or stress-controlled mode.

An expansion MicroConsole panel houses another set of three plug-in modules. Of these, two control the hydraulic actuator at the bottom of the frame, which in turn controls the confining pressure. The

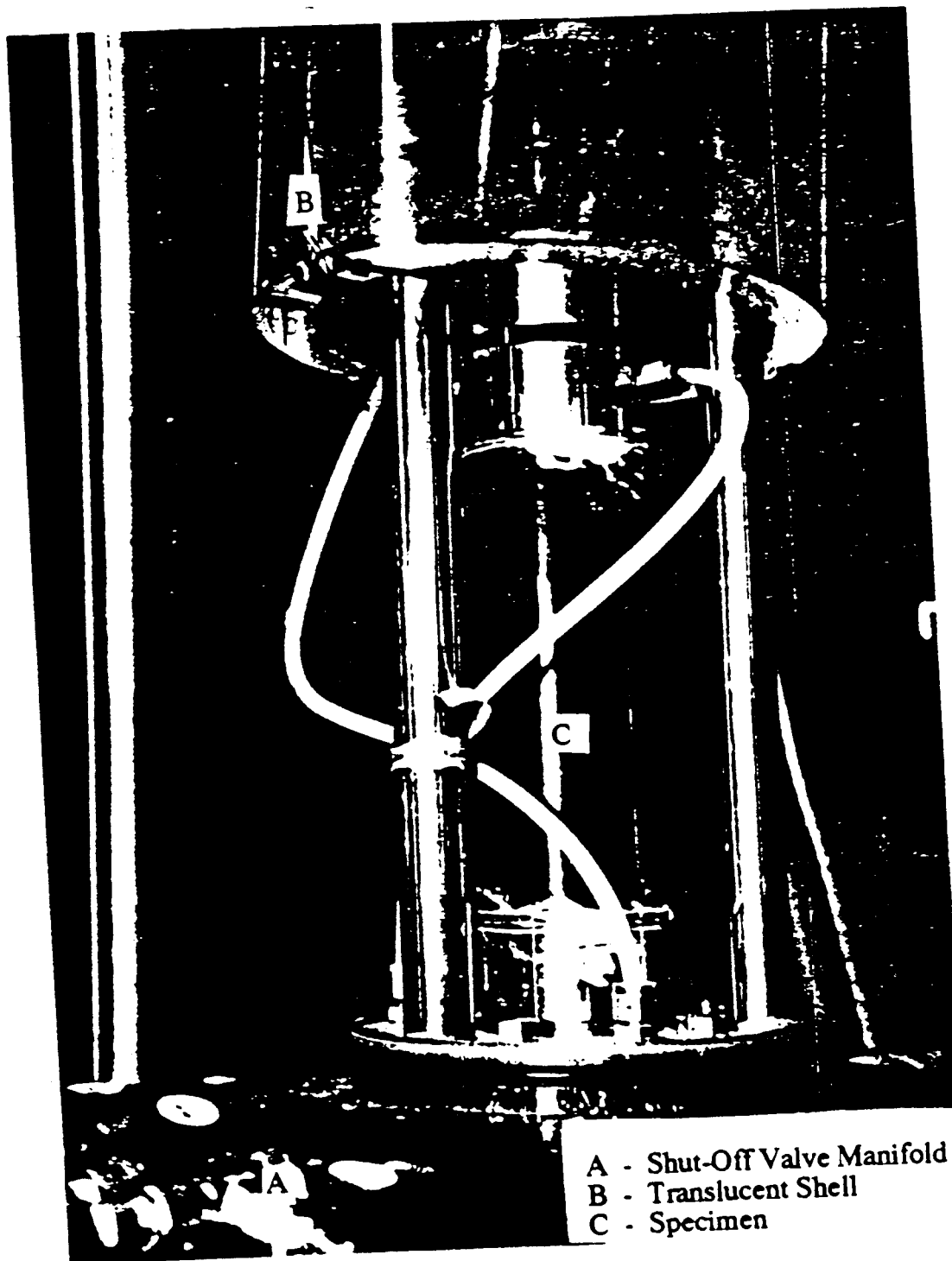


Figure 3.3 - Triaxial Testing Cell.

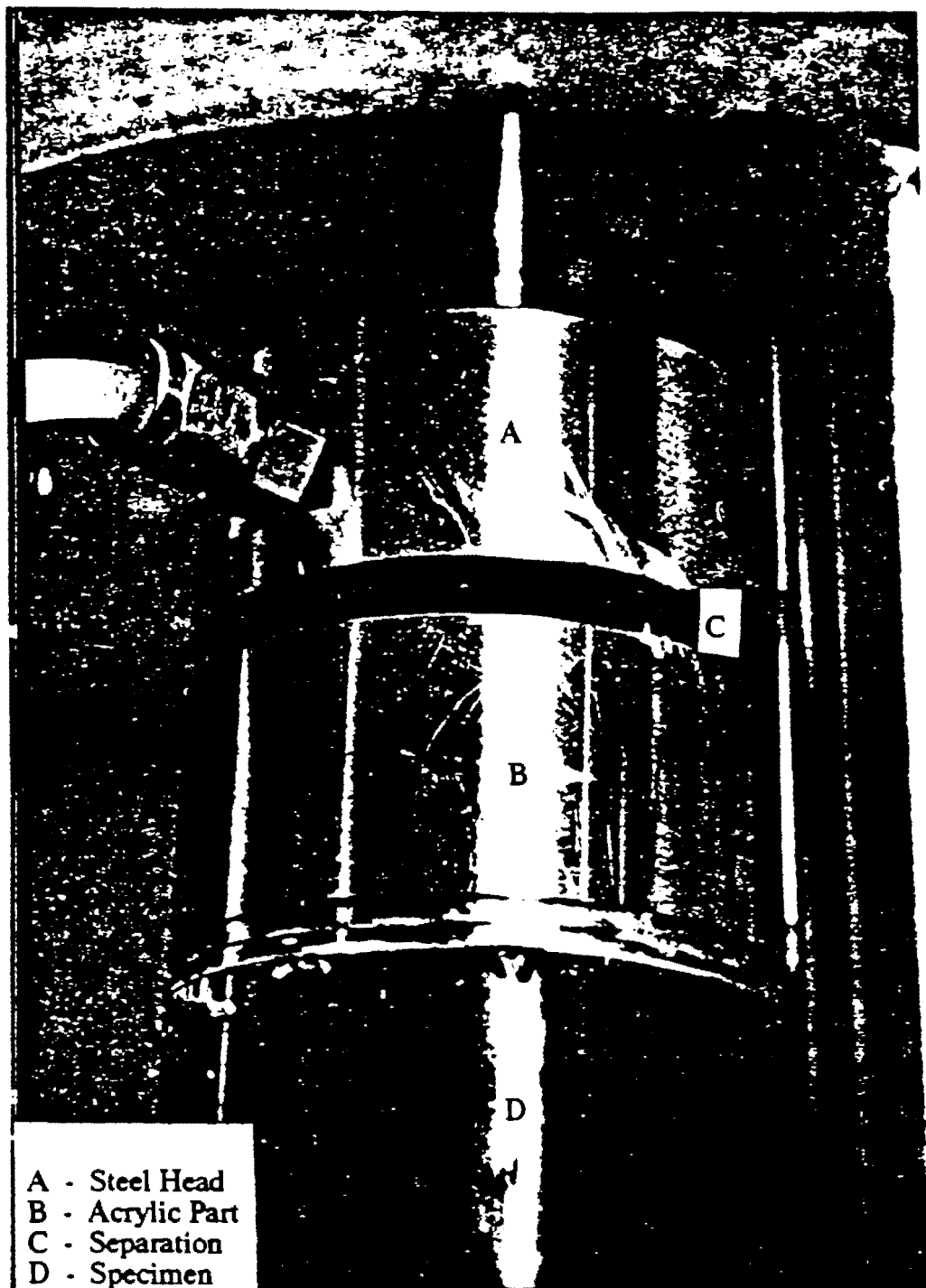
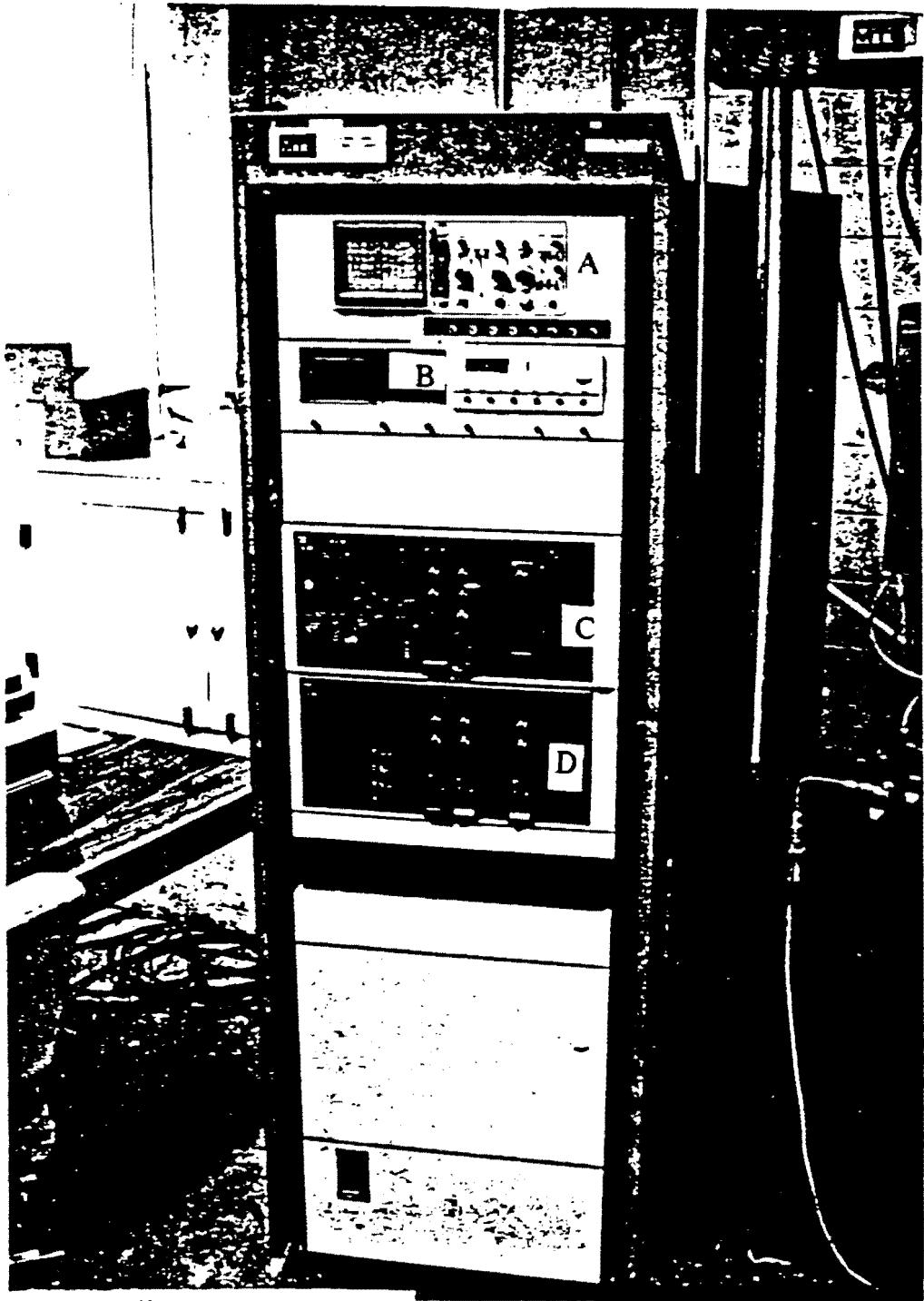


Figure 3.4 - Components of Upper Load Platen of Triaxial Cell.



- A - Oscilloscope
- B - Waveform Generator
- C - Microconsole
- D - Expansion Microconsole

Figure 3.5 - Components of Controller.

third module is used to monitor the pore pressure.

The MicroConsole is also equipped with two arbitrary waveform generators manufactured by Wavetek Inc. These two function-generators, that are used to control the motion of the two hydraulic actuators, have several built-in standard functions, such as sine, cosine, square, and haversine. The amplitude, frequency, and the DC-offset of these waves can be set to any arbitrary values. In addition, these standard waveforms can be readily edited to produce more complex functions. These input functions, as well as the output from any of the transducers mounted on the load frame or the load cell, can be monitored by an oscilloscope mounted above the waveform generators.

### **3.2.3. Hydraulic Power Supply**

The hydraulic power supply provides the high pressure fluid required for the operation of the system. The high pressure fluid is applied to one side of the actuator, causing it to move. A servovalve controls the movement of the actuator, by opening or closing in response to the Controller. The valve can be opened in either of two directions, allowing the high pressure fluid to flow into the cylinder on either side of the piston. This causes movement of the piston in either of two directions.

# Chapter 4

## Testing Procedures

### 4.1 Introduction

Recently much attention has been focused on conducting and implementing resilient modulus tests. As such, several new testing procedures and methodologies have been developed. The leading organization pursuing the implementation of resilient modulus tests, besides AASHTO, is the Strategic Highway Research Program (SHRP). This organization has suggested some improvement to the AASHTO T-274 procedure. Based upon the type of material to be tested, both AASHTO and SHRP have proposed two separate procedures. Granular materials are tested differently than cohesive materials. In this study, for each type of soil, the AASHTO method is compared to the SHRP method. Also, it was found that further modifications may be needed for granular materials.

In this chapter, granular and cohesive materials are defined first and then sample preparation methods are discussed. The AASHTO and SHRP testing procedures, as proposed are presented. A newly-developed procedure for granular materials is discussed. Finally, the implementation of these procedures in the UTEP device is explained.

### 4.2 Definition of Soil Types

As mentioned before, both SHRP and AASHTO distinguish between granular and cohesive materials. AASHTO and SHRP definitions of granular and cohesive materials are presented below.

#### 4.2.1 AASHTO Definitions

The AASHTO definition for cohesive soils is rather vague and unclear. In the 1986 AASHTO T-274

procedure, a cohesive soil is defined as a soil containing substantial amounts of clay. Therefore, cohesive soils are those soils classified as A-2-6, A-2-7, A-6 and A-7 using the criteria of AASHTO M-145. The definition of a granular soil is also vague. Basically, any material which is not cohesive can be considered as granular.

#### **4.2.2 SHRP Definitions**

SHRP divides soils into two well-defined categories -- Type 1 and Type 2. As per SHRP Protocol P-46 (SHRP, 1989), Type 1 materials include all unbound granular and subbase materials and all untreated subgrade soils which meet the criteria of less than 70 percent passing the No. 10 sieve and 20 percent or less passing the No. 200 sieve. Therefore, soils classified as A-1-a in AASHTO classification will always classify as Type 1. In addition, soils classified as A-1-b, A-2 and A-3 may or may not fall into this type. All other untreated soils not meeting the criteria for Type 1 soil will be classified as Type 2. Soils classified as A-4, A-5, A-6 and A-7 are Type 2 soils.

#### **4.3 Sample Preparation**

Depending upon the type of soil tested, different sample preparation methods were used. These methods are described below. For simplicity, SHRP Type 1 soils and AASHTO granular soils were broadly categorized as granular soils. Similarly, SHRP Type 2 soils and AASHTO cohesive soils are categorized as cohesive soils.

In this study, the sample preparation procedures proposed by SHRP were followed for both AASHTO and SHRP testing procedures. In this manner, the effects of sample preparation on the results could be minimized.

The soil preparation as described by AASHTO is complicated. The use of three different compaction methods, kneading, static or gyratory, is suggested. The compaction method used to prepare a sample depends on the field condition. Table 4.1 shows a reproduction of the table by AASHTO to determine the method of compaction for sample preparation. Once the compaction method and moisture content is determined, the sample is prepared and placed into the testing apparatus.

It was felt that the SHRP procedures were easier to follow and implement. In addition, the SHRP procedure would yield more repeatable samples and was better written.

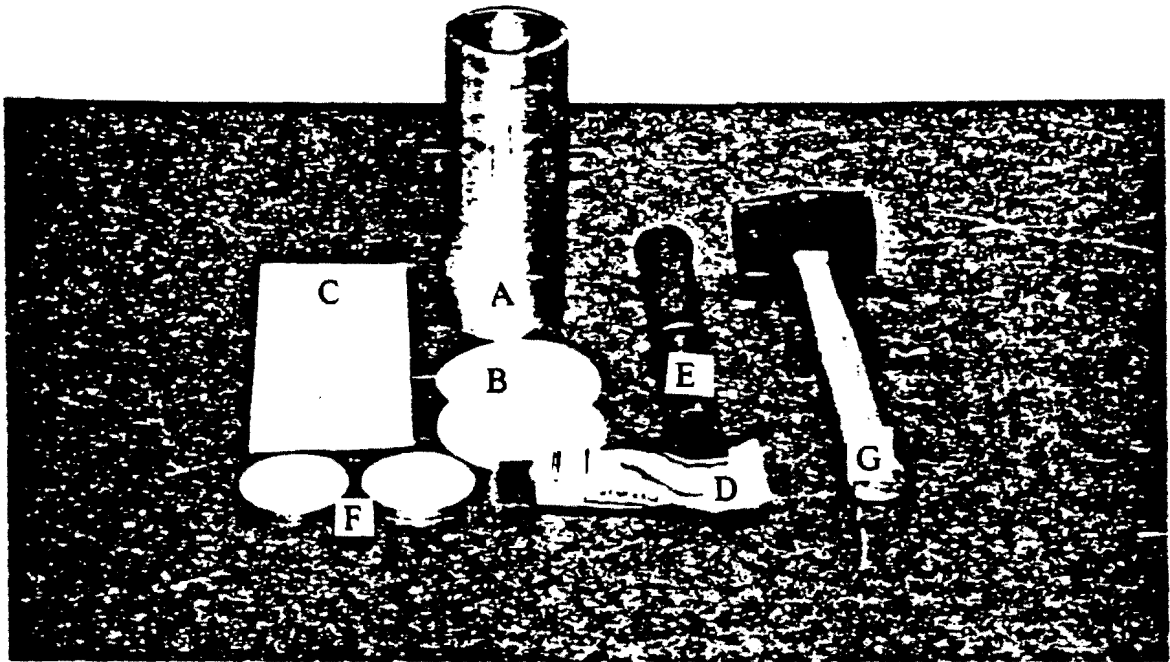
##### **4.3.1 Granular Soils**

The items needed for sample preparation for SHRP Type 1 soils are shown in Figure 4.1. A split mold, two filter papers, a rubber membrane, vacuum grease, tamping rod, two porous stones and a hammer were required.

The procedure followed for sample preparation is as follows. The bottom load platen was placed on a clean level surface and vacuum grease was applied around the platen. One porous stone and one filter paper was placed on top of the platen. The filter paper was placed in between the soil and the

Table 4.1 AASHTO's Guide to Selection of Compaction Method

| GYRATORY   | KNEADING   | STATIC  |
|--|--|---|
| Subgrades compacted at a water content less than 80% saturation and remain in that condition | Subgrades compacted at a water content less than 80% saturation and remain in that condition             | Subgrades compacted at a water content less than 80% saturation and remain in that condition            |
|  |  | Subgrades compacted at a water content less than 80% saturation and water content subsequently increase |
|  | Sample compacted at initial field water content & subjected to post construction change in water content |   |
|  | Subgrades compacted at a water content greater than 80% saturation                                       |   |



- A - Split Mold
- B - Filter Paper
- C - Rubber Membrane
- D - Vacuum Grease
- E - Tamping Rod
- F - Porous Stones
- G - Hammer

Figure 4.1 - Equipment for Preparing Specimens for Granular (Type 1) Materials.

porous stone, to minimize the clogging of the porous stone. The split mold was assembled and the rubber membrane stretched over the ends of the platen. Vacuum was applied to the mold through special nipples to securely hold the membrane against the mold. The soil to be tested was poured into the mold in three equal layers and compacted to the desired density with a tamping rod. For higher densities, a constant pressure was applied on top of the sample while the side of the mold was tapped with a hammer. The second filter paper and porous stone were placed on top of the sample. The sample was placed in the testing equipment. The vacuum hose was disconnected from the split mold and placed on one of the saturation lines of the triaxial cell. Both the mold and bottom load platen were picked up and placed inside the triaxial cell. The top load cell was lowered until it just touched the top porous stone and the bottom load platen was secured to the triaxial cell. Vacuum grease was applied to the top platen and the rubber membrane was removed from the mold and stretched over the top and lower platen. A rubber band was tied around the top load platen and the split mold was removed from the sample carefully. Another rubber band was tied around the lower load platen. The membrane was checked for leaks.

### 4.3.2 Cohesive Soils

The materials needed for sample preparation for Type 2 soils are standard Proctor hammer, standard Proctor mold with extension collar, 2 sealable plastic bags, rubber membrane, distilled water, water bottle, mixing pan, scale, extruder, and trimming device (see Figure 4.2).

An appropriate amount of distilled water was added to the soil until the desired moisture content was obtained. The soil and water were mixed in a mixing pan. The mixture was placed inside two plastic bags (double bagged), and sealed. The mixture was placed inside a humidity control room for 24 hours. After 24 hours, the mixture was removed from the bags and placed on a clean table. The standard Proctor mold as assembled with the extension collar in place and soil was placed into the mold in three equal layers. Twenty-five blows were applied with the standard Proctor hammer to each layer. The compacted soil was removed using an extruder. The sample was trimmed down to the proper dimensions of 2.8 inches in diameter and 6.0 inches in length. The rubber membrane was placed around the sample and the sample was placed in the testing equipment.

To secure the sample to the platens, a hydrostone mix was prepared and applied (Pezo et al, 1991). The hydrostone used in this study was provided by UT-Austin. Hydrostone is a gypsum type material which resembles plaster of paris. The hydrostone mix, which was used in a similar way as capping compound is used in concrete cylinder testing, gains strength relatively rapidly. The hydrostone was mixed to a paste and was applied between the sample and the platens (top and bottom). The hydrostone was allowed to dry for one and half hours. The drying time was relatively short due to the low humidity in El Paso. Pezo et al (1991) noticed that the results of resilient modulus tests using hydrostone were significantly more consistent and the results were more accurate. Saturation lines were plugged with paper to avoid clogging. The sample was placed inside the triaxial cell and the top load platen was lowered and a 2 psi pressure was applied. The hydrostone was inspected to ensure a complete coverage of the top and bottom of the sample. After the hydrostone was dried, the seating pressure was removed from the sample and rubber bands were tied around the top and bottom platens. Leaks in the membrane could not be checked because the saturation lines were plugged.

## **4.4 Testing Procedures**

As mentioned before, separate testing procedures were followed for the two types of soils. Three different procedures were followed for Type 1 soils namely, AASHTO, SHRP, and UTEP. For Type 2 soils, AASHTO and SHRP procedures were followed. The UTEP procedure was developed during the course of this study. All procedures are explained below.

### **4.4.1 Granular Soils**

#### **4.4.1.1 AASHTO Procedure**

The testing procedure suggested by AASHTO is rather lengthy because the specimen is tested under numerous different stress states and loading conditions. Table 4.2 shows the loading sequence proposed by AASHTO. At each loading condition, 200 cycles of load were applied. The resilient modulus is calculated from the results of the 200th cycle.

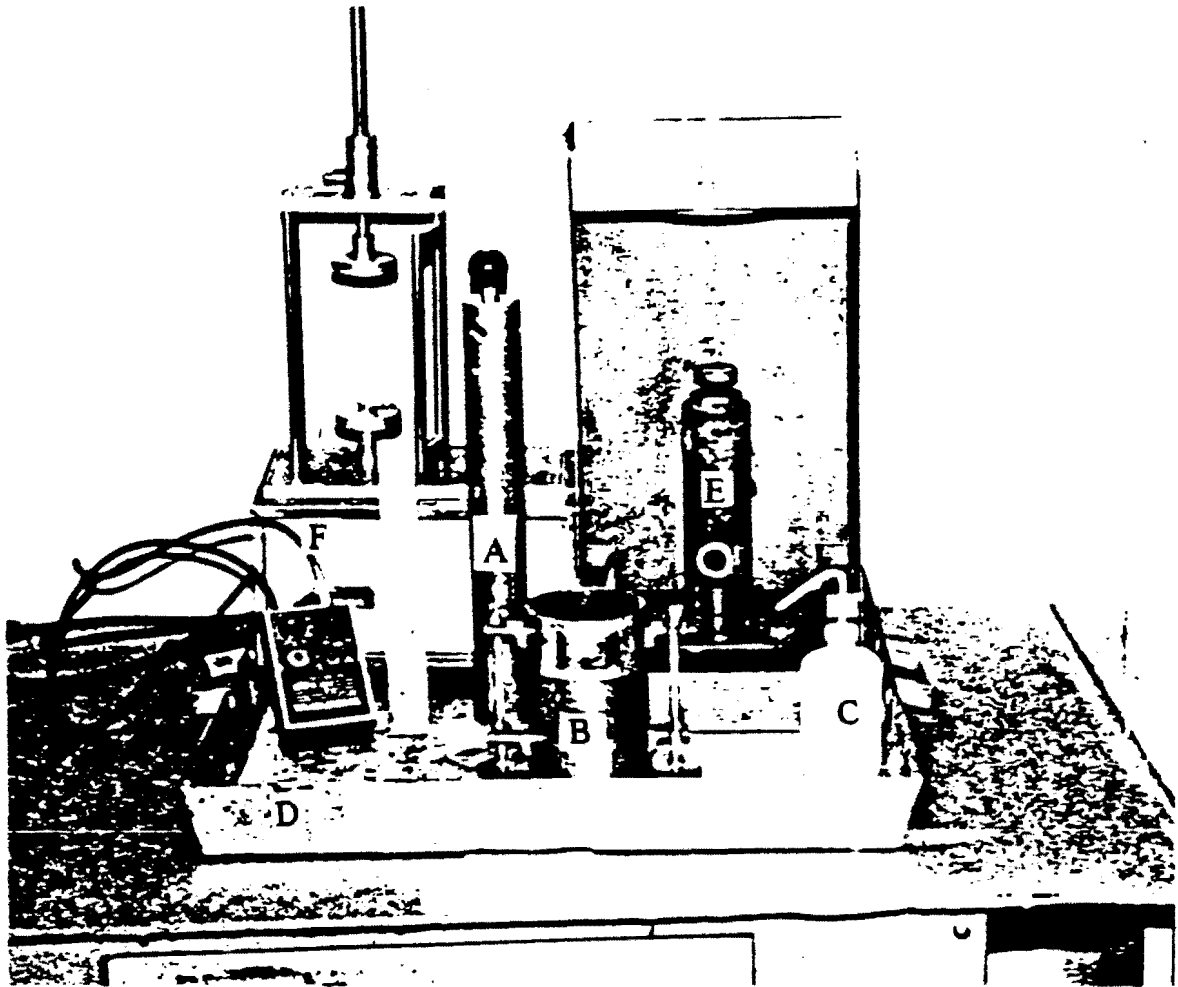
In Table 4.2, the first column indicates the loading steps. A total of 33 steps have to be followed. A detailed description of efforts involved in each step can be found in Section 4.6. The zeros in this column indicate conditioning steps. This pretest loading would presumably help the sample to become more homogeneous. In other words, during the conditioning steps, any voids in the sample are supposedly removed and a good contact between the sample and load platens is achieved. Data are not collected during these steps. In our experience, the six pretesting steps resulted in unrecoverable deterioration of many samples before the actual testing. This procedure involves five confining pressures and at each confining pressure increasing deviatoric stress is applied. The deviatoric stress ranges from 1 to 20 psi. The fourth column shows the number of cycles to be applied. This number is also the cycle for which the modulus is calculated. The last column shows if data is collected or not. In our experience, in order to perform a complete test, including sample preparation, the required time is about 4.5 hours.

#### **4.4.1.2 SHRP Procedure**

Table 4.3 shows the loading sequence for SHRP procedure. Contrary to AASHTO recommendation, only one conditioning step is required. Again, this is represented as 0 in the "Loading Sequence" column. No data is collected during this step. The conditioning step is performed for the same reason as mentioned previously. The substantial decrease in the number of pretesting steps would certainly decrease the chances for sample degradation or disturbance.

The actual test consists of 15 loading steps. The load is applied for 100 cycles with the 100th cycle being the cycle where the resilient modulus is calculated. In our experience, the procedure is easy to follow and perform. The test period is approximately 2.5 hours because of fewer loading steps and fewer cycles of load. This procedure requires five confining pressures with deviatoric stresses ranging from 3 to 40 psi. The fourth column is the number of cycles to apply and the last column shows if data is collected.

One major problem with the SHRP procedure is sample disturbance due to large deviatoric stresses



- A - Standard Proctor Hammer
- B - Standard Proctor Mold with Extension
- C - Water Bottle
- D - Mixing Pan
- E - Extruder
- F - Trimming Device

Figure 4.2 - Equipment for Preparing Specimens for Cohesive (Type 2 ) Materials.

Table 4.2 Loading Sequence Proposed by AASHTO for Granular Soils

| Loading Sequence | Deviatoric Stress, psi | Confining Pressure, psi | Number of Repetitions | Deformation Record(Y or N) |
|------------------|------------------------|-------------------------|-----------------------|----------------------------|
| 0                | 5                      | 5                       | 200                   | N                          |
| 0                | 10                     | 5                       | 200                   | N                          |
| 0                | 10                     | 10                      | 200                   | N                          |
| 0                | 15                     | 10                      | 200                   | N                          |
| 0                | 15                     | 15                      | 200                   | N                          |
| 0                | 20                     | 15                      | 200                   | N                          |
| 1                | 1                      | 20                      | 200                   | Y                          |
| 2                | 2                      | 20                      | 200                   | Y                          |
| 3                | 5                      | 20                      | 200                   | Y                          |
| 4                | 10                     | 20                      | 200                   | Y                          |
| 5                | 15                     | 20                      | 200                   | Y                          |
| 6                | 20                     | 20                      | 200                   | Y                          |
| 7                | 1                      | 15                      | 200                   | Y                          |
| 8                | 2                      | 15                      | 200                   | Y                          |
| 9                | 5                      | 15                      | 200                   | Y                          |
| 10               | 10                     | 15                      | 200                   | Y                          |
| 11               | 15                     | 15                      | 200                   | Y                          |
| 12               | 20                     | 15                      | 200                   | Y                          |
| 13               | 1                      | 10                      | 200                   | Y                          |
| 14               | 2                      | 10                      | 200                   | Y                          |
| 15               | 5                      | 10                      | 200                   | Y                          |
| 16               | 10                     | 10                      | 200                   | Y                          |
| 17               | 15                     | 10                      | 200                   | Y                          |
| 18               | 1                      | 5                       | 200                   | Y                          |
| 19               | 2                      | 5                       | 200                   | Y                          |
| 20               | 5                      | 5                       | 200                   | Y                          |

Table 4.2 Cont. - Loading Sequence Proposed by AASHTO for Granular Soils

| Loading Sequence | Deviatoric Stress,<br>psi | Confining<br>Pressure, psi | Number of<br>Repetitions | Deformation<br>Record(Y or N) |
|------------------|---------------------------|----------------------------|--------------------------|-------------------------------|
| 21               | 10                        | 5                          | 200                      | Y                             |
| 22               | 15                        | 5                          | 200                      | Y                             |
| 23               | 1                         | 1                          | 200                      | Y                             |
| 24               | 2                         | 1                          | 200                      | Y                             |
| 25               | 5                         | 1                          | 200                      | Y                             |
| 26               | 7.5                       | 1                          | 200                      | Y                             |
| 27               | 10                        | 1                          | 200                      | Y                             |

Table 4.3 Loading Sequence Proposed by SHRP for Type 1 Soils

| Loading Sequence | Deviatoric Stress, psi | Confining Pressure, psi | Number of Repetitions | Deformation Record(Y or N) |
|------------------|------------------------|-------------------------|-----------------------|----------------------------|
| 0                | 4                      | 15                      | 200                   | N                          |
| 1                | 3                      | 3                       | 100                   | Y                          |
| 2                | 6                      | 3                       | 100                   | Y                          |
| 3                | 9                      | 3                       | 100                   | Y                          |
| 4                | 5                      | 5                       | 100                   | Y                          |
| 5                | 10                     | 5                       | 100                   | Y                          |
| 6                | 15                     | 5                       | 100                   | Y                          |
| 7                | 10                     | 10                      | 100                   | Y                          |
| 8                | 15                     | 10                      | 100                   | Y                          |
| 9                | 30                     | 10                      | 100                   | Y                          |
| 10               | 10                     | 15                      | 100                   | Y                          |
| 11               | 15                     | 15                      | 100                   | Y                          |
| 12               | 30                     | 15                      | 100                   | Y                          |
| 13               | 15                     | 20                      | 100                   | Y                          |
| 14               | 20                     | 20                      | 100                   | Y                          |
| 15               | 40                     | 20                      | 100                   | Y                          |

applied at low confining pressures (loading steps number 9, 12 and 15) that is applied on to the specimen. It causes the sample to deform excessively, especially if the sample has a low modulus. During our testing program, several samples failed before the completion of all loading steps.

One advantage of the resilient modulus test is that it is a nondestructive test. The sample should not fail during testing, or its properties should not significantly alter between consecutive loading sequences. As such, the test had to be modified so that the sample would not be subjected to high stress levels. A new loading sequence for Type 1 soils has been developed that would minimize the disturbance to a sample during testing. This new procedure will be noted as the UTEP method.

#### **4.4.1.3 UTEP Procedure**

In the AASHTO and SHRP methods, the confining pressure is kept constant and the deviatoric stress is varied. But, in the UTEP method, the deviatoric stress is held constant while the confining pressure is increased.

The loading steps for UTEP procedure are shown in Table 4.4. As before, the first row or the "Loading Sequence" 0 is the conditioning step. It is the same as for the SHRP method. The conditioning step is run for 200 cycles and no data is collected for this step. The rest of the 15 loading steps are run for 100 cycles. To complete the test, including sample preparation, it takes approximately 2 hours. Three deviatoric stresses are used in this procedure. Five confining pressures are tested at each deviatoric stress. The confining pressure ranges from 3 to 20 psi. The fourth and fifth column are the number of load repetitions to apply at each loading step and whether data is collected or not, respectively.

The UTEP method was developed to minimize the disturbance to samples during staged testing as observed with the SHRP procedure. The stress levels are much lower than both the AASHTO and SHRP. The advantages of this testing procedure over others are discussed in Chapter 6.

### **4.4.2 Cohesive Soils**

#### **4.4.2.1 AASHTO Procedure**

As for granular soils, the AASHTO procedure testing is quite time consuming. Table 4.5 illustrates the loading sequence for cohesive soils proposed by AASHTO. The sample is initially conditioned by applying five different loading sequences. The zero in the first column of Table 4.5, signifies this fact. The actual testing procedure will proceed with 15 loading sequences. The resilient modulus is calculated at the 200th cycle. Three confining pressures are used with each confining pressure being tested at five deviatoric stresses that range from 1 to 10 psi.

#### **4.4.2.2 SHRP Procedure**

The testing does not take as much as time the AASHTO procedure. The loading steps for the SHRP procedure are shown in Table 4.6. The first row of the Table 4.6 is the conditioning step. The conditioning test is applied for 200 cycles. The rest of the test consists of a 15 loading step sequence.

Table 4.4 Loading Sequence Proposed by UTEP for Type 1 Soils

| Loading Sequence | Deviatoric Stress,<br>psi | Confining<br>Pressure, psi | Number of<br>Repetitions | Deformation<br>Record(Y or N) |
|------------------|---------------------------|----------------------------|--------------------------|-------------------------------|
| 0                | 5                         | 15                         | 200                      | N                             |
| 1                | 3                         | 3                          | 100                      | Y                             |
| 2                | 3                         | 6                          | 100                      | Y                             |
| 3                | 3                         | 10                         | 100                      | Y                             |
| 4                | 3                         | 15                         | 100                      | Y                             |
| 5                | 3                         | 20                         | 100                      | Y                             |
| 6                | 6                         | 3                          | 100                      | Y                             |
| 7                | 6                         | 6                          | 100                      | Y                             |
| 8                | 6                         | 10                         | 100                      | Y                             |
| 9                | 6                         | 15                         | 100                      | Y                             |
| 10               | 6                         | 20                         | 100                      | Y                             |
| 11               | 9                         | 3                          | 100                      | Y                             |
| 12               | 9                         | 6                          | 100                      | Y                             |
| 13               | 9                         | 10                         | 100                      | Y                             |
| 14               | 9                         | 15                         | 100                      | Y                             |
| 15               | 9                         | 20                         | 100                      | Y                             |

Table 4.5 Loading Sequence Proposed by AASHTO for Cohesive Soils

| Loading Sequence | Deviatoric Stress, psi | Confining Pressure, psi | Number of Repetitions | Deformation Record(Y or N) |
|------------------|------------------------|-------------------------|-----------------------|----------------------------|
| 0                | 1                      | 6                       | 200                   | N                          |
| 0                | 2                      | 6                       | 200                   | N                          |
| 0                | 4                      | 6                       | 200                   | N                          |
| 0                | 8                      | 6                       | 200                   | N                          |
| 0                | 10                     | 6                       | 200                   | N                          |
| 1                | 1                      | 6                       | 200                   | Y                          |
| 2                | 2                      | 6                       | 200                   | Y                          |
| 3                | 4                      | 6                       | 200                   | Y                          |
| 4                | 8                      | 6                       | 200                   | Y                          |
| 5                | 10                     | 6                       | 200                   | Y                          |
| 6                | 1                      | 3                       | 200                   | Y                          |
| 7                | 2                      | 3                       | 200                   | Y                          |
| 8                | 4                      | 3                       | 200                   | Y                          |
| 9                | 8                      | 3                       | 200                   | Y                          |
| 10               | 10                     | 3                       | 200                   | Y                          |
| 11               | 1                      | 0                       | 200                   | Y                          |
| 12               | 2                      | 0                       | 200                   | Y                          |
| 13               | 4                      | 0                       | 200                   | Y                          |
| 14               | 8                      | 0                       | 200                   | Y                          |
| 15               | 10                     | 0                       | 200                   | Y                          |

Table 4.6 Loading Sequence Proposed by SHRP for Type 2 Soils

| Loading Sequence | Deviatoric Stress, psi | Confining Pressure, psi | Number of Repetitions | Deformation Record(Y or N) |
|------------------|------------------------|-------------------------|-----------------------|----------------------------|
| 0                | 4                      | 6                       | 200                   | N                          |
| 1                | 2                      | 6                       | 100                   | Y                          |
| 2                | 4                      | 6                       | 100                   | Y                          |
| 3                | 6                      | 6                       | 100                   | Y                          |
| 4                | 8                      | 6                       | 100                   | Y                          |
| 5                | 10                     | 6                       | 100                   | Y                          |
| 6                | 2                      | 4                       | 100                   | Y                          |
| 7                | 4                      | 4                       | 100                   | Y                          |
| 8                | 6                      | 4                       | 100                   | Y                          |
| 9                | 8                      | 4                       | 100                   | Y                          |
| 10               | 10                     | 4                       | 100                   | Y                          |
| 11               | 2                      | 2                       | 100                   | Y                          |
| 12               | 4                      | 2                       | 100                   | Y                          |
| 13               | 6                      | 2                       | 100                   | Y                          |
| 14               | 8                      | 2                       | 100                   | Y                          |
| 15               | 10                     | 2                       | 100                   | Y                          |

Three levels of confining pressure are used. For each confining pressure, the deviatoric stress is varied between 2 and 10 psi. Each one of the 15 loading steps is applied for 100 cycles. The resilient modulus is calculated for the last cycle.

The SHRP procedure is simpler to use than the AASHTO procedure. The guidelines are relatively easy to follow. In our experience, the entire duration of one test, including set-up time, is approximately two hours.

#### **4.5 Testing Procedure For One Loading Step**

A detailed explanation of the equipment used at UTEP for resilient modulus testing was included in Chapter 3. In the present section, a detailed description of the steps required for conducting tests at one confining pressure and one deviatoric stress is discussed.

The equipment is first switched to a displacement-controlled mode. The desired confining pressure is applied to the sample. To ensure proper application of the confining pressure, a slight separation between the two parts of the upper load platen is maintained (see Chapter 3, Figure 3.4). As soon as the confining pressure reaches equilibrium, the two parts are closed, and the device is switched to the load-controlled mode. One of the saturation lines connected to the upper part of the top platen is opened to check for any possible leak. If no leak is detected, a small vacuum is applied to ensure intimate and rigid connection between the two parts. Otherwise, the equipment is switched back to the displacement-controlled mode, the upper section of the top platen is lowered slightly, and checked for leaks again. In all these steps, the voltage output of the load cell is monitored to ensure that no axial load is applied on the sample.

In the next step, the amplitude of the input half-sine axial load is adjusted so that the desired deviatoric stress could be applied to the specimen. The deviatoric stress is applied to the sample. Simultaneously, a stop watch is activated so that the number of cycles of load can be determined. As the repeat frequency of the loading is equal to 1 Hz, the number of cycles is the time in seconds.

Four cycles (four seconds) before the desired number of cycles, the analyzer is triggered and eight seconds (eight cycles) of data are collected. After the data has been collected, the input voltage, corresponding to the amplitude of the axial load is reduced to zero. The collected data is saved for future data reduction.

If the next loading stage involved only a change in the deviatoric stress, the amplitude of the input half-sine is simply changed and the testing is repeated.

For the case where the confining pressure has to be changed, the process is slightly more involved. The vacuum holding the two parts of the upper platen is released. The machine is switched to the displacement-controlled mode. Upon releasing the confining pressure, the two parts are separated. At this time, the new confining pressure is applied and the test is continued repeating the entire process described in this section.

## 4.6 Post Testing Steps

After all the loading sequences are completed, the sample is removed from the equipment. The sample is divided into three pieces. Each piece is weighed and placed in the oven for 24 hours so that the water content can be measured. In the event that the hydrostone mix is used, the two ends contaminated with the mix are first removed.

## 4.7 Reduction of Data

Once the resilient modulus test is complete, the data collected is reduced. Since large amounts of data are collected for each test, a computer program has been developed to automatically calculate the resilient modulus. The program is called **MRREDUCE**.

**MRREDUCE** is a user friendly program. The program has the options to plot the data on the screen for viewing. It also creates an output file for each loading step. Each output file contains the name of the file, the length and diameter of the sample, and information on the loading sequence. The stress, strain and resilient modulus for eight consecutive cycles are determined and reported in a comprehensive manner. A summary file containing the loading sequence, the average resilient modulus, and the scatter associated with the modulus is generated. Finally, an appropriate constitutive model for each specimen is determined and reported.

Appendix A contains a detail user's manual on the use of the **MRREDUCE** program.

# Chapter 5

## Synthetic Specimens

### 5.1 Introduction

Three synthetic specimens were tested before testing actual soil specimens, to evaluate the performance of the device. These samples were constructed and tested at The University of Texas at Austin (UT-Austin) before delivery to The University of Texas at El Paso (UTEP). This chapter discusses the properties of the synthetic specimens and results obtained from tests on these samples.

### 5.2 Properties of Synthetic Samples

The synthetic samples were composed of a two-component urethane elastomer resin. The two components were manufactured by Conap, Inc. of Olean, New York (Stokoe et al, 1990). The three samples were named TU-700, TU-900 and TU-960. All samples had one common component: dicyclohexylmethane -4,4' -diisocyanate. The other component for TU-700 and TU-900 was diethyltoluene diamine while for TU-960 it was 4,4' -methylenedianiline. According to Stokoe et al (1990) the hardness of the samples is controlled by the molecular structure of the prepolymer. It was therefore relatively easy to develop a sample of desired stiffness.

Procedures followed in preparing the samples are briefly discussed below. Details of the process can be found in Stokoe et al (1990). The two components were mixed together and poured into a cylindrical mold. This was done under a vacuum to remove entrapped air. Mixing and pouring was completed within 20 minutes. The mixture was allowed to cure for seven days. The specimens were then machined to the final dimensions.

Stokoe et al (1990) extensively tested similar samples using the static compression test and

torsional resonant column test. Young's moduli obtained from the static compression tests for soft (TU-700), medium (TU-900) and hard (TU-960) samples were 1670, 6550 and 32300 psi, respectively. The Poisson's ratio was determined to be 0.48, 0.50 and 0.47 for the soft, medium and hard, respectively.

Moduli obtained from the resonant column tests were also reported. Young's moduli for the soft, medium and hard samples were 2430, 10070 and 52000 psi, respectively. They attributed the difference in the numbers to the loading frequency. In other words, the elastomer samples exhibited viscoelastic behavior.

Figure 5.1 shows a typical graph of the results from the resonant column tests on three samples similar to those used in this study. For all three samples, the modulus values are constant over a wide range of strain levels. Therefore, the materials behave linearly over a wide range of strains. Also, superimposed on the figure is the approximate range of strains covered by the AASHTO testing procedure. As seen in the graph, for a given confining pressure, the resilient modulus values are mostly measured in the linear range.

The frequency dependency of the moduli of these samples was studied by combining the results from cyclic torsional and resonant column tests. The variation in modulus with frequency for the three samples are shown in Figure 5.2. For each sample, the modulus value is minimum for static compression tests and maximum for the resonant column tests.

It should be mentioned that both the cyclic torsional shear and resonant column tests can accurately measure shear modulus and shear strain. To obtain Young's modulus and axial strain, the following equations were utilized:

$$E = 2G(1 + \nu) \quad (5.1)$$

$$\epsilon_a = \gamma / (1 + \nu) \quad (5.2)$$

where:

E = Young's modulus

G = Shear modulus

$\nu$  = Poisson's ratio

$\epsilon_a$  = axial strain

$\gamma$  = shear strain.

In both equations, Poisson's ratio has to be estimated or measured.

At each loading frequency, tests were carried out at several strain levels. It was found that over the range of strains tested, the moduli is independent of strain.

Furthermore, for each sample, Stokoe et al normalized the moduli at a particular strain level and at different frequencies with the corresponding modulus measured at a frequency of 0.01 Hz. The normalized results are shown in Figure 5.3. The normalized moduli can be reasonably described by one curve, independent of the stiffness of the sample. Therefore, the necessary corrections for the frequency dependency of the properties can be easily achieved.

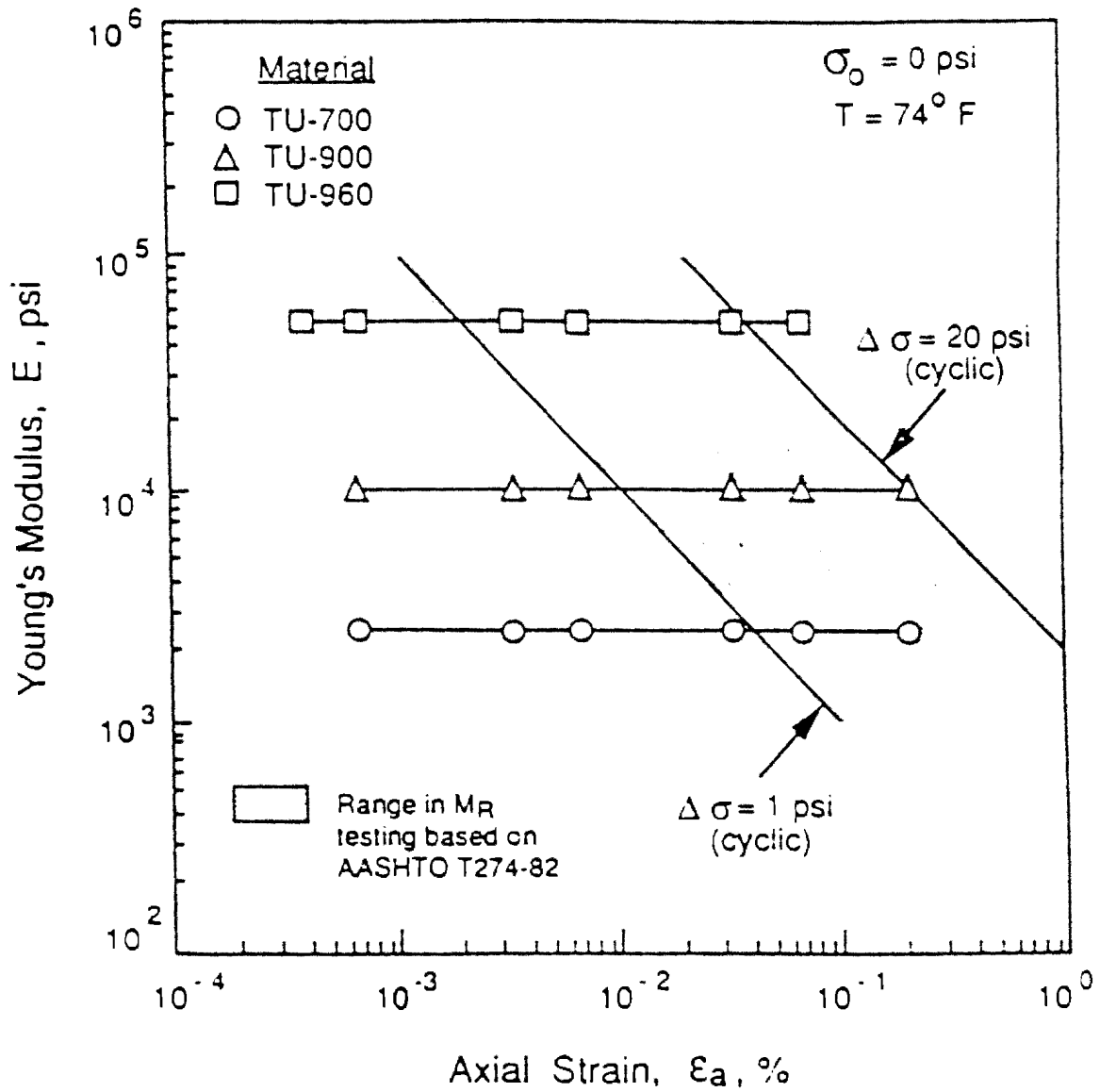


Figure 5.1 - Comparison of Axial Strains Generated in MR Testing with those Generated in Calibrating the Synthetics Specimens (from Stokoe et al, 1990).

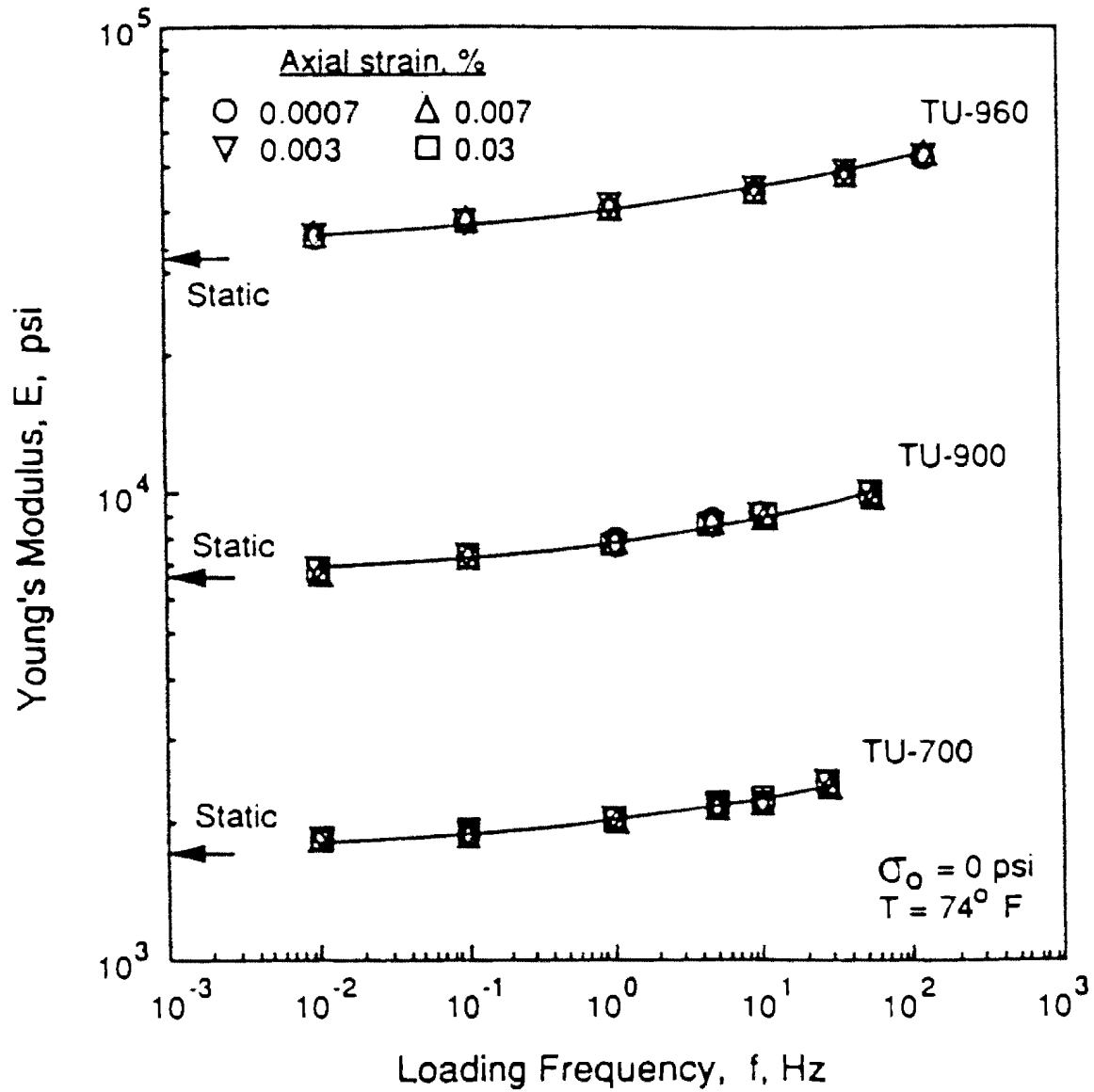


Figure 5.2 - Variation in Young's Modulus with Axial Strain Amplitude and Loading Frequency as Determined by Cyclic Torsional and Resonant Column Tests at Zero Confining Pressure (from Stokoe et al, 1990).

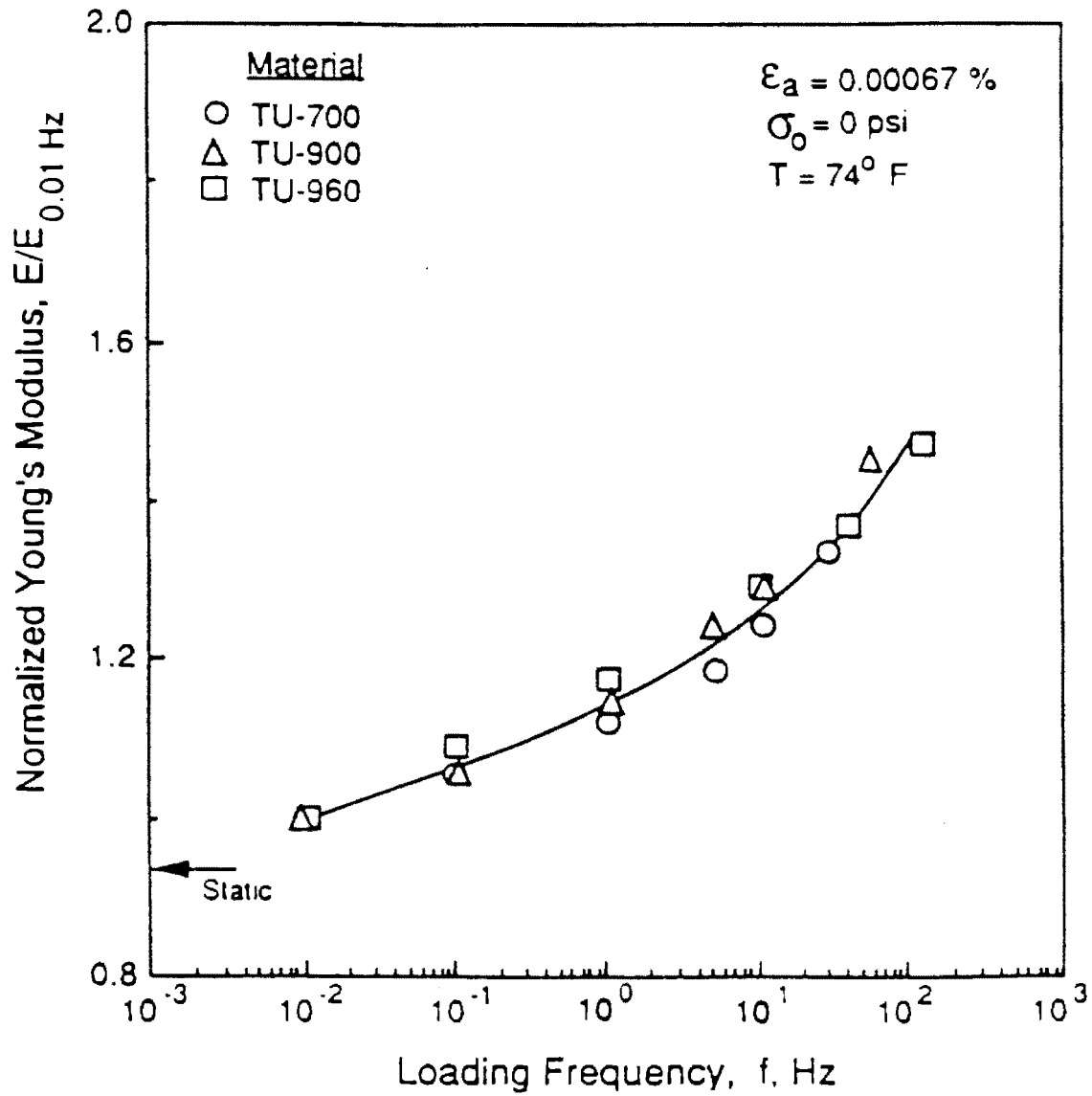


Figure 5.3 - Variation in Normalized Young's Modulus with Loading Frequency as Determined by Cyclic Torsional Tests (from Stokoe et al, 1990).

The temperature dependency of stiffness for the samples were also addressed by Stokoe et al. Shown in Figure 5.4 is the variation in modulus with frequency for three temperatures. The change in modulus is roughly equal to 1 percent per degree (F). The effect of temperature is more prominent at higher frequencies.

In summary, Stokoe et al (1990) demonstrated that the elastomer samples were excellent tools for evaluating a resilient modulus device. However, three correction factors have to be applied to each specimen before the accurate resilient modulus of a given elastomer sample can be found. These three corrections compensate for: 1) loading frequency, 2) testing temperature, and 3) mode of testing (torsional vs axial). Even though the shear modulus of the elastomer samples are measured with an accuracy of 3 percent (Stokoe, et al, 1990), it is felt that the resilient modulus of the samples are known with an accuracy of about 5 percent. This matter is presently under theoretical investigation.

### **5.3 Testing Matrix**

As mentioned before, three elastomer samples were utilized to evaluate UTEP's resilient modulus device. The three samples were designated as soft (TU-700), medium (TU-900) and hard (TU-960). All three samples were approximately 2.8-in. in diameter and 6.5 in. in height.

An extensive amount of data was collected for each sample. Basically, each sample was tested following the procedures proposed by SHRP and AASHTO. The loading sequences proposed for the granular (or Type 1) and cohesive (or Type 2) materials were both utilized. In addition, the UTEP procedure was evaluated. Tests were carried out securing the sample on the platens with and without the hydrostone mix.

The reasons for such an extensive testing program are several. First, any inconsistency associated with the loading sequences could be found. Second, the sample is subjected to numerous combinations of confining pressures and deviatoric stresses. Most tests were repeated at least three times. Although not shown here, in all cases the results were quite repeatable and demonstrated small deviations. It should be mentioned that all tests were carried out at a temperature of about 70°F.

### **5.4 Presentation of Results**

Typical results from resilient modulus tests on the medium (TU-900) sample are discussed here. The results from the other two samples are included in Appendix B. The elastomer material should more or less behave like a cohesive (Type 2) material. The results from this type of testing are described first.

Shown in Figure 5.5 is the variation in modulus with deviatoric stress for the medium sample following AASHTO procedure for cohesive soils. Typically, the modulus slightly decreased with an increase in deviatoric stress. This can be partially due to the increase in the strain levels.

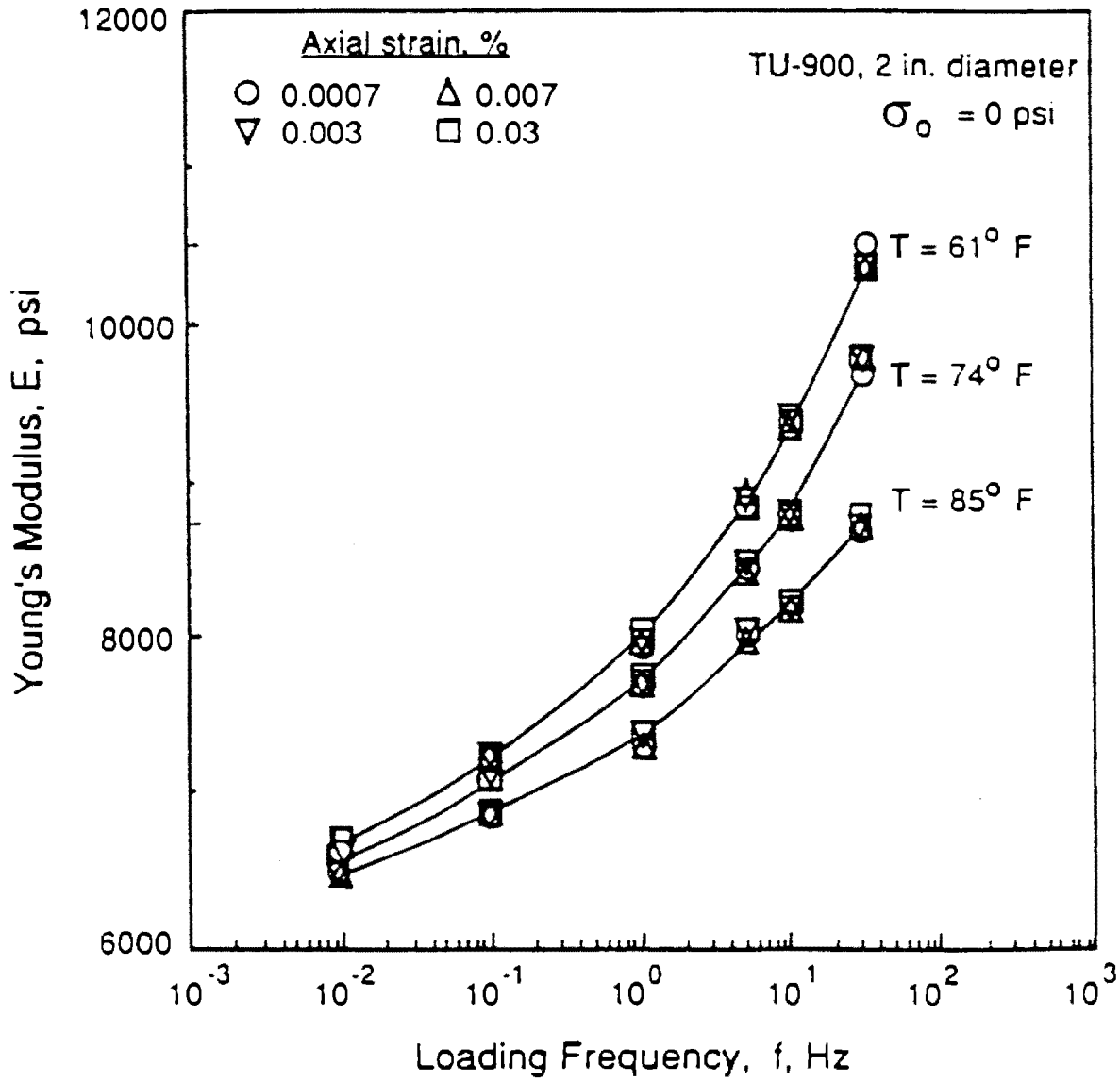


Figure 5.4 - Variation in Young's Modulus with Temperature for Specimen TU-900 Tested at Various Loading Frequencies (from Stokoe et al, 1990).

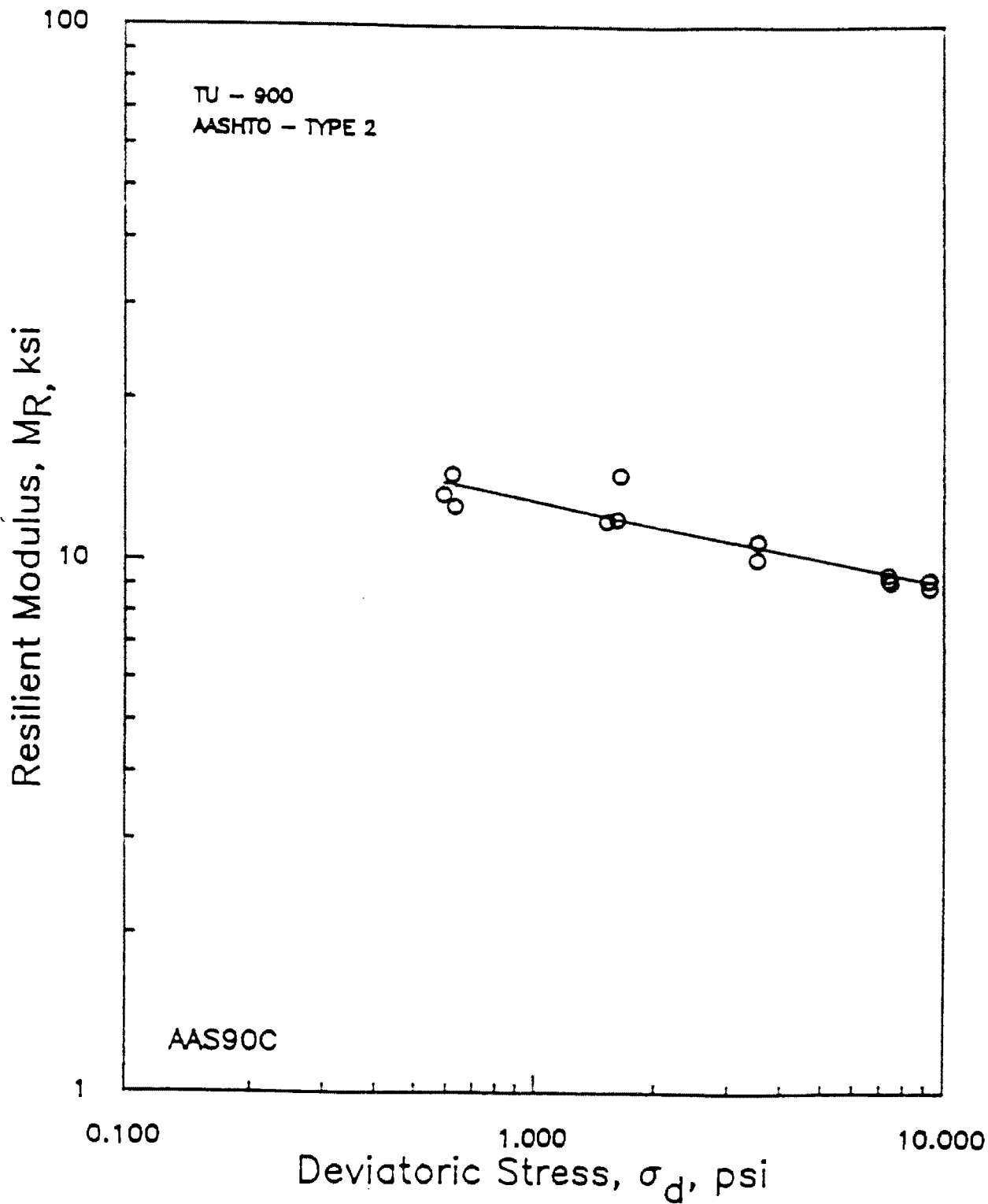


Figure 5.5 - Variation in Resilient Modulus with Deviatoric Stress for Sample TU-900 using AASHTO Cohesive Procedure and Hydrostone.

Another reason for this decrease in modulus can be the friction in the piston bearing. This was investigated and found to be negligible for 2.8 in. samples at low confining pressures (confining pressures less than 25 psi).

For each deviatoric stress level, three data points were plotted. These three data points correspond to the three levels of confining pressure proposed by AASHTO. For deviatoric stress levels above 2 psi, the modulus values were independent of confining pressure as reported by Stokoe et al (1990). Little scatter was seen in the data.

The variation in modulus with deviatoric stress following the SHRP protocol is shown in Figure 5.6. Practically speaking, the results from this series of tests were quite similar to those measured from AASHTO testing process. Therefore, all the discussions presented above for the AASHTO testing process hold for this process as well.

The AASHTO and SHRP results for the granular (Type 1) testing procedures are summarized in Figures 5.7 and 5.8, respectively. The results from the two sets are similar. Much scatter in data is evident from the AASHTO procedure due to the numerous steps involving deviatoric stress levels of less than 2 psi. If the modulus corresponding to these stress levels are ignored, the results from the SHRP and AASHTO procedures are quite compatible. For both cases, the modulus is not affected by the bulk stresses and is more or less constant.

The results from the UTEP procedure are shown in Figure 5.9. The results and trends are similar to those obtained from the AASHTO and SHRP procedures. Some scatter is evident in the data. This is because the tests were accidentally performed at deviatoric stresses of slightly less than 2 psi (instead of 3 psi).

## **5.5 Discussion of Results**

The average modulus obtained from each testing procedure is summarized in Tables 5.1 through 5.3 for the soft material (TU-700), medium material (TU-900) and the hard material (TU-960), respectively. Also included in the tables are the standard deviation and coefficient of variation associated with each procedure.

The effects of the grouting of the samples to the top and bottom platens were also studied. Tests were conducted on each sample with and without applying the hydrostone mix. The results are compared herein. The addition of the grouting agent would ensure a good contact between the sample and the platen. It should be mentioned that precision machining was required in order to obtain flat surfaces necessary for performing the tests without the grouting agent.

The resilient modulus values for three elastomer samples corrected for loading frequency, temperature and mode of vibration were determined to be 2318 psi, 9794 psi and 42083 psi, for the soft, medium and hard samples, respectively.

Average moduli from different testing procedures generally compare reasonably well with those measured using the torsional devices. The average values are summarized in Table 5.4. For the

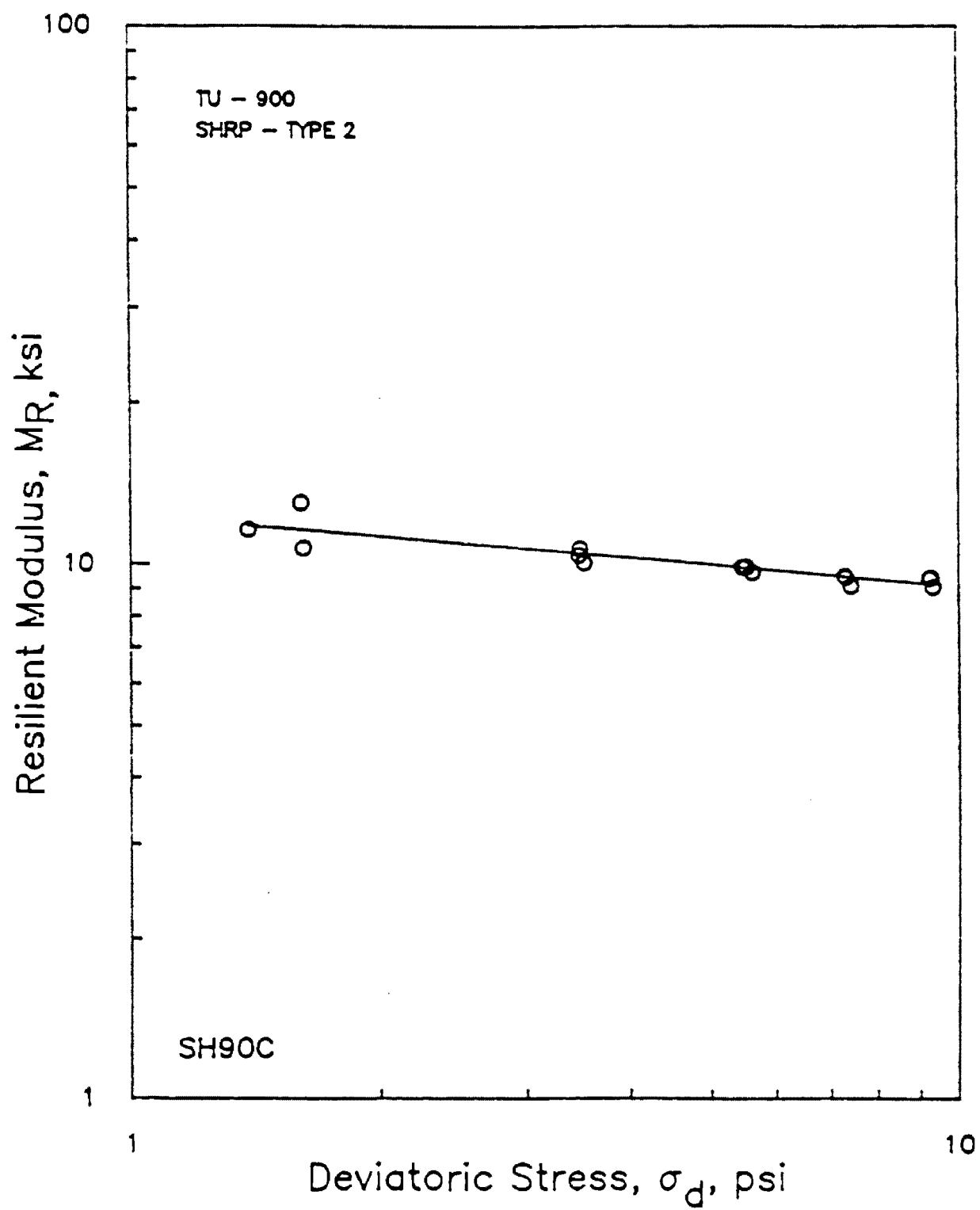


Figure 5.6 - Variation in Resilient Modulus with Deviatoric Stress for Sample TU-900 using SHRP Type 2 Procedure and Hydrostone.

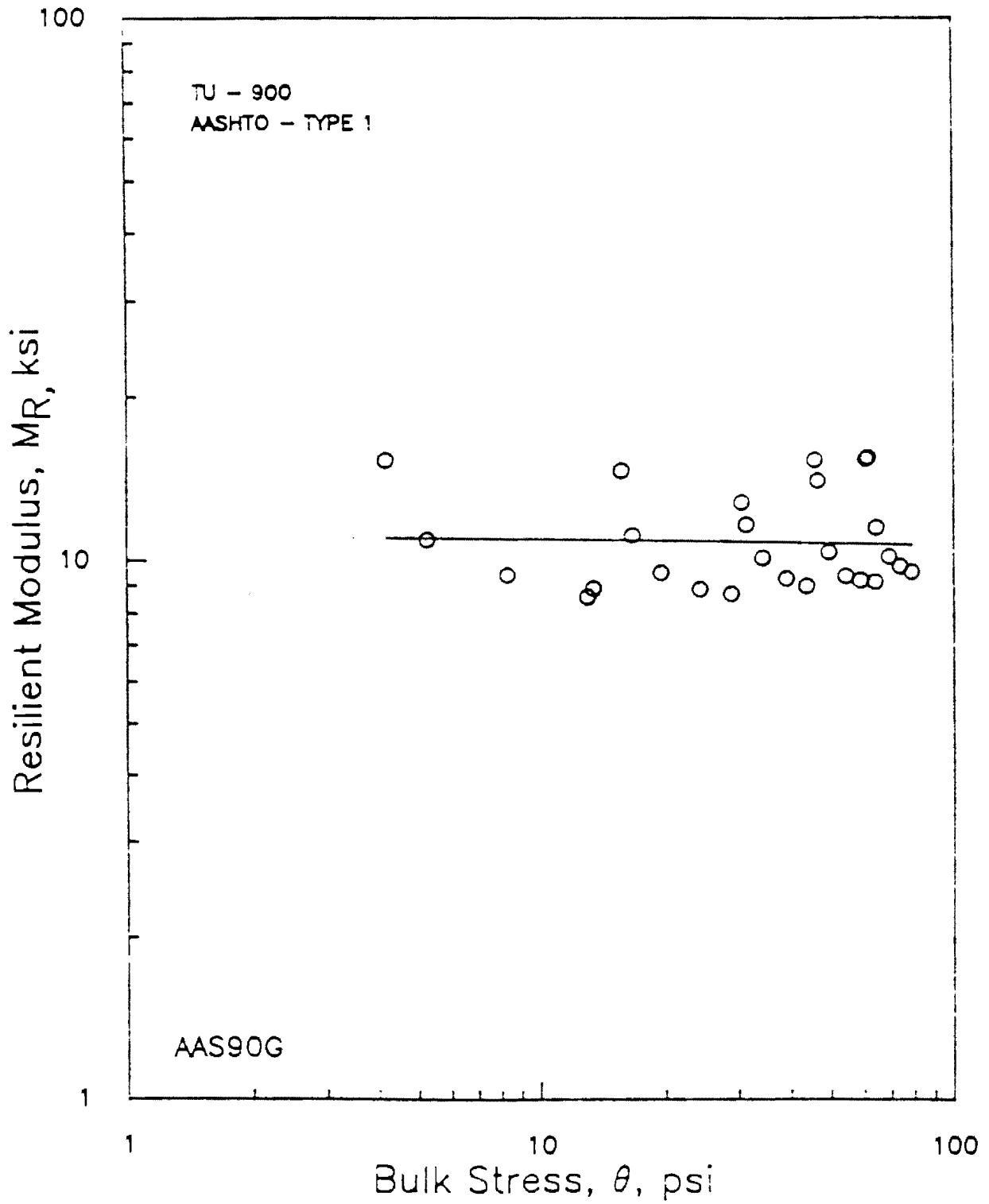


Figure 5.7 - Variation in Resilient Modulus with Bulk Stress for Sample TU-900 using AASHTO Granular Procedure and Hydrostone.

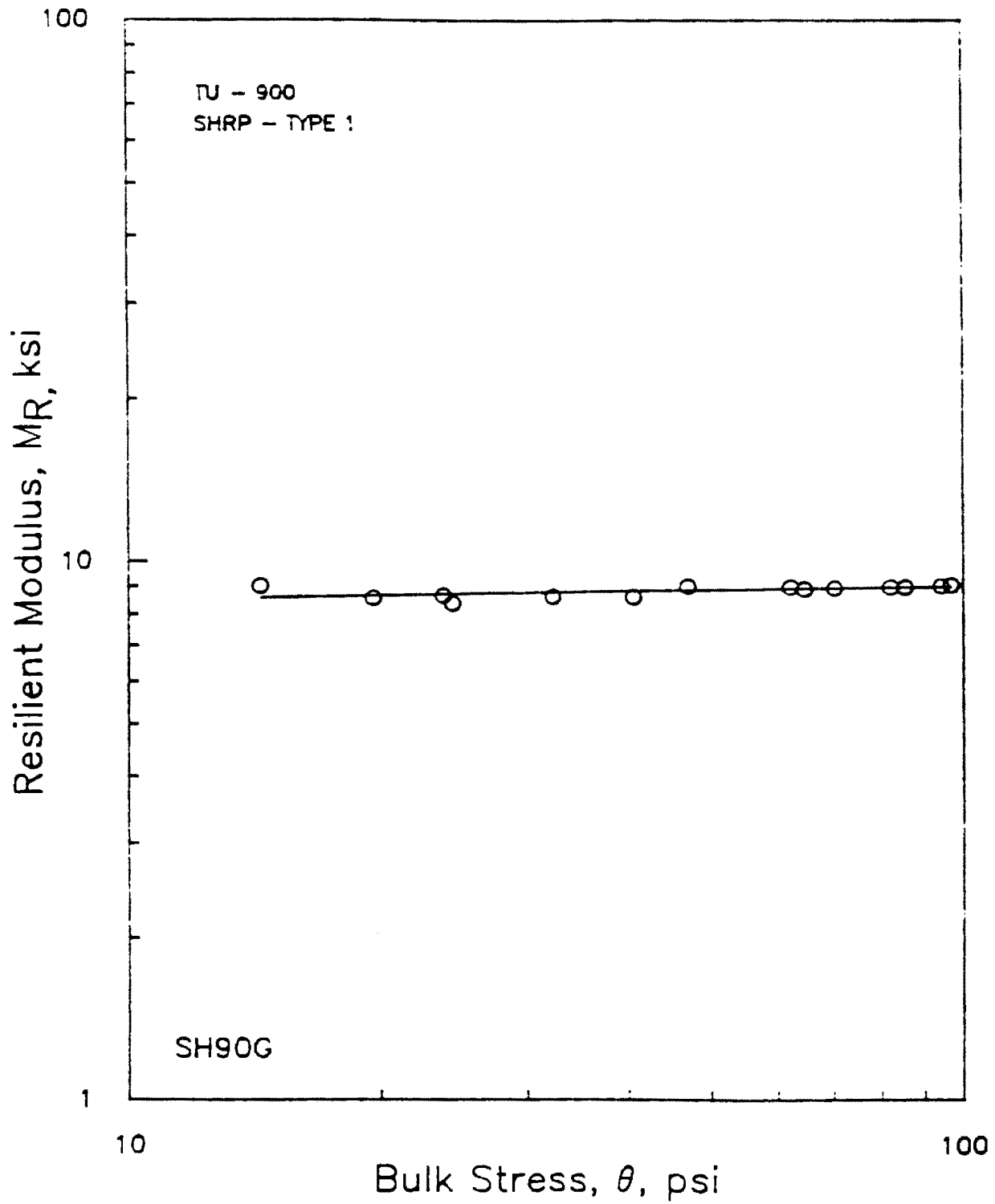


Figure 5.8 - Variation in Resilient Modulus with Bulk Stress for Sample TU-900 using SHRP Type I Procedure and Hydrostone.

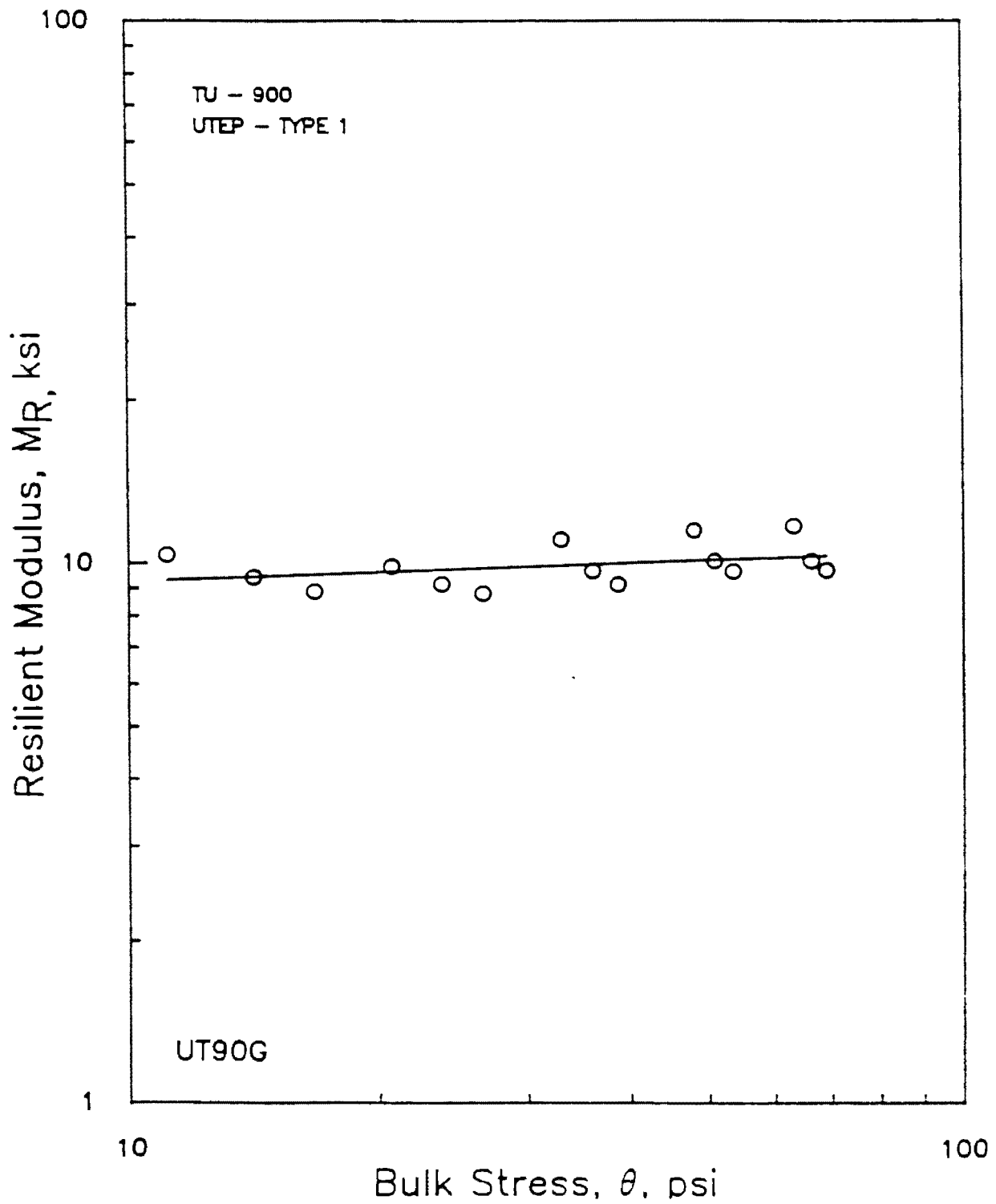


Figure 5.9 - Variation in Resilient Modulus with Bulk Stress for Sample TU-900 using UTEP Type 1 Procedure and Hydrostone.

Table 5.1 Summary of the Results for TU-700

| Testing Method                                    | Hydrostone | Modulus (psi) | Standard Deviation (psi) | Coefficient of Variation (percent) | Percent Difference* |
|---|------------|---------------|--------------------------|------------------------------------|---------------------|
| Type 1-SHRP                                       | Y          | 2420          | 160                      | 6.6                                | 4.4                 |
|   | N          | 2360          | 83                       | 3.5                                | 1.8                 |
| Type 2-SHRP                                       | Y          | 2440          | 200                      | 8.2                                | 5.3                 |
|   | N          | 2606          | 290                      | 11.1                               | 12.4                |
| Granular-AASHTO with $\sigma_d$ of 1 and 2 psi    | Y          | 2800          | 380                      | 13.6                               | 20.8                |
|   | N          | 2460          | 370                      | 15.0                               | 6.1                 |
| Granular-AASHTO without $\sigma_d$ of 1 and 2 psi | Y          | 2570          | 160                      | 6.2                                | 10.9                |
|   | N          | 2340          | 60                       | 2.6                                | 1.0                 |
| Cohesive-AASHTO with $\sigma_d$ of 1 and 2 psi    | Y          | 2580          | 400                      | 15.5                               | 11.3                |
|   | N          | 2210          | 190                      | 8.6                                | -4.7                |
| Cohesive-AASHTO without $\sigma_d$ of 1 and 2 psi | Y          | 2340          | 140                      | 6.0                                | 1.0                 |
|   | N          | 2104          | 160                      | 7.6                                | -9.2                |
| Type 1-UTEP                                       | Y          | 2390          | 190                      | 8.0                                | 3.1                 |

$$\text{Percent Difference} = \frac{\text{Modulus from this Study} - \text{Modulus from Torsional Tests}}{\text{Modulus from Torsional Tests}}$$

Table 5.2 Summary of the Results for TU-900

| Testing Method  | Hydrostone | Modulus<br>(psi) | Standard Deviation<br>(psi) | Coefficient of Variation<br>(percent) | Percent Difference<br>(percent) |
|---|------------|------------------|-----------------------------|---------------------------------------|---------------------------------|
| Type 1-SHRP   | Y          | 8850             | 256                         | 2.9                                   | -9.6                            |
|   | N          | 10140            | 610                         | 6.0                                   | 3.5                             |
| Type 2-SHRP   | Y          | 10110            | 1050                        | 10.4                                  | 12.9                            |
|   | N          | 9060             | 970                         | 10.7                                  | -7.5                            |
| Granular-AASHTO<br>with $\sigma_d$ of<br>1 and 2 psi    | Y          | 11060            | 2400                        | 21.7                                  | 12.9                            |
|   | N          | 10100            | 830                         | 8.2                                   | 3.1                             |
| Granular-AASHTO<br>without $\sigma_d$ of<br>1 and 2 psi | Y          | 9320             | 480                         | 5.2                                   | -4.8                            |
|   | N          | 10150            | 410                         | 4.0                                   | 3.6                             |
| Cohesive-AASHTO<br>with $\sigma_d$ of<br>1 and 2 psi    | Y          | 11040            | 1960                        | 17.8                                  | 12.7                            |
|   | N          | 9550             | 540                         | 5.7                                   | -2.5                            |
| Cohesive-AASHTO<br>without $\sigma_d$ of<br>1 and 2 psi | Y          | 9669             | 750                         | 7.8                                   | -1.3                            |
|   | N          | 9740             | 240                         | 2.5                                   | -0.5                            |
| Type 1-UTEP   | Y          | 9950             | 911                         | 9.2                                   | 4.5                             |

Table 5.3 Summary of the Results for TU-960

| Testing Method  | Hydrostone | Modulus<br>(psi) | Standard Deviation<br>(psi) | Coefficient of Variation<br>(percent) | Percent Difference<br>(percent) |
|---|------------|------------------|-----------------------------|---------------------------------------|---------------------------------|
| Type 1-SHRP   | Y          | 45700            | 1440                        | 3.2                                   | 4.4                             |
|   | N          | NA               | NA                          | NA                                    | NA                              |
| Type 2-SHRP   | Y          | 45600            | 1200                        | 2.6                                   | 4.2                             |
|   | N          | NA               | NA                          | NA                                    | NA                              |
| Granular-AASHTO<br>with $\sigma_d$ of<br>1 and 2 psi    | Y          | 46270            | 3700                        | 8.0                                   | 5.7                             |
|   | N          | 38660            | 4780                        | 12.4                                  | -11.7                           |
| Granular-AASHTO<br>without $\sigma_d$ of<br>1 and 2 psi | Y          | 46270            | 1050                        | 2.3                                   | 5.7                             |
|   | N          | 41260            | 3000                        | 7.3                                   | -5.7                            |
| Cohesive-AASHTO<br>with $\sigma_d$ of<br>1 and 2 psi    | Y          | 45000            | 1520                        | 3.4                                   | 2.8                             |
|   | N          | 39442            | 1270                        | 3.2                                   | -9.9                            |
| Cohesive-AASHTO<br>without $\sigma_d$ of<br>1 and 2 psi | Y          | 43970            | 840                         | 1.9                                   | .5                              |
|   | N          | 39860            | 900                         | 2.3                                   | -8.9                            |
| Type 1-UTEP   | Y          | 44580            | 1260                        | 2.8                                   | 1.9                             |

Table 5.4 Minimum and Maximum Moduli for Synthetic Samples

| Interpretion Method               | Moduli, psi |         |         |         |         |         |
|-----------------------------------|-------------|---------|---------|---------|---------|---------|
|                                   | TU-700      |         | TU-900  |         | TU-960  |         |
|                                   | Minimum     | Maximum | Minimum | Maximum | Minimum | Maximum |
| With $\sigma_d$ of 1 and 2 psi    | 2104        | 2800    | 8850    | 11060   | 38660   | 46270   |
| Without $\sigma_d$ of 1 and 2 psi | 2104        | 2606    | 8850    | 10150   | 39860   | 46270   |

soft sample, the modulus varies from a minimum of 2104 psi to a maximum of 2800 psi. As mentioned before, the UTEP device is not capable of yielding consistent results at deviatoric stresses of 1 and 2 psi. Ignoring the two AASHTO cases where the deviatoric stresses of 1 and 2 psi were considered, the lower and upper bounds would change to 2104 psi and 2606 psi, respectively. Similarly, for the medium samples, the modulus varied between 8850 psi and 10150 psi, and for the hard sample between 39860 psi and 46270 psi. In almost all cases, the deviations in modulus from those determined from the torsional tests were within a 10 percent range.

The results discussed here are important. Many possible sources of error which can be encountered in practical application of the resilient modulus tests are incorporated in the data. These factors include the friction between the piston and push-rod, inaccuracies with LVDT readings, seating of the specimen on the pedestal, and the load-induced nonlinearities. Given all these factors, the UTEP resilient modulus device is well-suited for performing tests. In the following sections, the effects of each of these factors are discussed.

## **5.6 Variability in Results**

The largest variation in the results is typically from the two AASHTO procedures when the 1 and 2 psi deviatoric stresses were considered. Ignoring results from these deviatoric stresses in determining the average moduli, the coefficients of variation were always less than 10 percent and typically less than 8 percent. The AASHTO and SHRP procedures associated with the cohesive (Type 2) soils usually yielded the largest coefficient of variation, especially for the soft and medium samples. For these procedures, the material may undergo some reduction in modulus due to the high strains applied to the samples. In other cases, it may yield a coefficient of variation of less than 6 percent.

## **5.7 Effects of Utilizing Grouting Agent**

The effects of grouting the samples were also studied. In general, the variation in results among the samples grouted and those not grouted was about 10 percent. It was notable that the variation was random in nature. That is, in some cases the grouted samples yielded higher modulus; and in other cases the ungrouted samples yielded higher modulus. It seems that with the grout in place, moduli should be equal to or greater than those of ungrouted samples. Although extremely unlikely, it is possible that the grout had not set completely before the tests were performed. This would account for some variations in the results. No other reason other than random scatter in data can be found for this matter.

One advantage of grouting is that in some instances, the scatter in data decreases as judged by the coefficient of variation. It should be emphasized that favorable results shown here for ungrouted materials was possible after the ends of the samples were precisely machined. It is important that the two ends of any specimen should be flat and parallel. Without this precision

machining, practically any modulus value could be obtained depending upon the setup of the specimen.

This page replaces an intentionally blank page in the original.

-- CTR Library Digitization Team

# Chapter 6

## Clay Specimens

### 6.1 Introduction

The second phase of the testing program consisted of characterizing and testing of clay. The clay used was obtained from El Paso County, near the Rio Grande River, in an area known as the Upper Valley. The properties of the clay are described in this chapter. Due to the extensive research that UT-Austin has conducted on characterizing clay materials, the efforts of this study have focused on characterizing granular and mixtures of clayey and granular materials. The clay was basically characterized so that it could be used in the clay-sand mixtures.

### 6.2 Index Properties

As indicated, the clay is local to El Paso. The material, which was light brown, was first sieved. Tests were only carried out on the portion passing the No. 200 sieve.

Hydrometer tests were performed on the clay. The grain size distribution from two sets of tests are shown in Figure 6.1. It can be seen that the results are repeatable. The Atterberg Limits were also determined. The liquid limit and plastic limit were 44.1 percent and 20.5 percent, respectively. Therefore, the plasticity index is 23.6 percent.

Based on the Atterberg limits, the clay is classified as A-7-6 according to the AASHTO classification system and classified as CL in the Unified Classification system.

The Proctor moisture-density test was also performed on the clay. The moisture-density relationship for the clay is shown in Figure 6.2. The maximum dry density of the clay was 107 lb/ft<sup>3</sup> at an optimum water content of 16.0 percent using standard proctor procedure.

### **6.3 Testing Matrix**

A total of 18 specimens were tested. Twelve samples were tested following the AASHTO T-274 procedure and six following the SHRP testing protocol. For each procedure, two samples were tested at the optimum water content, two samples at 2 percent wet of optimum and two samples at 2 percent dry of optimum water content. Six additional tests were carried out at optimum water contents following the AASHTO procedure to evaluate the repeatability of the results. Each sample was stored in a sealed bag for about three weeks in a moist room before testing. This was done to ensure equilibrium within the properties of the samples.

The samples tested using the AASHTO procedure were not grouted to the top and bottom platens. On the other hand, those samples tested following the SHRP protocol were grouted before testing.

### **6.4 Presentation Of Results**

Shown in Figure 6.3 is a typical variation in modulus with deviatoric stress for a clay sample at the optimum water content, tested following the AASHTO procedure. Much scatter in the data is evident. At each deviatoric stress, the modulus values are dependent on the confining pressure.

To evaluate repeatability of the results, six very similar samples were prepared and tested at the optimum water content. Variations in modulus with deviatoric stress for these samples are presented in Appendix C. Practically speaking, much scatter is evident in the data, suggesting that the results are not repeatable. The same trends were evident for samples tested dry and wet of optimum water contents.

The results from the tests following the SHRP protocol are also shown in Appendix C. The actual water content of each sample is reported in each corresponding figure. The variation in modulus with deviatoric stress, for a sample which should have been at optimum water content, is illustrated in Figure 6.4. It can be seen that there is little scatter in the data. Some effects of the confining pressure at each deviatoric stress can be seen. The results from a second set of tests on a similar sample are shown in Figure 6.5. The results are repeatable. Typical results from specimens two percent wet and two percent dry of optimum are presented in Figures 6.6 and 6.7, respectively.

In general, repeatable results were obtained from the SHRP procedure. The constitutive model associated with the clay is discussed in Chapter 9.

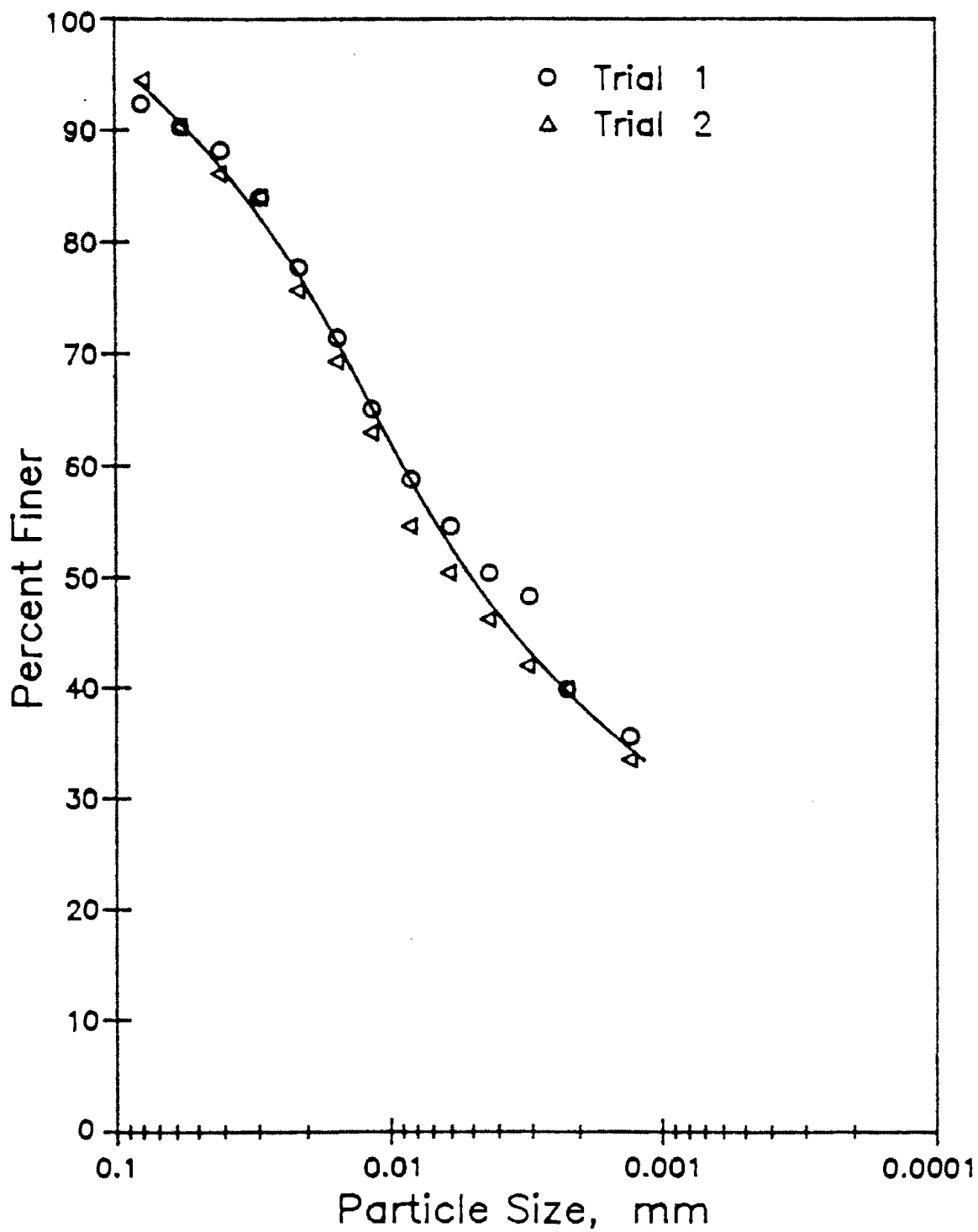


Figure 6.1 Grain Size Distribution for Clay Soil.

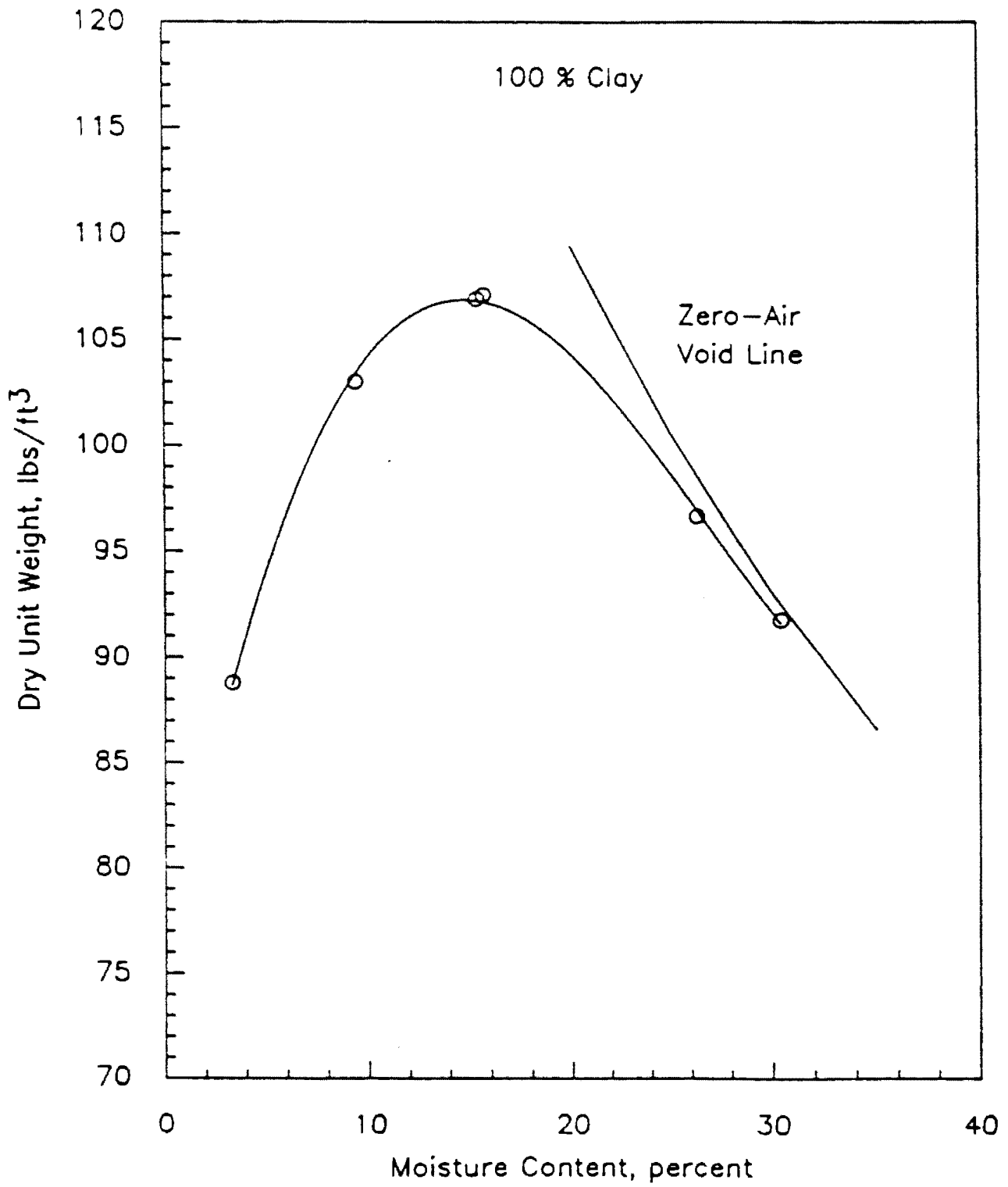


Figure 6.2 - Variation of Dry Unit Weight with Moisture Content for Pure Clay.

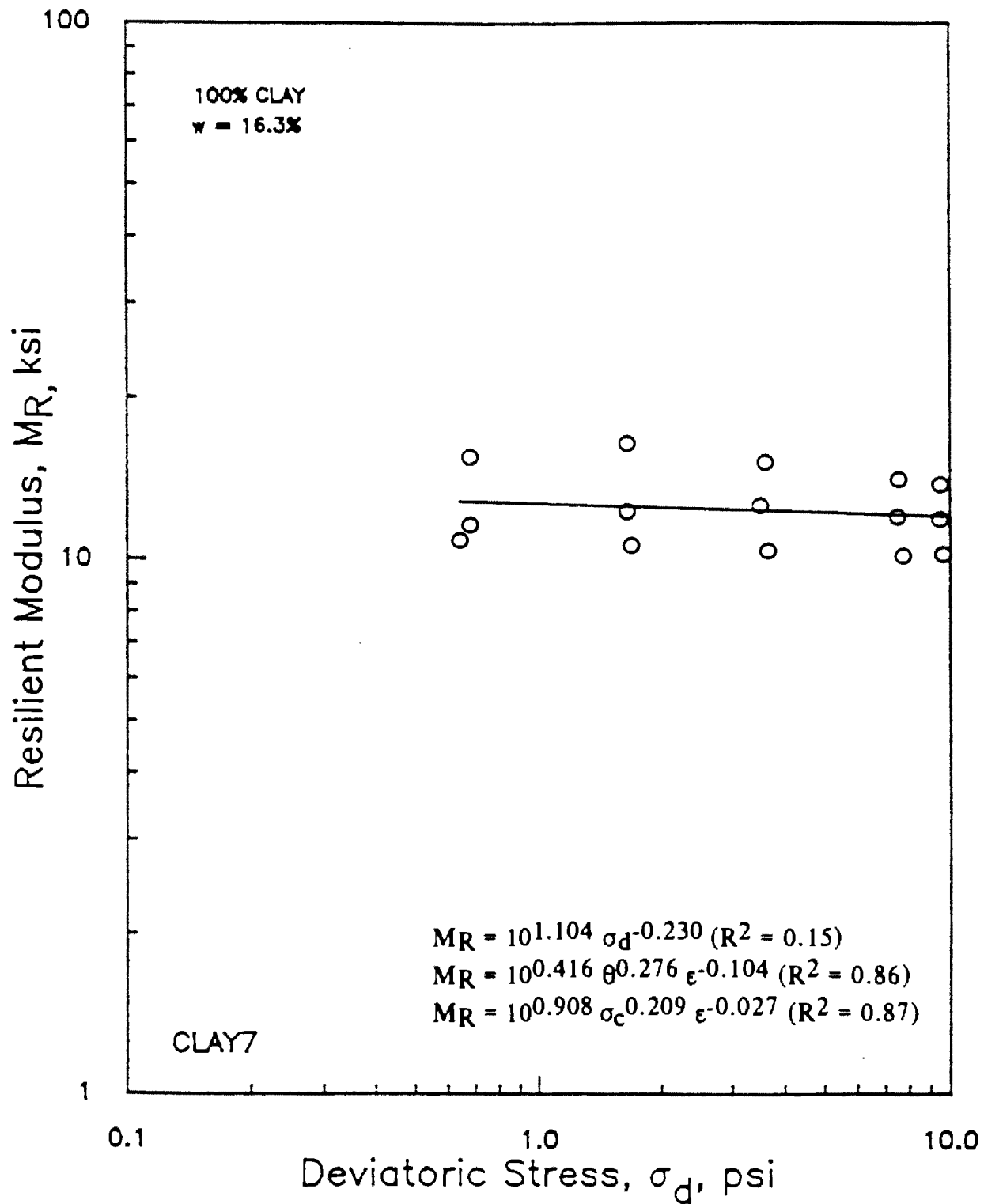


Figure 6.3 - Variation in Resilient Modulus with Deviatoric Stress for a Clay Sample at Optimum Water Content Following AASHTO Procedure.

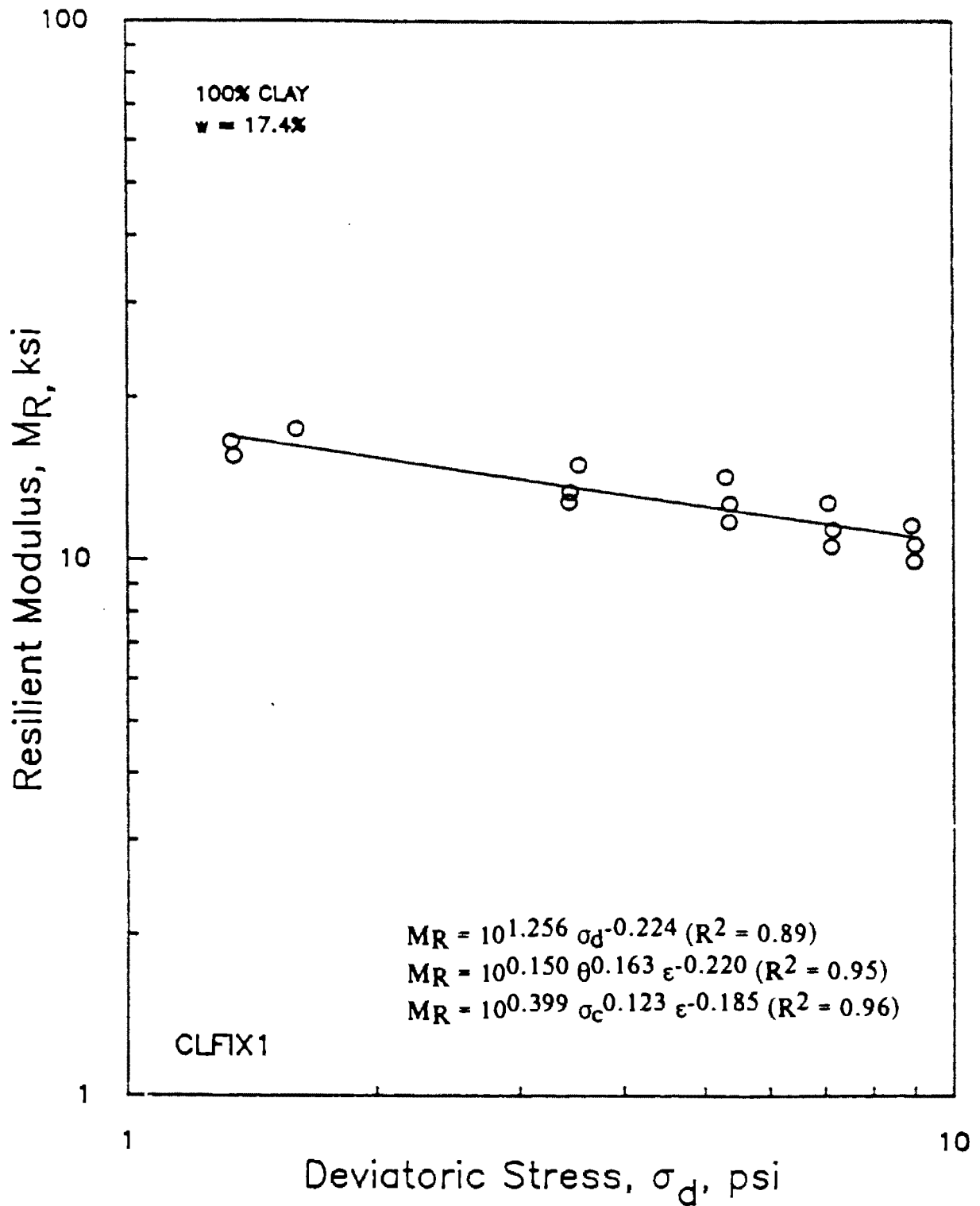


Figure 6.4 - Variation in Resilient Modulus with Deviatoric Stress for a Clay Sample at 17.4 percent Water Content Following SHRP Procedure.

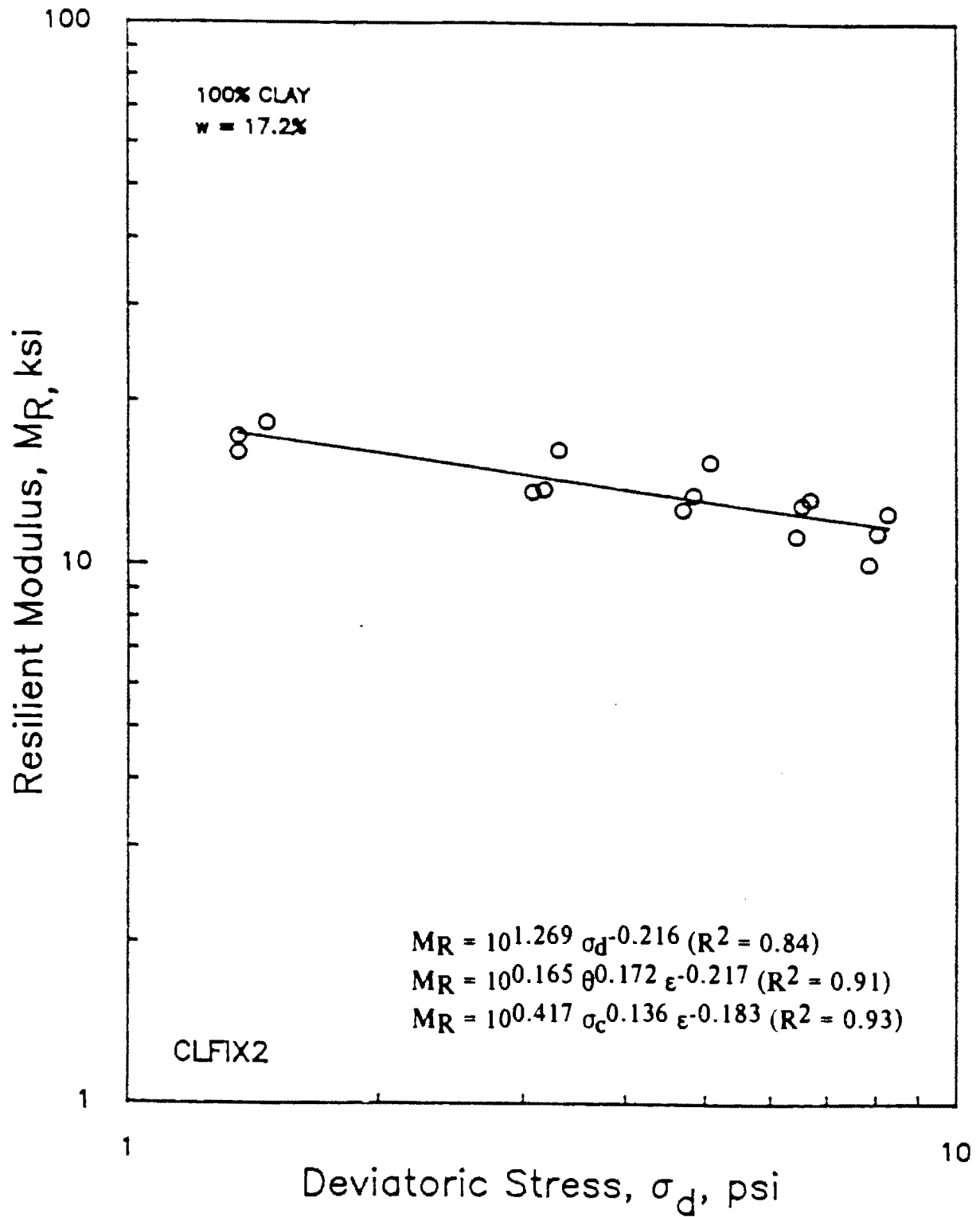


Figure 6.5 - Variation in Resilient Modulus with Deviatoric Stress for a Clay Sample at 17.2 percent Water Content Following SHRP Procedure.

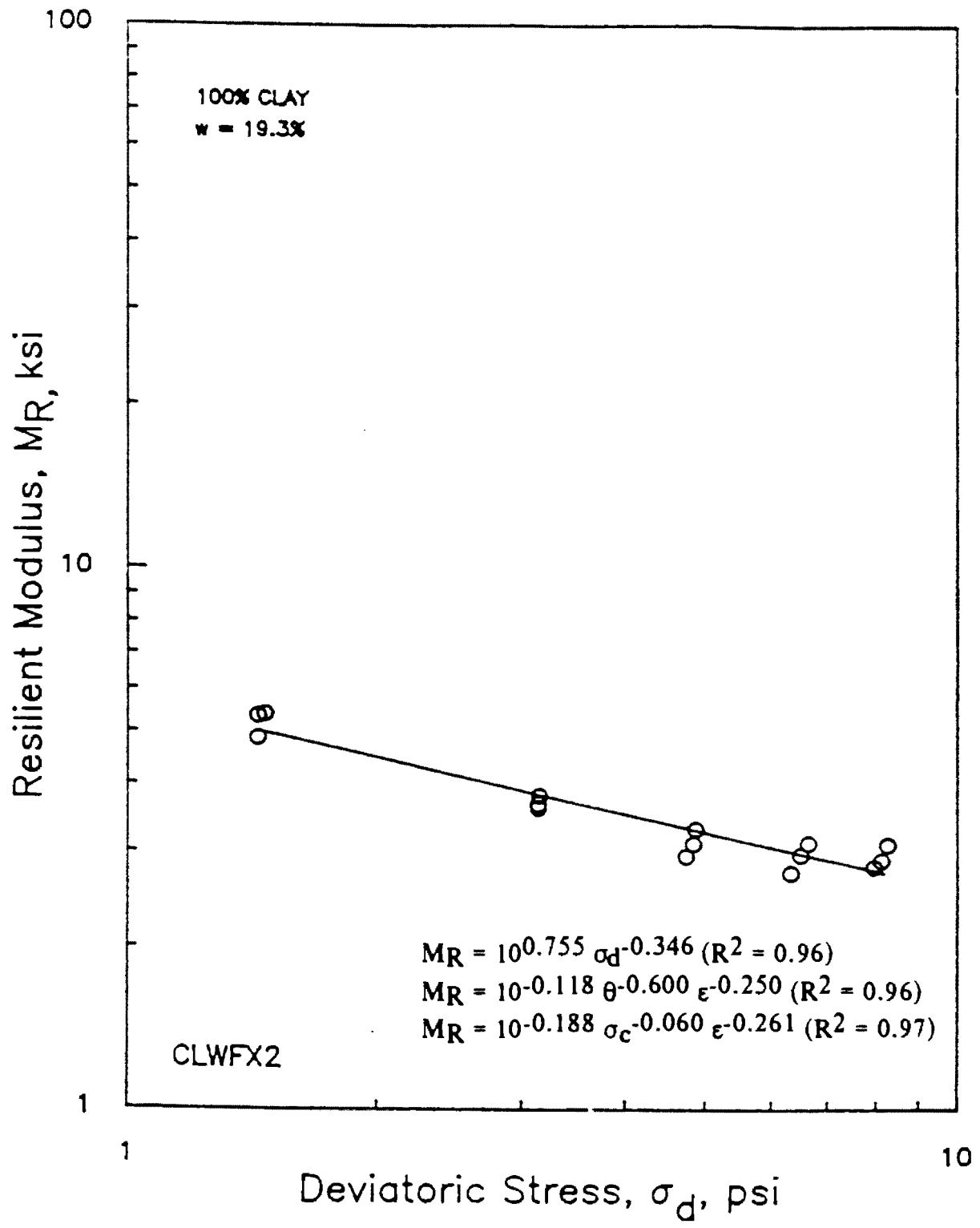


Figure 6.6 - Variation in Resilient Modulus with Deviatoric Stress for a Clay Sample at 19.3 percent Water Content Following SHRP Procedure.

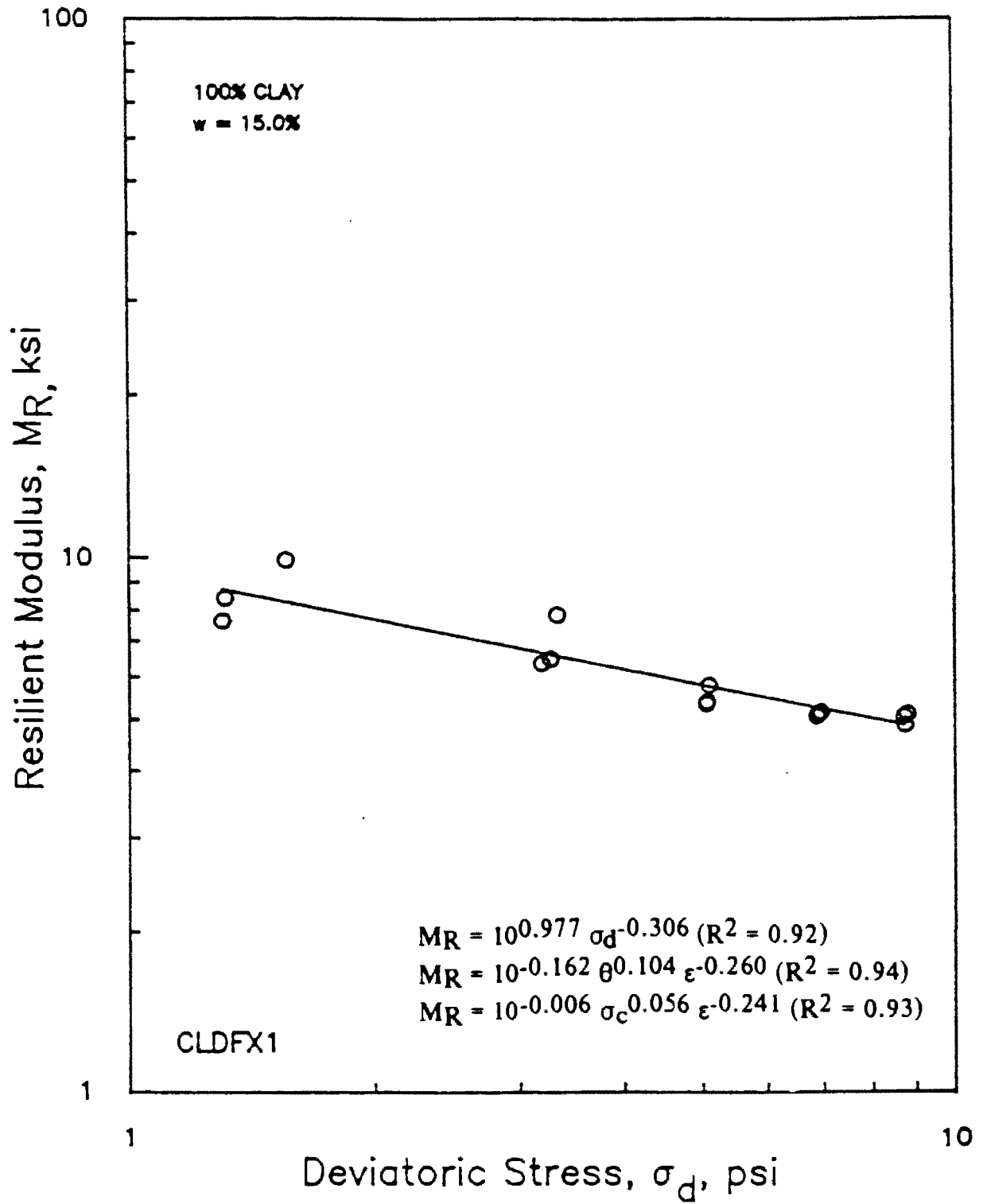


Figure 6.7 - Variation in Resilient Modulus with Deviatoric Stress for a Clay Sample at 15.0 percent Water Content Following SHRP Procedure.

This page replaces an intentionally blank page in the original.

-- CTR Library Digitization Team

# Chapter 7

## Sand Specimens

### 7.1 Introduction

The third phase of the testing program consisted of characterizing and testing a sand commonly found in El Paso. The properties of the sand, and the development of the UTEP method are described in this chapter.

### 7.2 Index Properties

The sand was first sieved. Only the fraction passing #40 sieve and retained on #60 sieve was utilized. This sand was extensively used by De Lara (1989). Its static properties are discussed there.

The maximum density is determined following ASTM D-4253 procedure. According to this procedure, soil is poured in the mold using a scoop or pouring funnel. Care is taken to minimize segregation during the pouring process. The soil surface is leveled and the mold is struck a few times so that the surcharge base plate has good contact with the soil surface. Next, the mold is attached to the vibrating table. The guide sleeve is attached to the mold and the surcharge weight is lowered on to the surcharge base plate. The whole assembly is vibrated, to get double amplitude of about 0.0130.002 in. at 60 Hz. The system is vibrated for 8 minutes. After 8 minutes, the surcharge weight, surcharge plate and guide sleeve are detached from the mold. The maximum dry density is calculated by dividing the mass of dry density by its densified volume.

However, the designated method for determining the maximum density using electromagnetic vibratory table had to be modified. The rheostat dial which controlled the amplitude of vibration

was not calibrated and the specified double amplitude of 1.013-0.002 in. for a 60 Hz vibrating table could not be measured. The determination of the maximum density was conducted in the following manner.

Approximately 25 lbs of dry sand were taken and poured into the cylindrical mold. The surcharge plate, surcharge weight and guide sleeve with the mold were assembled and bolted to the vibrating table in similar fashion as mentioned in standard ASTM procedure. The dial setting to get double amplitude was marked from 0 to 100. As a first step, the dial was set at 5. The table was then vibrated for 8 minutes. After 8 minutes, the surcharge (plate and weight) and guide sleeve were removed and necessary measurements were accounted. Similarly, the complete process was repeated for dial settings 5 through 90.

The density curve for the sand is shown in Figure 7.1. The minimum and maximum densities for the sand were 106.86 lbs/ft<sup>3</sup> and 93.2 lbs/ft<sup>3</sup>, respectively. Based on the gradation, the sand was classified as A-3 by AASHTO soil classification and as SP in the Unified Classification System.

The minimum dry density is determined following the ASTM D-4254 procedure. According to this procedure, soil is placed in the mold in its loosest form. This form of soil structure of the specimen is achieved by using the specially designed pouring device (or funnel) fitted with a spout. The pouring device is held upright and vertical. The soil is poured through the spout. The height of spout is maintained at 1 in. for free fall of soil. The pouring device is moved in a spiral path from outside to center of the mold to form each layer of equal thickness. The mold is filled approximately 0.5 to 1.0 in. above the top of the mold. The excess soil is then screed off and the soil surface is leveled. During screeding, care must be taken to avoid any rearrangement and settlement of soil particles inside the mold. The minimum dry density is calculated by dividing the mass of the dry specimen by its volume.

### **7.3 Testing Matrix**

A total of 13 specimens were tested. Three samples were tested at a relative density,  $r_d$ , of 100 percent following the SHRP testing protocol. Seven samples were tested at a  $r_d$  of 100 percent following the UTEP procedure. In addition, three samples was tested at a  $r_d$  of 70 percent following the UTEP procedure.

Three samples, with relative density of 100 percent, were tested to develop and evaluate the UTEP procedure. Each sample was tested at different deviatoric stresses. This was done to analyze the effects of deviatoric stress on specimen disturbance. A more detailed explanation is provided in the following sections.

### **7.4 Presentation of Results**

A typical variation in modulus with bulk stress for a sand sample using the SHRP protocol is illustrated in Figure 7.2. The scatter in the data is relatively small. Generally, the modulus

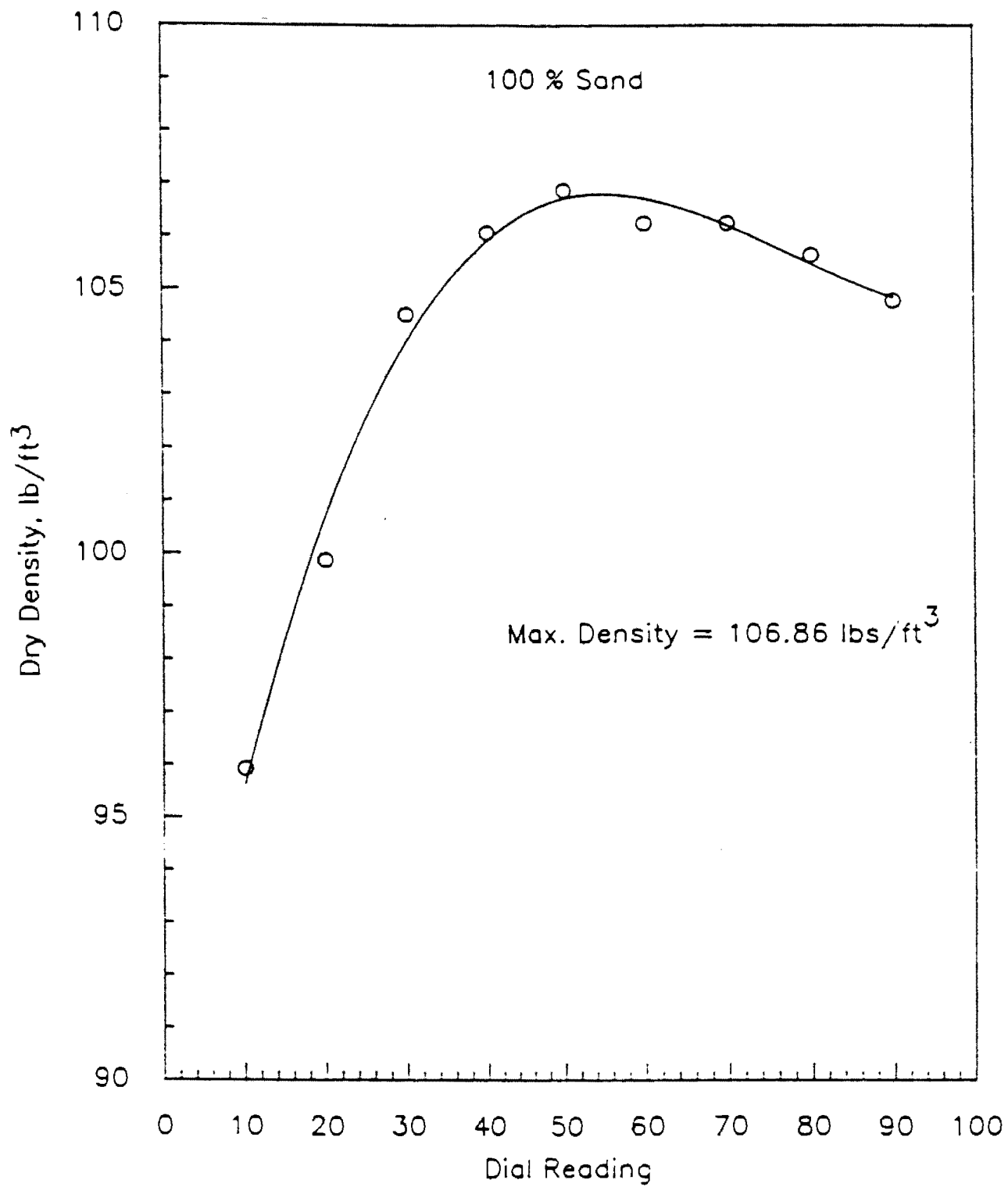


Figure 7.1 - Variation of Relative Density with Dial Reading for Sand.

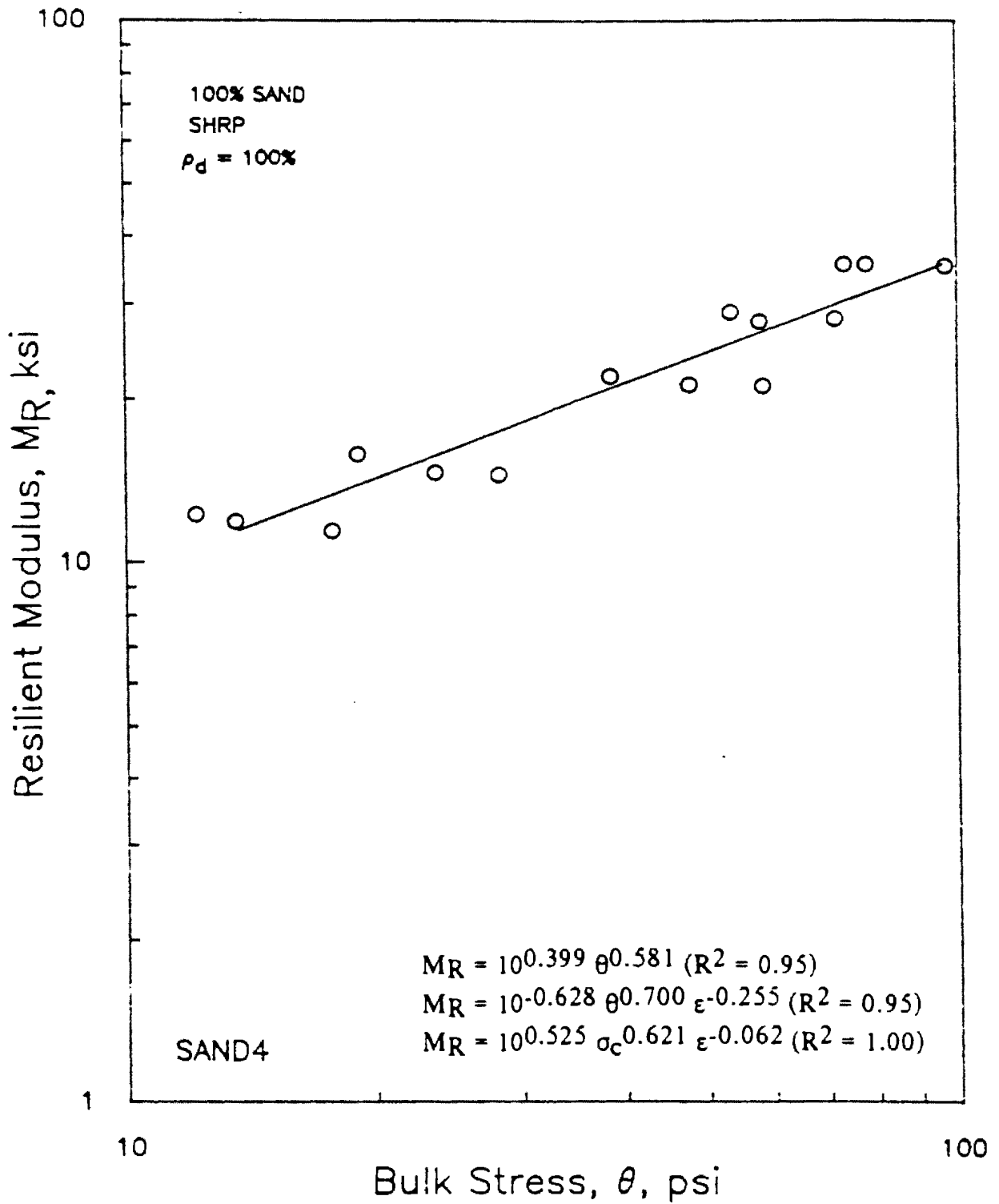


Figure 7.2 - Variation in Resilient Modulus with Bulk Stress for a Sand Sample at a Relative Density of 100 percent Following SHRP Procedure.

increases with the bulk stress. The data is clustered into five groups corresponding to the five different confining pressures.

Repeatability was checked by testing three samples. The results were the same for the first confining pressure. However, when the sample was subsequently tested at a different confining pressure, the results obtained were erratic. This indicated possible degradation of the specimen at high deviatoric stresses, suggesting that the SHRP procedure required some modifications.

The modifications were discussed in Chapter 4 and the method incorporating these modifications will be called the UTEP method for convenience. The UTEP method is a stage testing procedure. As indicated before, the properties of the material should not be altered between two consecutive states of stress. High ratios of deviatoric stress to confining pressure (as high as three), suggested by SHRP, would result in severe degradation of the sample. Sample degradation is considerably reduced in the UTEP procedure.

The variation in resilient modulus with bulk stress for a sand sample at 100 percent relative density (similar to the sample tested with the SHRP procedure) at deviatoric stresses 3, 6 and 9 psi is shown in Figure 7.3. The scatter in data is relatively small. The modulus increases linearly with bulk stress. To demonstrate that the sample degradation is minimal, two other similar samples were tested. The first sample was tested at deviatoric stresses of 6 and 9 psi (Figure 7.4) and the final sample was tested at only the deviatoric stress of 9 psi (Figure 7.5). The results from the three samples compare very closely. This degree of repeatability cannot be achieved with the SHRP procedure. For the first level of confining pressures, similar results could be achieved. However, for the subsequent confining pressures, the moduli would be substantially less and the results were not repeatable.

After repeatability of results with the UTEP procedure was established, four other samples were tested at 100 percent relative density. Variations in modulus with the bulk stress for these samples are presented in Appendix D. These results are similar to those presented in Figure 7.3. Two tests are almost identical, with moduli from the last test being slightly higher. The variations of the modulus with bulk stress for these samples are presented in Appendix D. Three tests yield almost identical results, with moduli from the last test being slightly lower. In any case, the variation in modulus is quite small between the four specimens.

Finally, three samples were tested at a relative density of 70 percent. Variation in modulus with bulk stress for one representative sample at this relative density is shown in Figure 7.6. The resilient modulus increases with an increase in bulk stress. However, some scatter in data is evident. The results for the other two samples are included in Appendix D. One sample behaves similar to the one shown in Figure 7.6, whereas, the other one differs from this trend. The difference in this plot is the amount of scatter. In addition, the moduli for this test is slightly less than the other two plots. However, the moduli from the three tests are within ten percent of each other. The reason for this discrepancy is not known at this time. However, as the minimum and maximum densities of the sand are close, it maybe that the relative density of one of the specimens was deviating from 75 percent. The constitutive model for sand is described in Chapter 9.

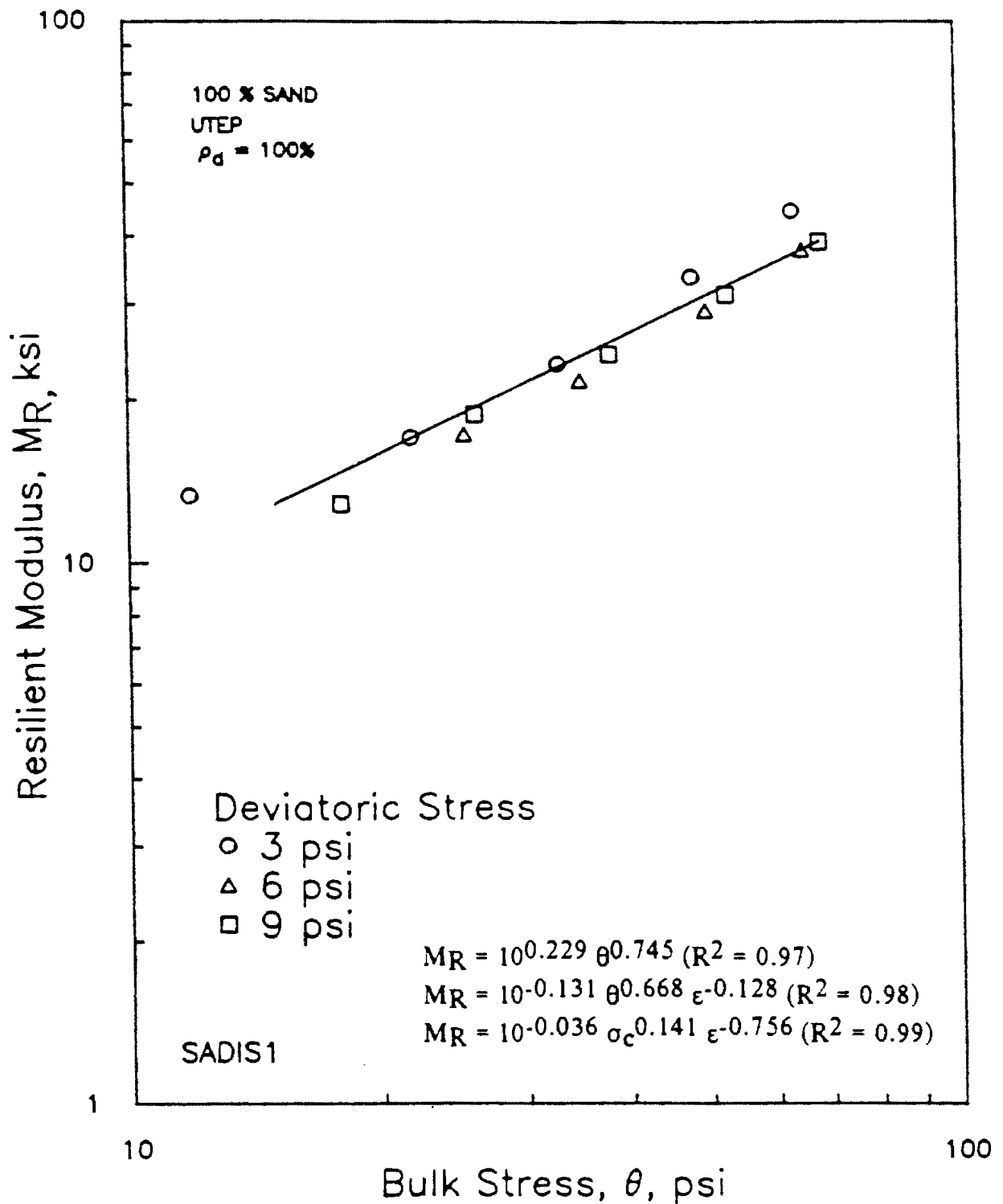


Figure 7.3 - Variation in Resilient Modulus with Bulk Stress for a Sand Sample at a Relative Density of 100 percent Following UTEP Procedure.

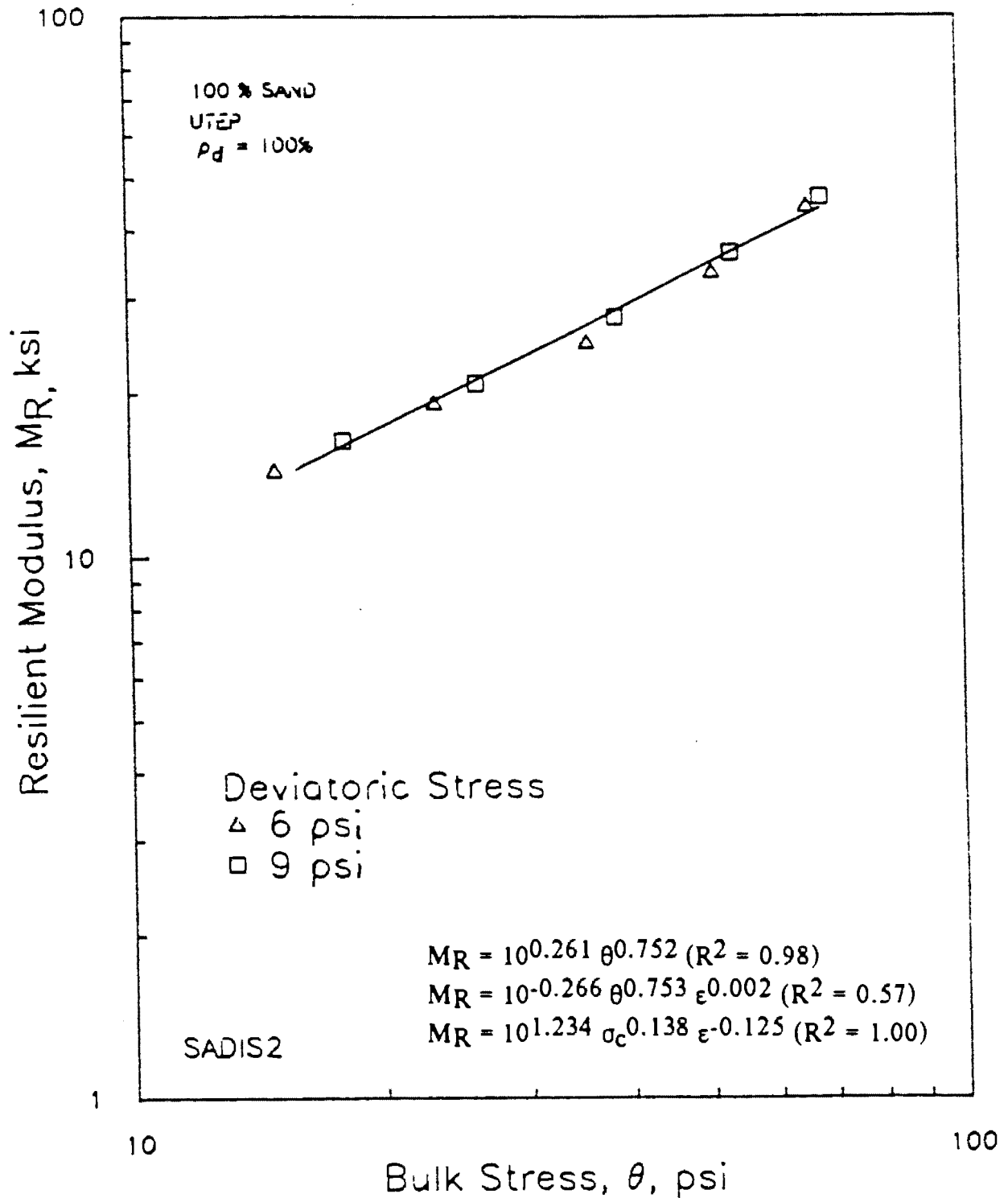


Figure 7.4 - Variation in Resilient Modulus with Bulk Stress for a Sand Sample at a Relative Density of 100 percent Following Modified UTEP Procedure.

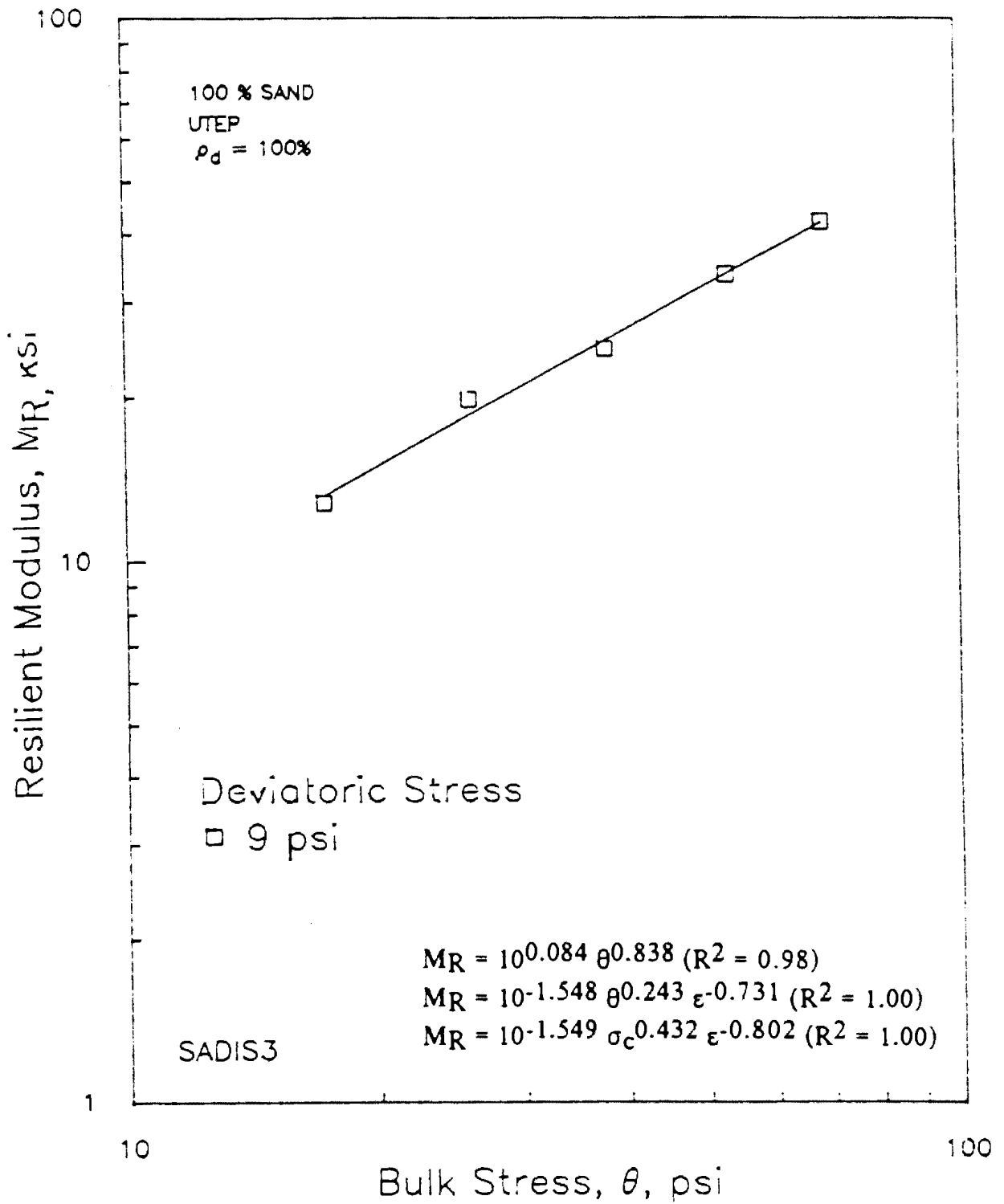


Figure 7.5 - Variation in Resilient Modulus with Bulk Stress for a Sand Sample at a Relative Density of 100 percent Following Modified UTEP Procedure.

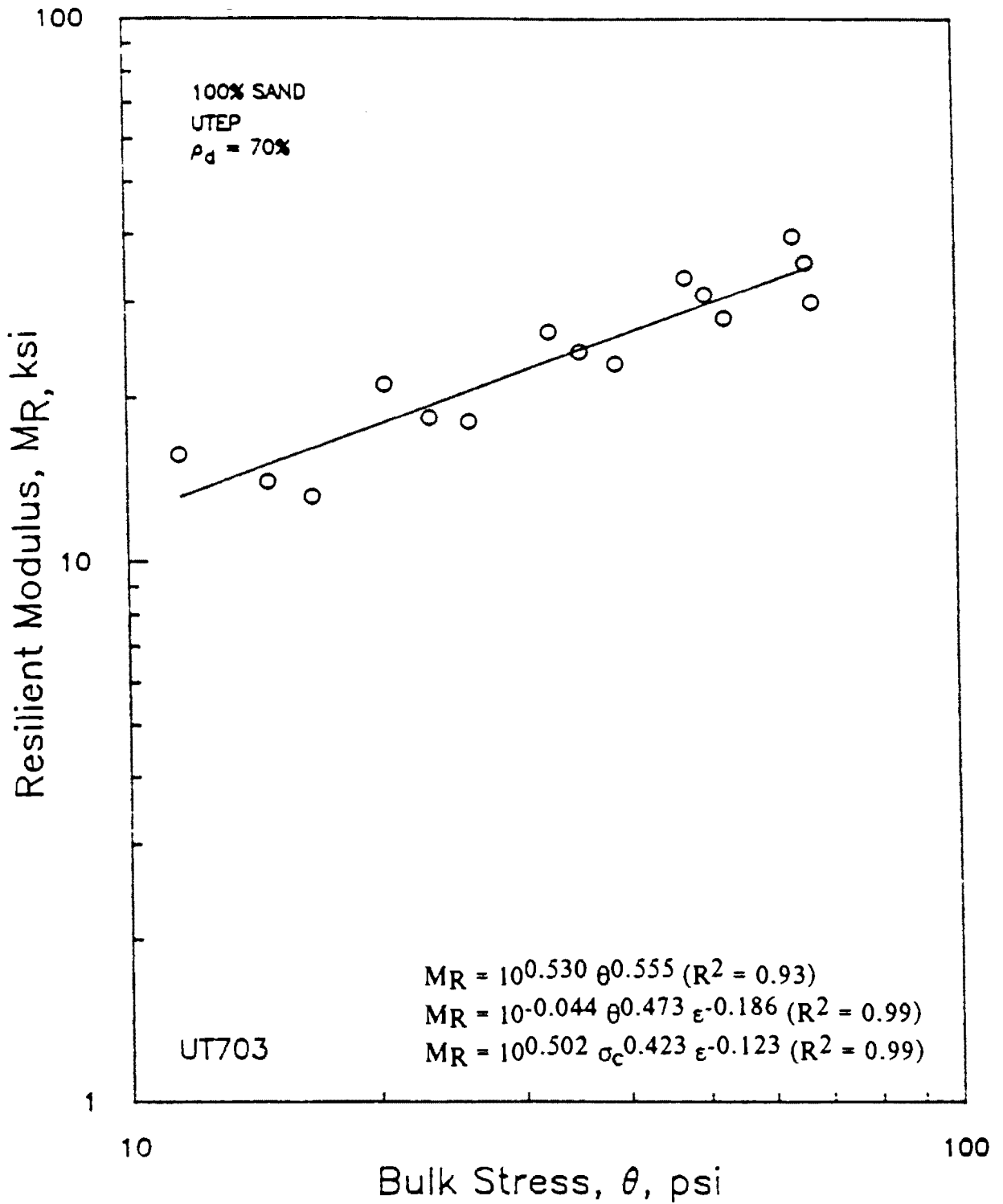


Figure 7.6 - Variation in Resilient Modulus with Bulk Stress for a Sand Sample at a Relative Density of 70 percent Following UTEP Procedure.

This page replaces an intentionally blank page in the original.

-- CTR Library Digitization Team

# Chapter 8

## Specimens of Clay-Sand Mixes

### 8.1 Introduction

The aim of the fourth and last phase of testing was to characterize and test mixtures of clay and sand. Mixtures of 90% clay-10% sand, 80% clay-20% sand, 70% clay-30% sand, 50% clay-50% sand, 30% clay-70% sand, 20% clay-80% sand, 15% clay-85% sand, 10% clay-90% sand and 5% clay-95% sand were examined. In this chapter, the properties and the testing matrix are described, and results of the tests are presented.

### 8.2 Index Properties

The samples were composed of a mixture of clay and sand. The clay and sand used were the same materials described in Chapters 6 and 7. The Atterberg limits and Proctor moisture-density tests were performed on each mixture. The liquid limit, plastic limit and plasticity index for each mixture are shown in Table 8.1. Values obtained for the pure sand and clay are also included in the table for the sake of completeness. The maximum dry density and optimum moisture content for each mixture, as well as the classification of each mixture using the AASHTO soil classification and the Unified Soil Classification System (USCS), are contained in Table 8.1.

The variation in Atterberg limits with clay content is shown in Figure 8.1. As expected, the plasticity index increases as the clay content increases. Also shown in the figure is the variation in liquid limit and plastic limit with clay content. As the clay content increases from 30 percent to 100 percent the liquid limit increases by a factor of 2.5; whereas the plastic limit increases by about only 50 percent. The equation of best fit line corresponding to these three parameters are also shown in the figure.

Table 8.1 Liquid Limit , Plastic Limit, Classification and Plasticity Index for Mixtures

| Mixtures<br>clay (%)/sand(%) | Liquid Limit<br>(percent) | Plastic Limit<br>(percent) | Plasticity Index<br>(percent) | Classification<br>(AASHTO/USC<br>S) |
|------------------------------|---------------------------|----------------------------|-------------------------------|-------------------------------------|
| 100/0                        | 44.7                      | 20.5                       | 24.2                          | A-6/CL                              |
| 90/10                        | 37.5                      | 18.6                       | 18.9                          | A-6/CL                              |
| 70/30                        | 30.5                      | 16.3                       | 14.2                          | A-6/CL                              |
| 50/50                        | 23.2                      | 15.7                       | 7.5                           | A-6/ML-CL                           |
| 30/70                        | 17.3                      | 13.8                       | 3.5                           | A-2-4/SC                            |
| 15/85                        | ---                       | ---                        | NP                            | A-3/SM                              |
| 10/90                        | ---                       | ---                        | NP                            | A-3/SW-SM                           |
| 5/95                         | ---                       | ---                        | NP                            | A-3/SP                              |
| 0/100                        | ---                       | ---                        | NP                            | A-3/SP                              |

Table 8.2 Maximum Dry Density and Optimum Moisture Content

| Mixtures<br>clay (%)/sand(%) | Maximum Density<br>(lb/ft <sup>3</sup> ) | Optimum Moisture Content<br>(percent) |
|------------------------------|--|---------------------------------------|
| 100/0                        | 107.0                                    | 16.0                                  |
| 90/10                        | 123.0                                    | 18.4                                  |
| 70/30                        | 106.8                                    | 16.9                                  |
| 50/50                        | 112.8                                    | 15.2                                  |
| 30/70                        | 115.7                                    | 10.3                                  |
| 15/85                        | 109.8                                    | 11.0                                  |
| 10/90                        | 106.8                                    | 10.5                                  |
| 5/95                         | 102.4                                    | 12.0                                  |

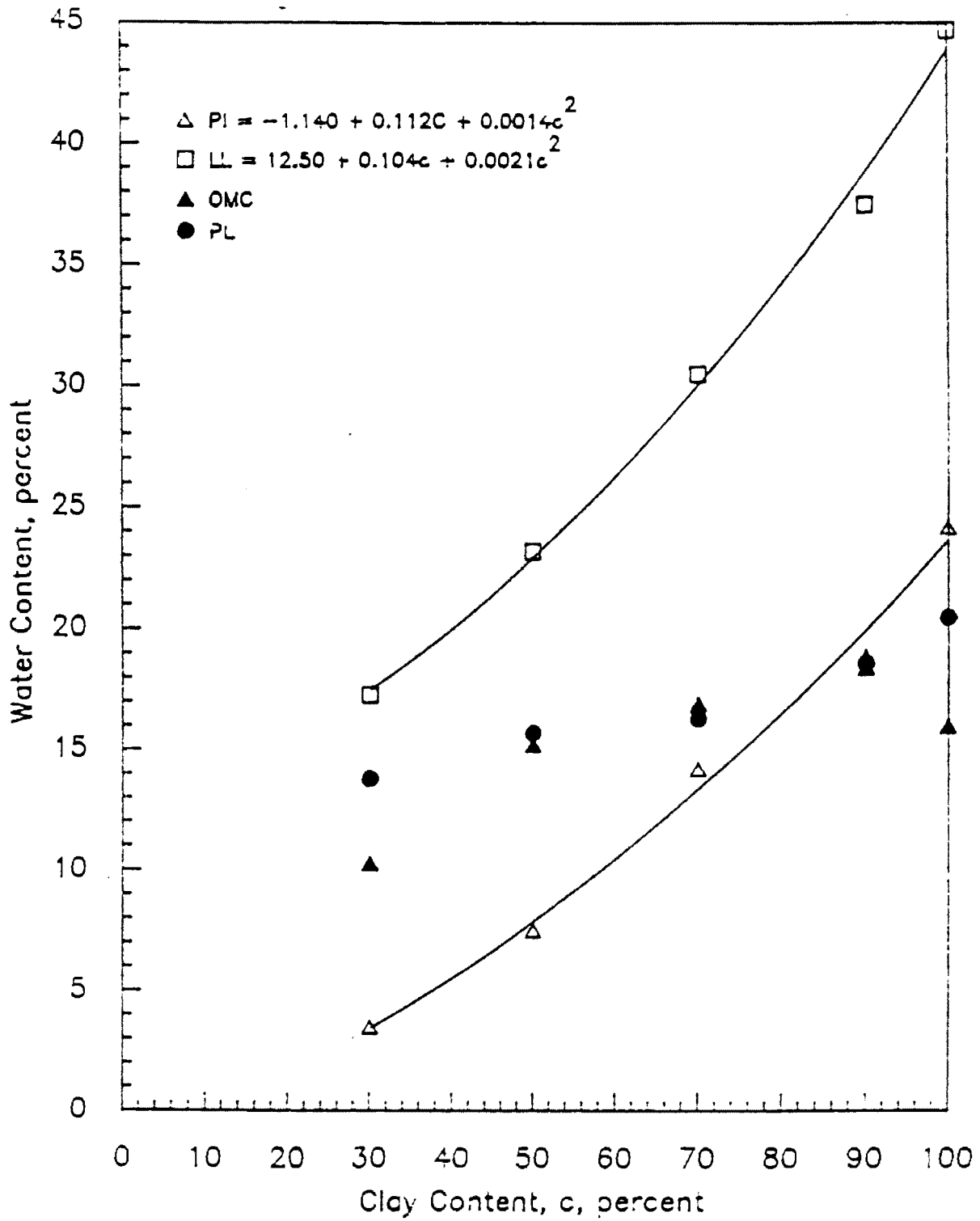


Figure 8.1 - Variation in Water Content with Clay Content for Mixtures.

The variation in maximum dry density with clay content is shown in Figure 8.2. The density increases almost linearly with an increase in the clay content up to a clay content of 30 percent. Beyond this value, the dry density decreases up to a clay content of 70 percent and presumably remains constant there on. One anomaly is apparent in the data. At clay contents of 80 and 90 percent, the maximum dry densities increase, tremendously. At this time the reason for this matter is unknown.

The variation in optimum water content with the clay content of the mixture is presented in Figure 8.3. Some scatter is evident in the data. It would not be unreasonable to assume a linear increase in optimum water content with clay content for clay contents above 30 percent and a constant optimum water content when the clay content is less than 20 percent.

### **8.3 Testing Matrix**

A total of 75 specimens were tested. The SHRP protocol was followed for the Type 2 soils and the UTEP procedure for the Type 1 specimens. As such, 33 samples were tested using the UTEP procedure and 42 samples were tested using the SHRP procedure. Each mixture was tested at three moisture contents: optimum, optimum plus 2 percent and optimum minus 2 percent. The repeatability of the numbers was checked by testing three samples at each moisture content.

Each sample was stored in a sealed bag for about three weeks in a moist room before testing. This was done to ensure equilibrium within the properties of the samples.

### **8.4 Presentation Of Results**

A typical variation in modulus with deviatoric stress for the Type 2 sample, 90% clay-10% sand, at optimum moisture content is shown in Figure 8.4. There is not much scatter in the data. At each deviatoric stress, the slight variation in modulus is due to the variation in confining pressure. This trend holds true for the remaining plots for all the Type 2 soils which are presented in Appendix E.

A typical variation in modulus with bulk stress is displayed in Figure 8.5 for a Type 1 sample consisting of 10% clay-90 % sand, at optimum moisture content. Some scatter in the data is evident because at each deviatoric stress, the modulus is dependent on the confining pressure. This is well reflected in Figure 8.6.

At each clay content, the repeatability of the method was checked by testing three samples. The results of the three tests are displayed in Appendix E. The samples tested at wet and dry of optimum, also yielded repeatable results.

Due to vast amounts of data collected, comprehensive comparison of results to check repeatability would be rather tedious. However, the variation in resilient modulus with clay

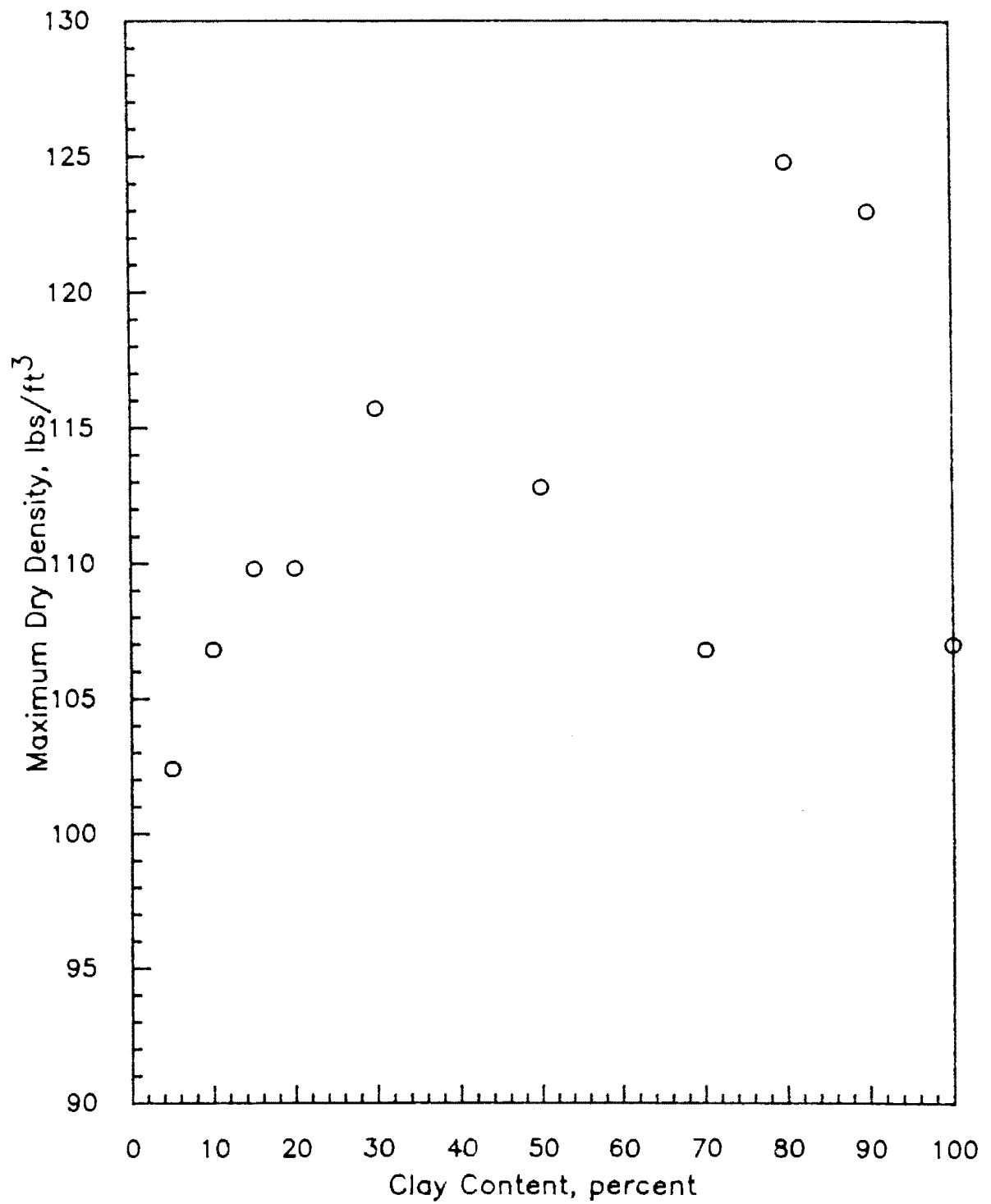


Figure 8.2 - Variation in Maximum Dry Density with Clay Content for Mixtures.

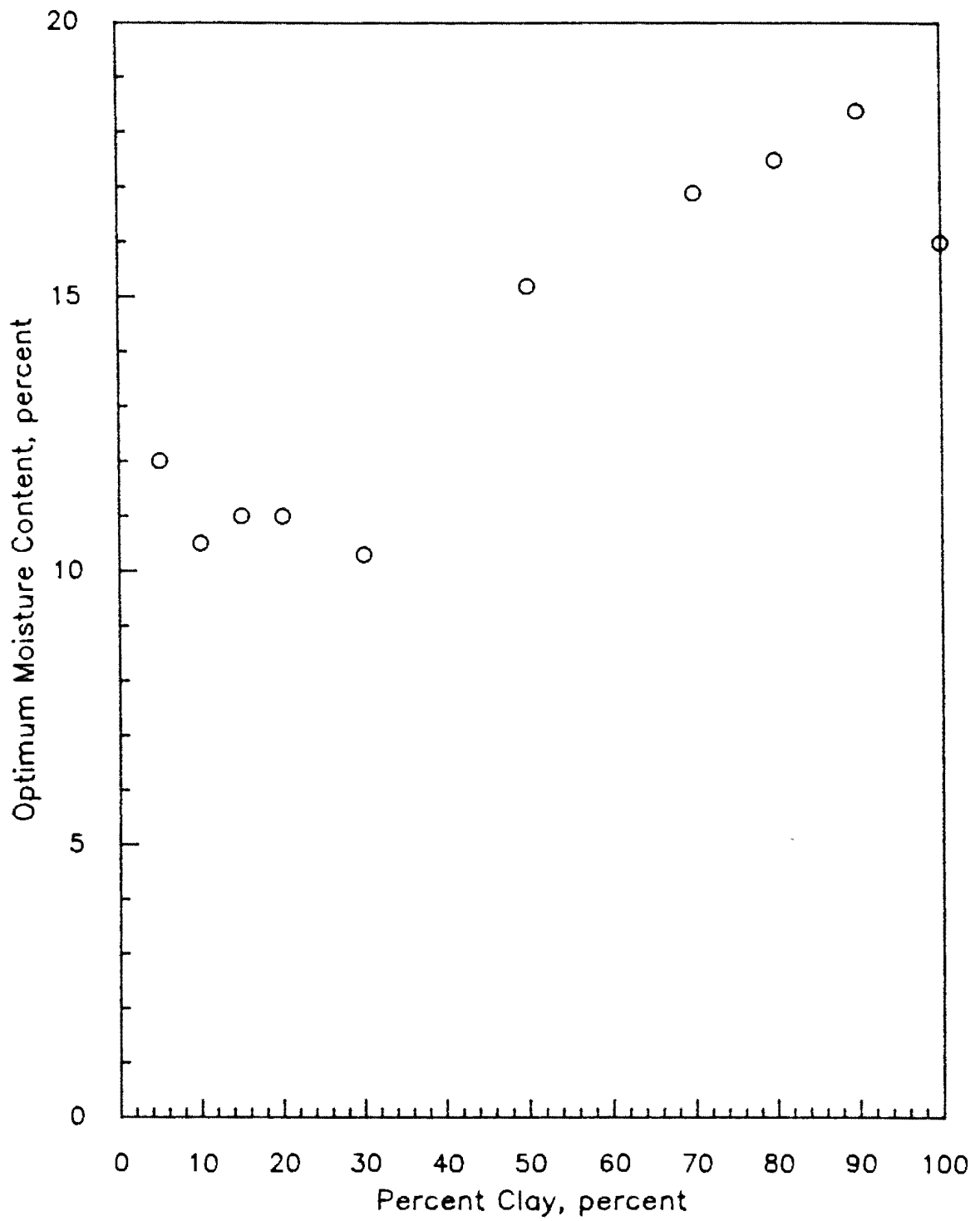


Figure 8.3 - Variation in Optimum Moisture Content with Percent Clay for Mixtures.

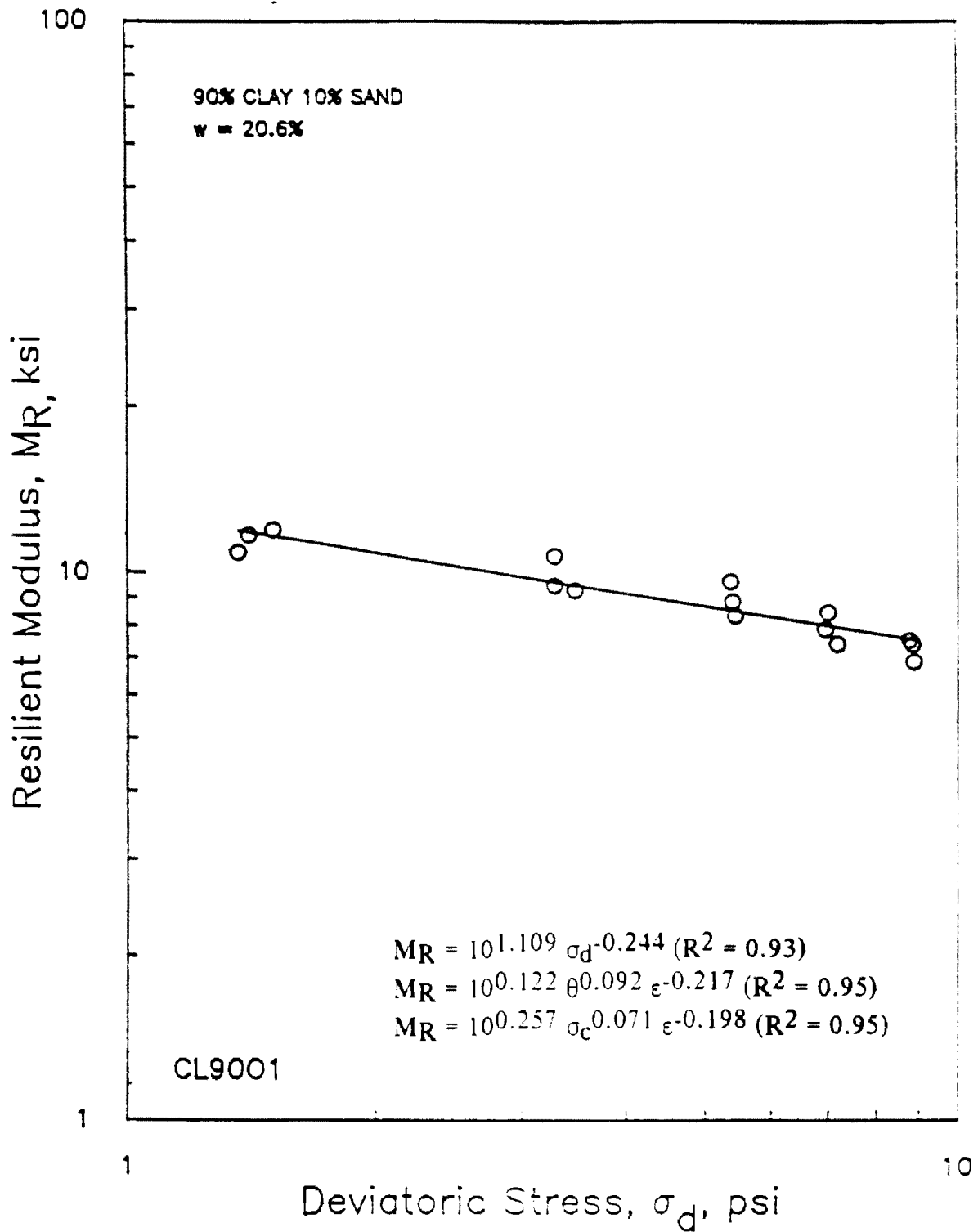


Figure 8.4 - Variation in Resilient Modulus with Deviatoric Stress for a 90% Clay-10% Sand Specimen at a Moisture Content of 20.6 percent Following SHRP Procedure.

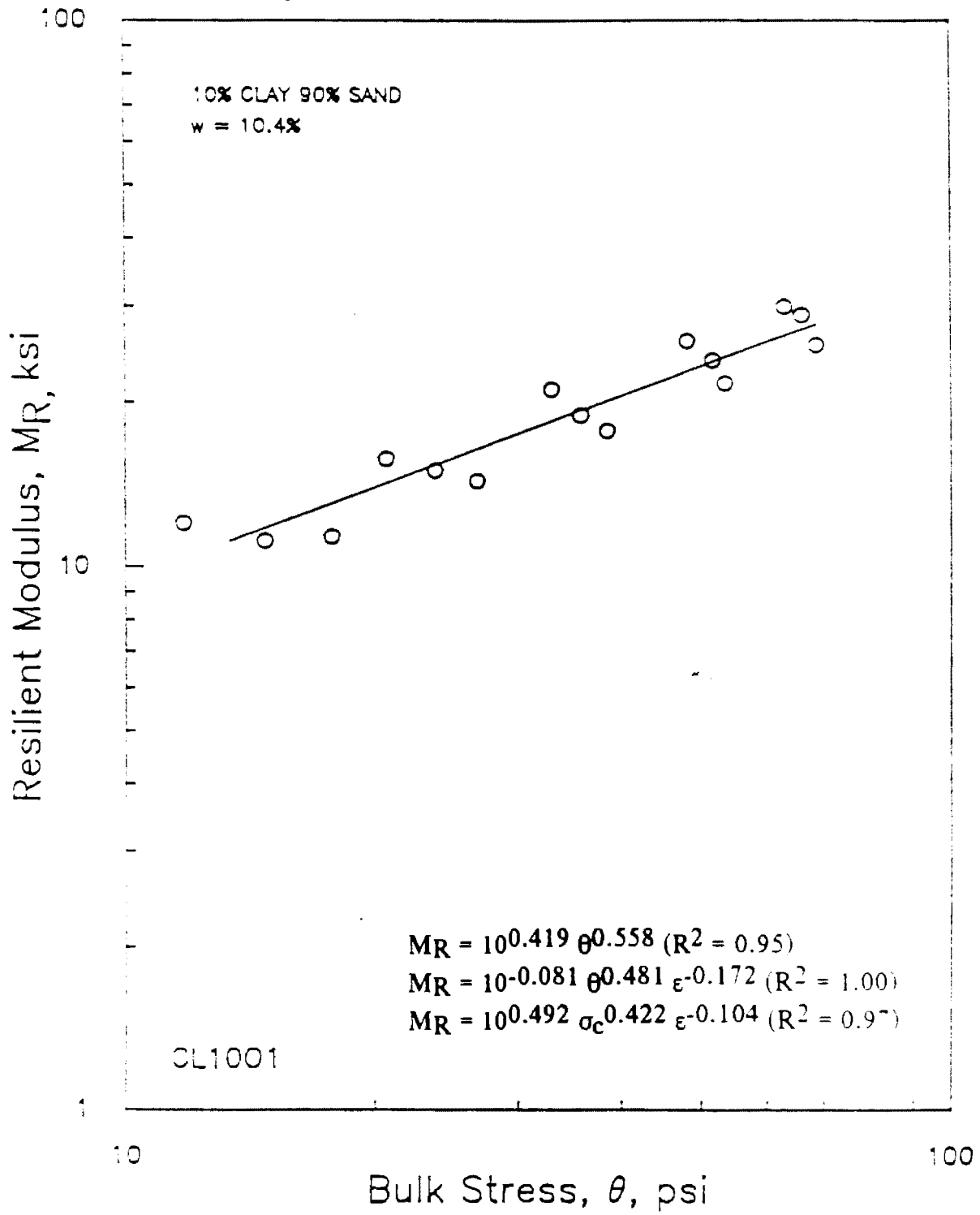


Figure 8.5 - Variation in Resilient Modulus with Bulk Stress for a 10% Clay-90% Sand Specimen at a Moisture Content of 10.4 percent Following UTEP Procedure.

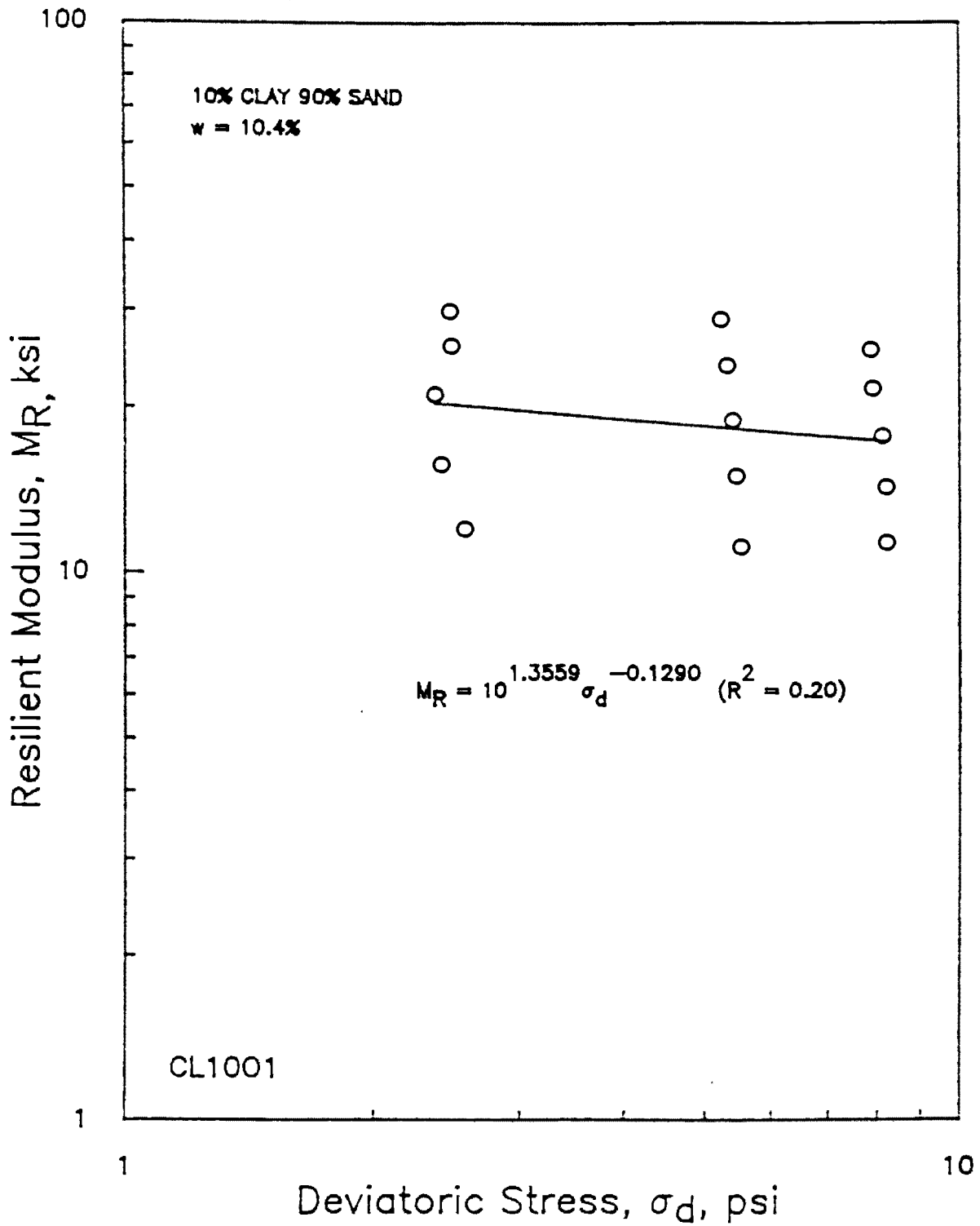


Figure 8.6 - Variation in Resilient Modulus with Deviatoric Stress for a 10% Clay-90% Sand Specimen at a Moisture Content of 10.4 percent Following UTEP Procedure.

content for the optimum water content at one confining pressure and one deviatoric stress is included in Figure 8.7. The modulus values at 6 psi confining pressure and 6 psi deviatoric stress were used since this state of stress is common to tests performed with Type 1 and Type 2 soils.

Modulus values obtained from three different experiments are also shown in the Figure 8.7. The level of scatter is relatively small. The maximum deviation in the actual modulus from the average modulus is about 15 percent. Also shown in the figure is the least-square best-fit polynomial through the data. The resilient modulus is sensitive to the clay content. The maximum modulus is obtained at clay contents of 5 percent and pure clay. The minimum value, which is about 50 percent less than the maximum, occurs at a clay content of about 50 percent.

The variation in resilient modulus with clay content for samples at wet of optimum moisture content is shown in Figure 8.8. Trends in the results are similar to those obtained from samples tested at optimum water content. However, for samples wet of the optimum water content, the minimum modulus was measured at a clay content of about 70 percent. The modulus deviates by a maximum of about 20 percent from the average values. As seen in Figures 8.7 and 8.8, the pure clay specimens resulted in an increase in modulus. The maximum modulus occurs at five percent clay content and minimum at about seventy percent content.

The variation in resilient modulus with clay content for samples at dry of optimum moisture content is shown in Figure 8.9. It appears the resilient modulus is dependent on the clay content. The effect of the clay content, however is not as prominent as for samples tested at optimum water content and wet of optimum water content. The amount of scatter in the data is relatively small. The maximum modulus occurs at five percent clay content while the minimum modulus is measured at a clay content of about 50 percent.

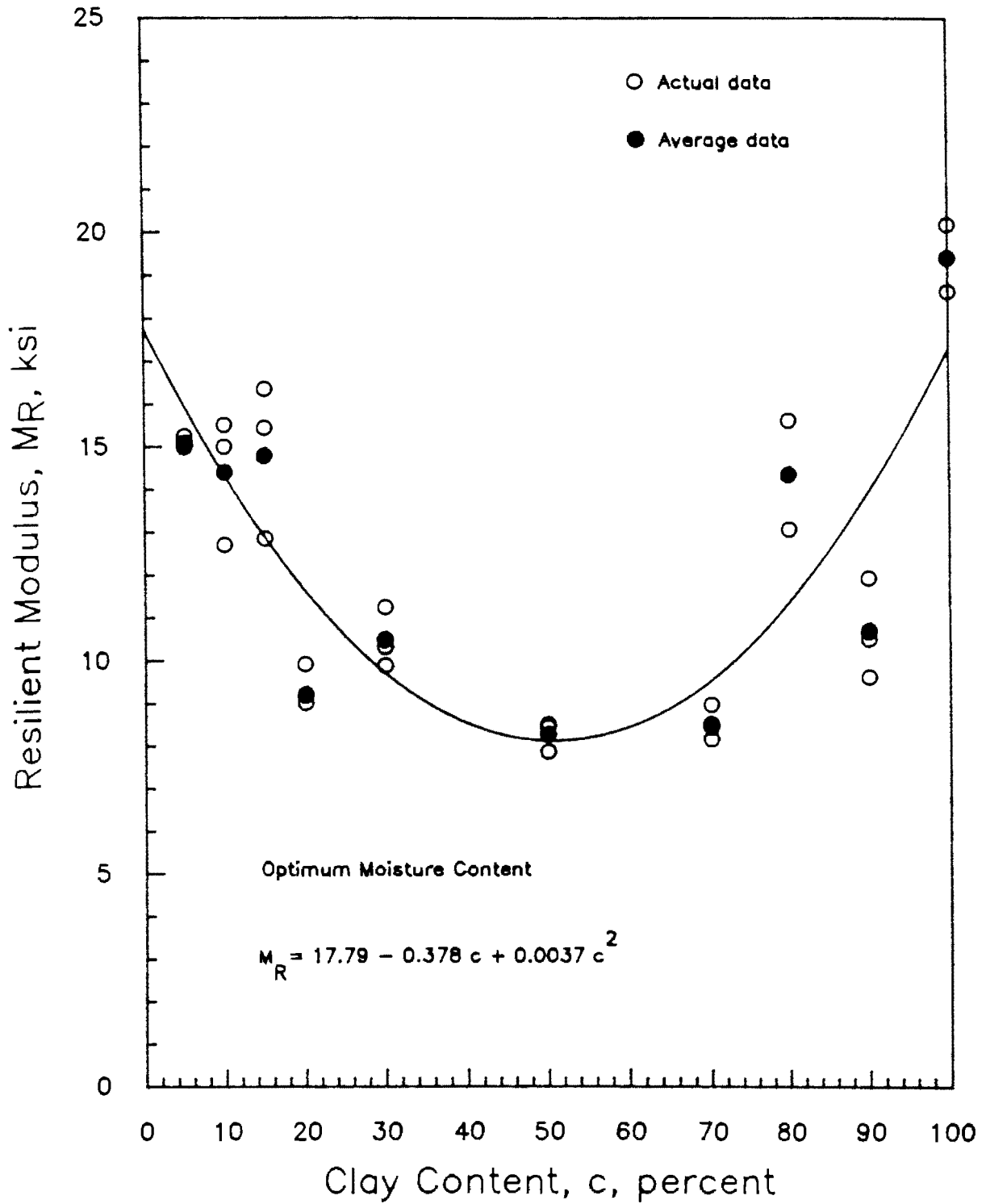


Figure 8.7 Variation in Resilient Modulus with Clay Content at Optimum Water Content for 6 psi Confining Pressure and 6 psi Deviatoric Stress.

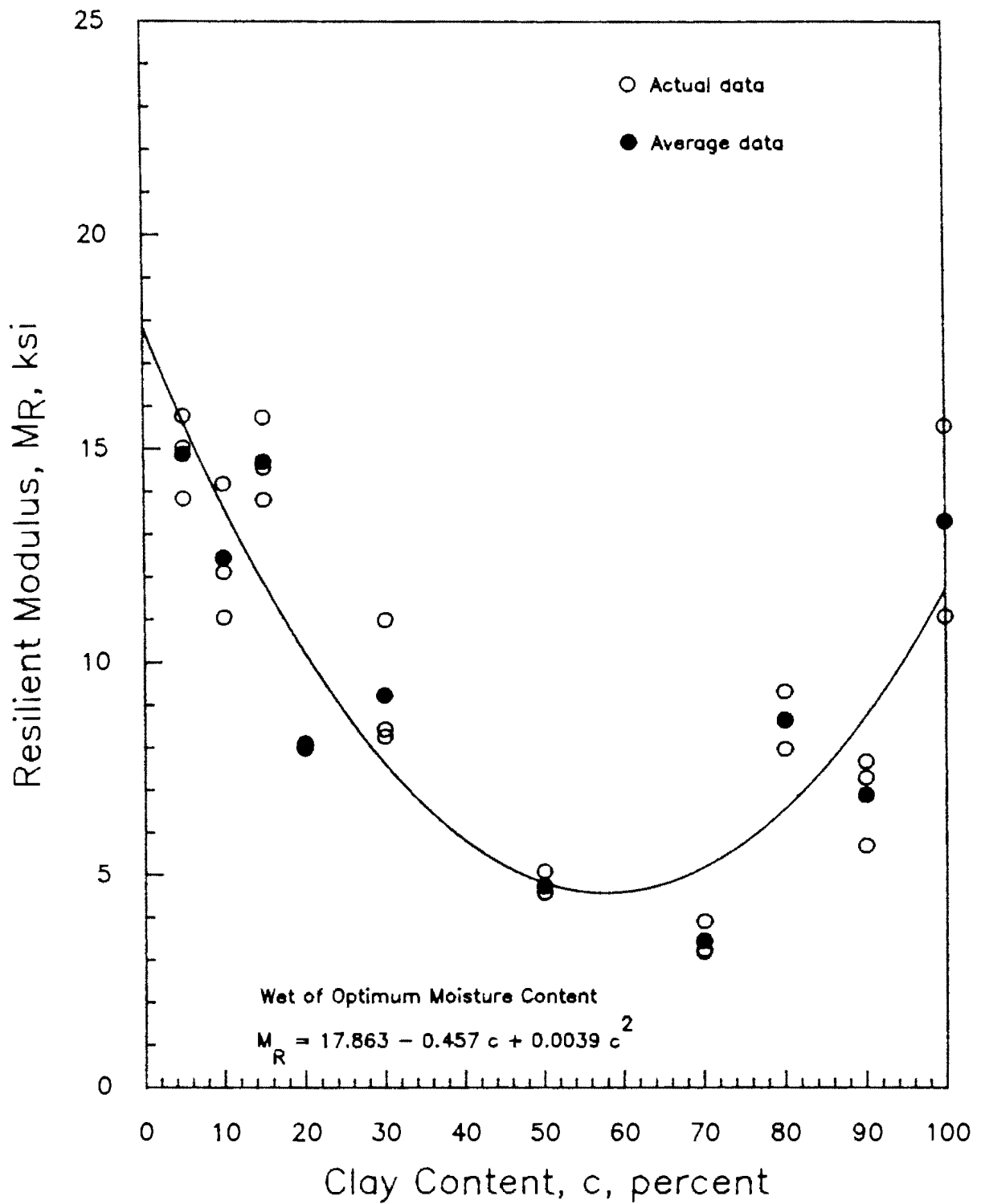


Figure 8.8 Variation in Resilient Modulus with Clay Content at Wet of Optimum Water Content for 6 psi Confining Pressure and 6 psi Deviatoric Stress.

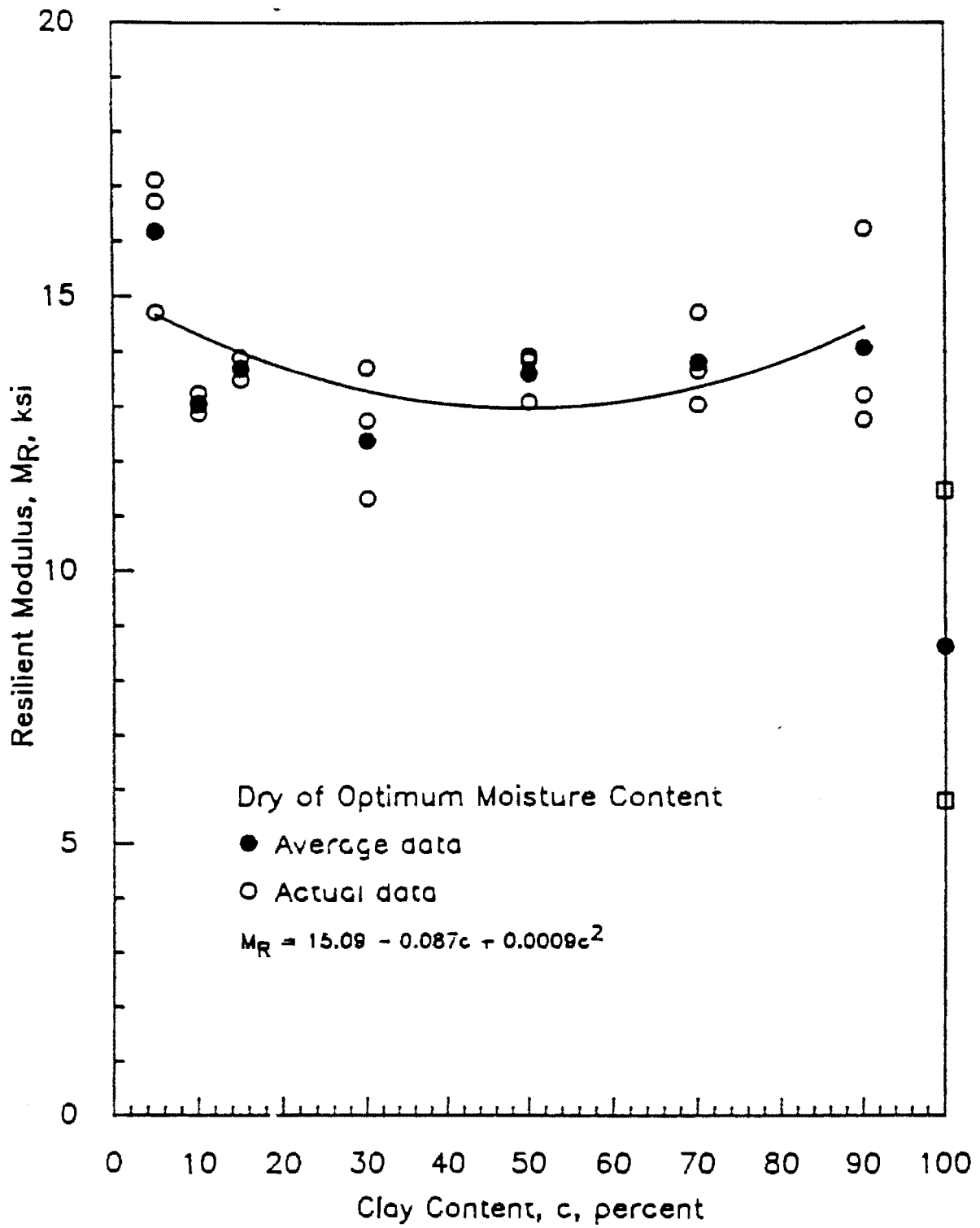


Figure 8.9 Variation in Resilient Modulus with Clay Content at Dry of Optimum Water Content for 6 psi Confining Pressure and 6 psi Deviatoric Stress.

# Chapter 9

## Constitutive Models

### 9.1 Introduction

The results of resilient modulus tests on pure sand, pure clay and several proportions of mixtures of these two materials were described in Chapters 6 through 8. In this chapter, the results from these tests are combined to develop appropriate constitutive models. Simplified relationships for estimating the regression constants of these models as a function of clay content are also proposed.

### 9.2 Evaluation of Existing Models

For each case, the corresponding constitutive model as proposed by SHRP or AASHTO was first used. These models were presented in Chapter 2. However, these relationships are repeated herein for completeness. For granular materials, both SHRP and AASHTO recommend a relationship between resilient modulus,  $M_R$  and bulk stress,  $\theta$ . This relationship is written as:

$$M_R = 10^{k_1} \theta^{k_2} \quad (9.1)$$

Similarly, both AASHTO and SHRP recommend a relationship between the resilient modulus and deviatoric stress,  $\sigma^d$ . This relationship can be written as:

$$M_R = 10^{k_1} \sigma_d^{k_2} \quad (9.2)$$

The constants  $k_1$  and  $k_2$  corresponding to the constitutive model of each soil specimen were determined. For each specimen, described in Chapters 6 through 8, the constitutive model is reflected in a corresponding figure in Appendices C through E. In each figure, the least-squares best-fit line corresponding to the constitutive model obtained by AASHTO or SHRP are also presented as a solid line. For the sake of brevity, these models are not repeated in this chapter. Each appendix contains a table summarizing the constant values. In these tables, the R-squared values are reported as well. An inspection of these values reveals that these models do not adequately represent the data. This matter will be discussed in the following sections.

For the sandy material reported in Chapter 6, Equation 9.1 yields R-squared values ranging from 0.78 to 0.98 with an average of about 0.85. Given the recent emphasis on improving the experimental aspects of resilient modulus tests, such level of correlation may not be adequate.

For the clay specimens tested, the R-squared values are quite low. For the samples tested using AASHTO method, the R-squared values were generally less than 0.25. A better correlation was achieved for the specimens tested following SHRP protocol. In this case, the R-squared values were generally between 0.85 and 0.95.

For the mixtures tested following UTEP procedure, the AASHTO/SHRP relationships yielded R-squared values which varied between 0.77 and 0.98 with an average value of 0.83. Those specimens of clay and sand mixtures tested following the SHRP protocol resulted in R-squared values which again varied between 0.78 and 0.98 with an average of about 0.90. Once again, much attention is focused on improving the testing aspects of the method. The modelling aspects of these tests should be improved so that the modifications in the laboratory testing aspects can be justified. To achieve this goal, two new constitutive models are proposed in the next section.

### 9.3. Proposed New Models

As mentioned in Chapter 2, for a given soil, Hardin and Drnevich (1972) found that two parameters significantly contribute to the stiffness (modulus) of soils. These two parameters (besides void ratio) are the state of stress and the strain level. As such, the two models proposed by AASHTO and SHRP are not complete. The model proposed for granular materials, directly considers the effects of the state of stress (bulk stress) but ignores the effects of strain amplitude. On the other hand, the model proposed for the cohesive soils, directly considers the effects of strain level (deviatoric stress) but virtually ignores the effects of the state of stress. Two models were studied which consider both these factors. These two models are of the form:

$$M_R = 10^{k_1} \theta^{k_2} \varepsilon^{k_3} \quad (9.3)$$

and

$$M_R = 10^{k_1} \sigma_c^{k_2} \varepsilon^{k_3} \quad (9.4)$$

In both models, the strain level is considered as a direct parameter. However, in the first model, bulk stress represents the state of stress, and in the second model the effects of stress state is included through the confining pressure,  $\sigma_c$ . These two models yield more representative constitutive models. The model presented in Equation 9.3 will be called Model One and the model presented in Equation 9.4 will be called Model Two, hereafter.

When Model One was applied to the resilient moduli from different tests, the R-squared values were generally above 0.95 except for some isolated cases (mostly for clays tested following AASHTO procedure). The difference between the measured modulus and calculated modulus from the AASHTO/SHRP equation for a granular material is shown in Figure 9.1. The figure corresponds to the modulus values obtained from three similar specimens tested at a relative density of 100 percent. The results from one specimen were shown in Figure 7.2. A significant difference exists between the actual and modelled data. The deviation between the two is as high as 45 percent but typically within 30 percent. The similar plot for the same data, but for the model presented in Equation 9.3 is shown in Figure 9.2. The measured and calculated moduli compare better and the scatter is usually less than 15 percent.

Finally, the model introduced in Equation 9.4 was evaluated. The difference in the calculated and measured data is presented in Figure 9.3. The calculated moduli from Equation 9.4 are typically within 20 percent of the measured values. Therefore, in this case, Equation 9.3 may be a better representation of the data collected. However, the difference is rather small. The R-squared values for Equations 9.3 and 9.4 are 0.97 and 0.95, respectively. The R-squared value from AASHTO/SHRP equation (Equation 9.1) is about 0.90. This shows that a change in R-squared of 0.05 (between 0.95 and 0.90) results in a significant increase in scatter.

A typical example of the variation between the calculated and measured moduli for a clay utilizing Equations 9.2, 9.3 and 9.4 is also included. This example corresponds to the data shown in Figure 6.4. The differences between the calculated and measured values are shown in Figures 9.4 through 9.6. The AASHTO/SHRP model, which yields an R-squared of about 0.87, results in a variation of up to 15 percent. The other two proposed models (Equations 9.3 and 9.4) yield slightly better correlation. The R-squared values for models proposed in Equations 9.3 and 9.4 were about 0.93 and 0.94. The variation between the calculated and measured values for both models are typically within 10 percent. Once again, a slight increase in R-squared values resulted in a significant decrease in the scatter. It should be mentioned that the correlation for other clay specimens are typically lower than the one used for this example. The two models proposed here in most cases yielded essentially R-square values above 0.95.

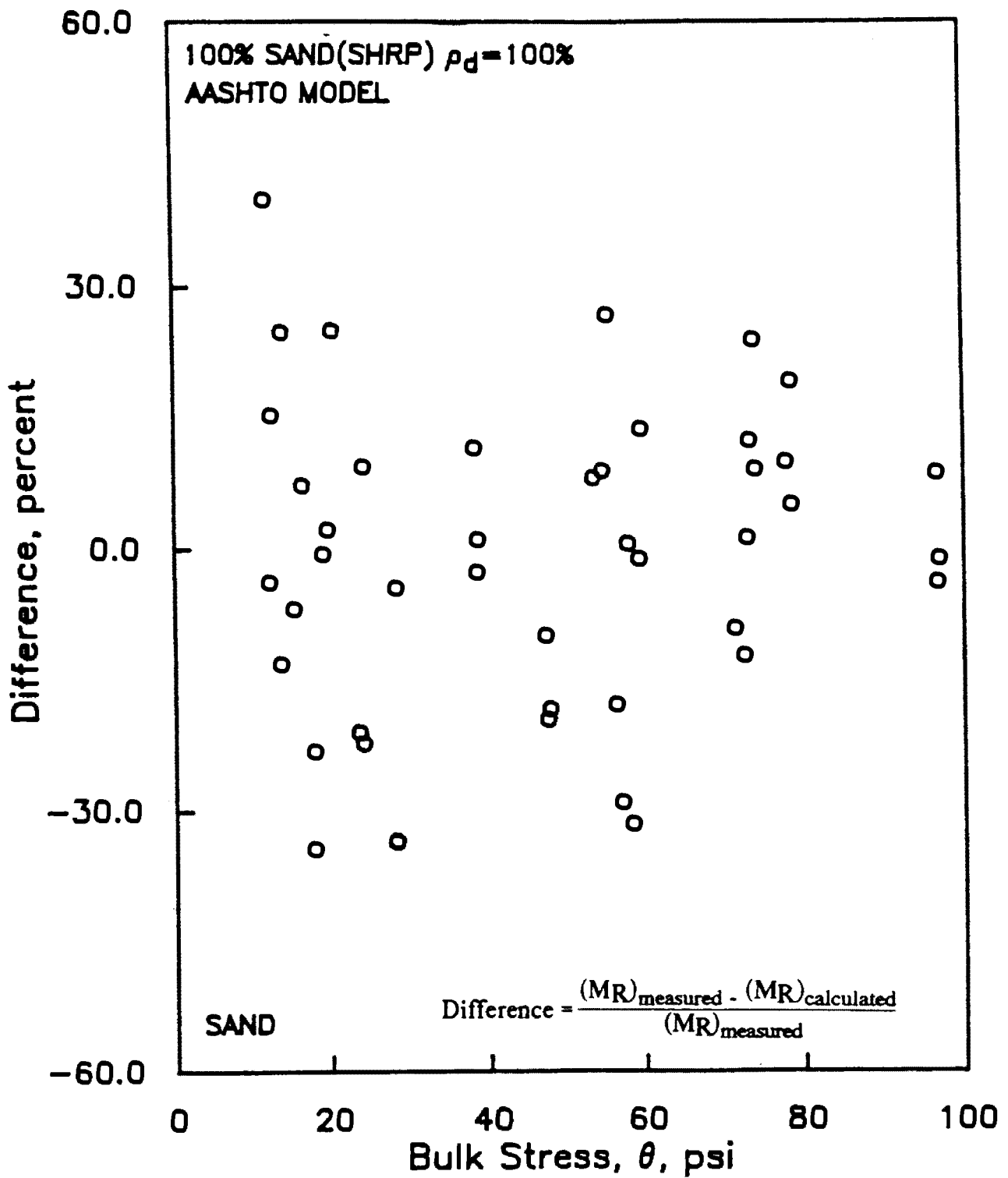


Figure 9.1 - Typical Variation in Percent Difference Between Measured and Modelled Moduli Using AASHTO/SHRP Model on a Sand Specimen.

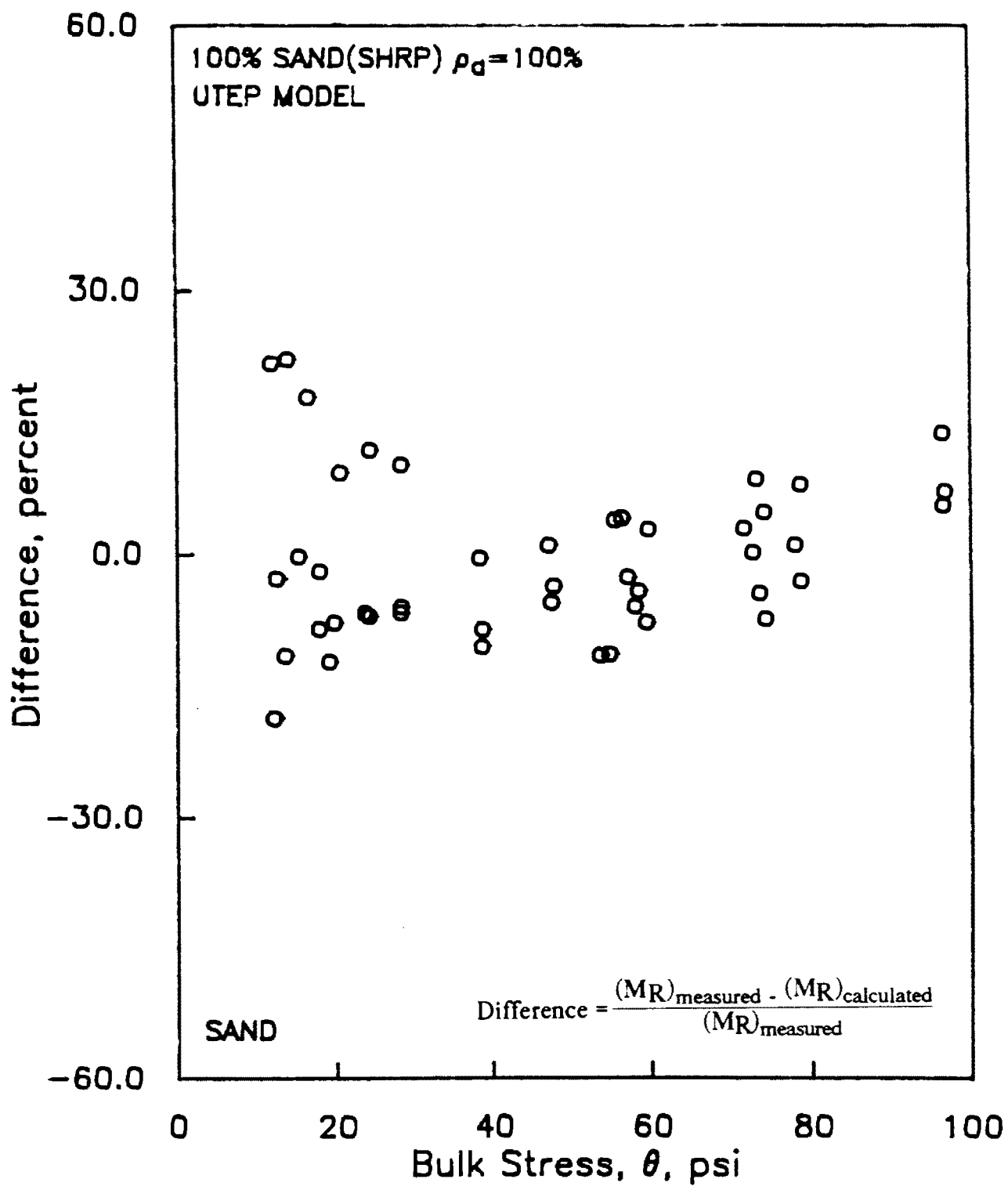


Figure 9.2 - Typical Variation in Percent Difference Between Measured and Modelled Moduli Using Model One on a Sand Specimen.

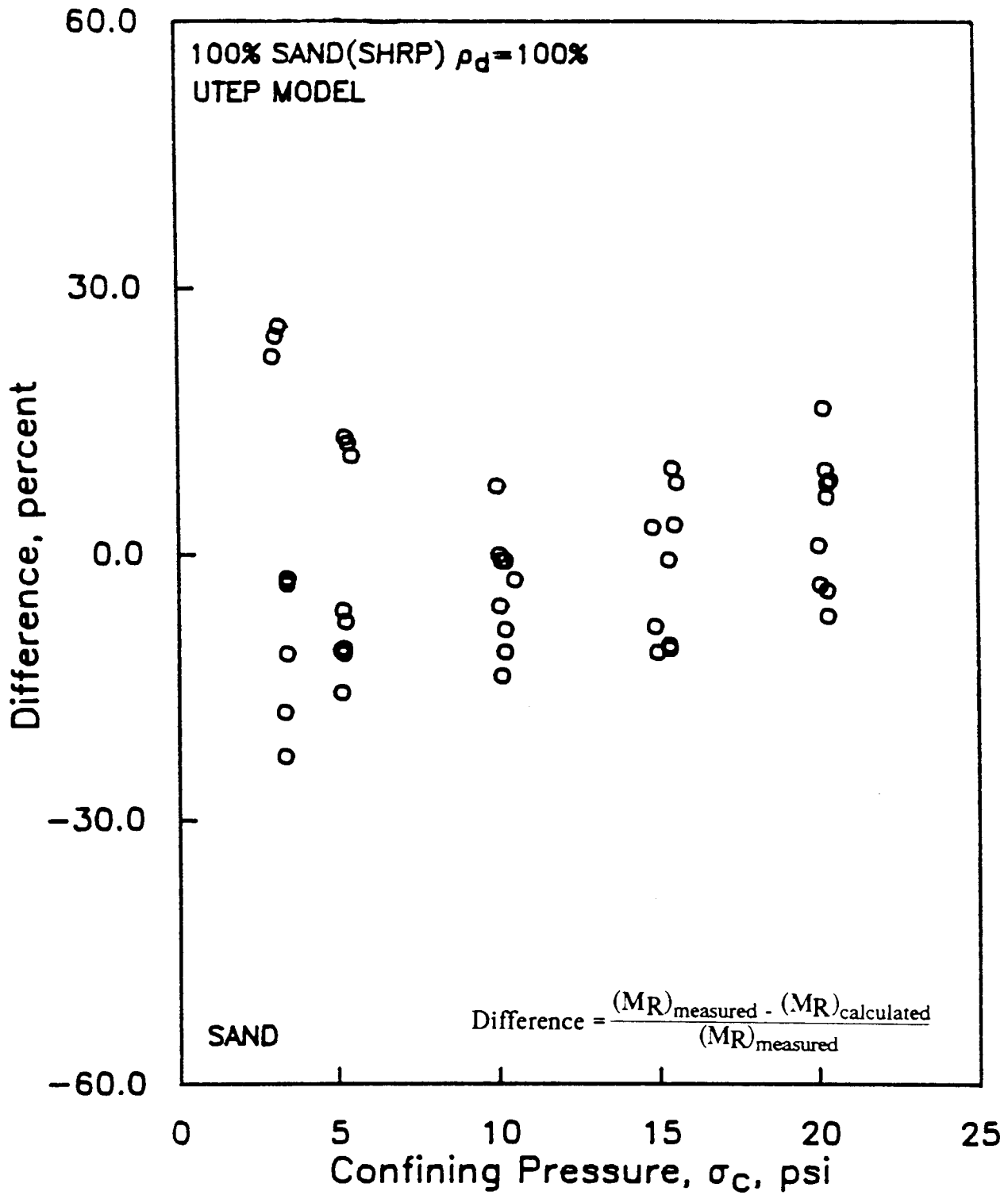


Figure 9.3 - Typical Variation in Percent Difference Between Measured and Modelled Moduli Using Model Two on a Sand Specimen.

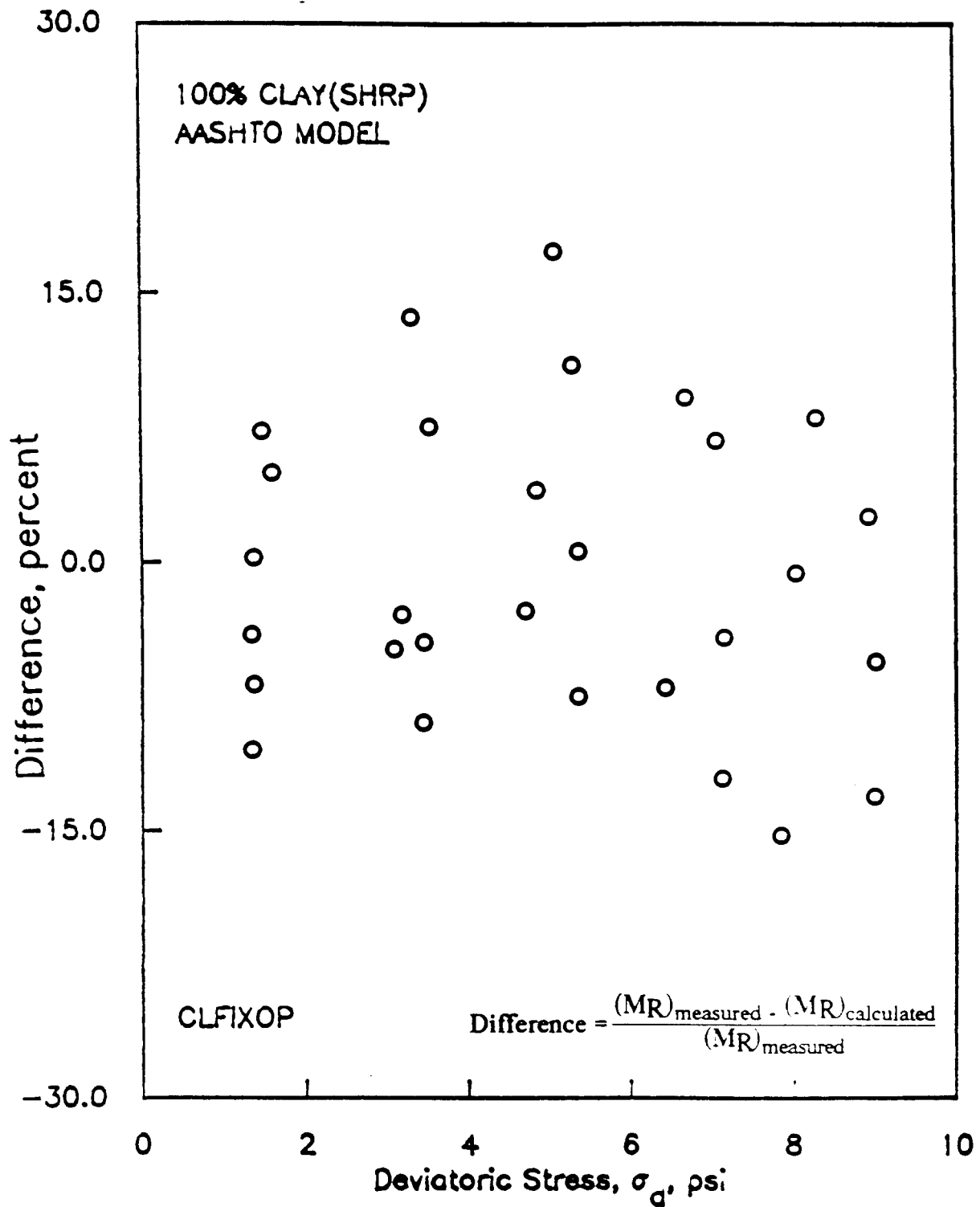


Figure 9.4 - Typical Variation in Percent Difference Between Measured and Modelled Moduli Using AASHTO/SHRP Model on a Clay Specimen.

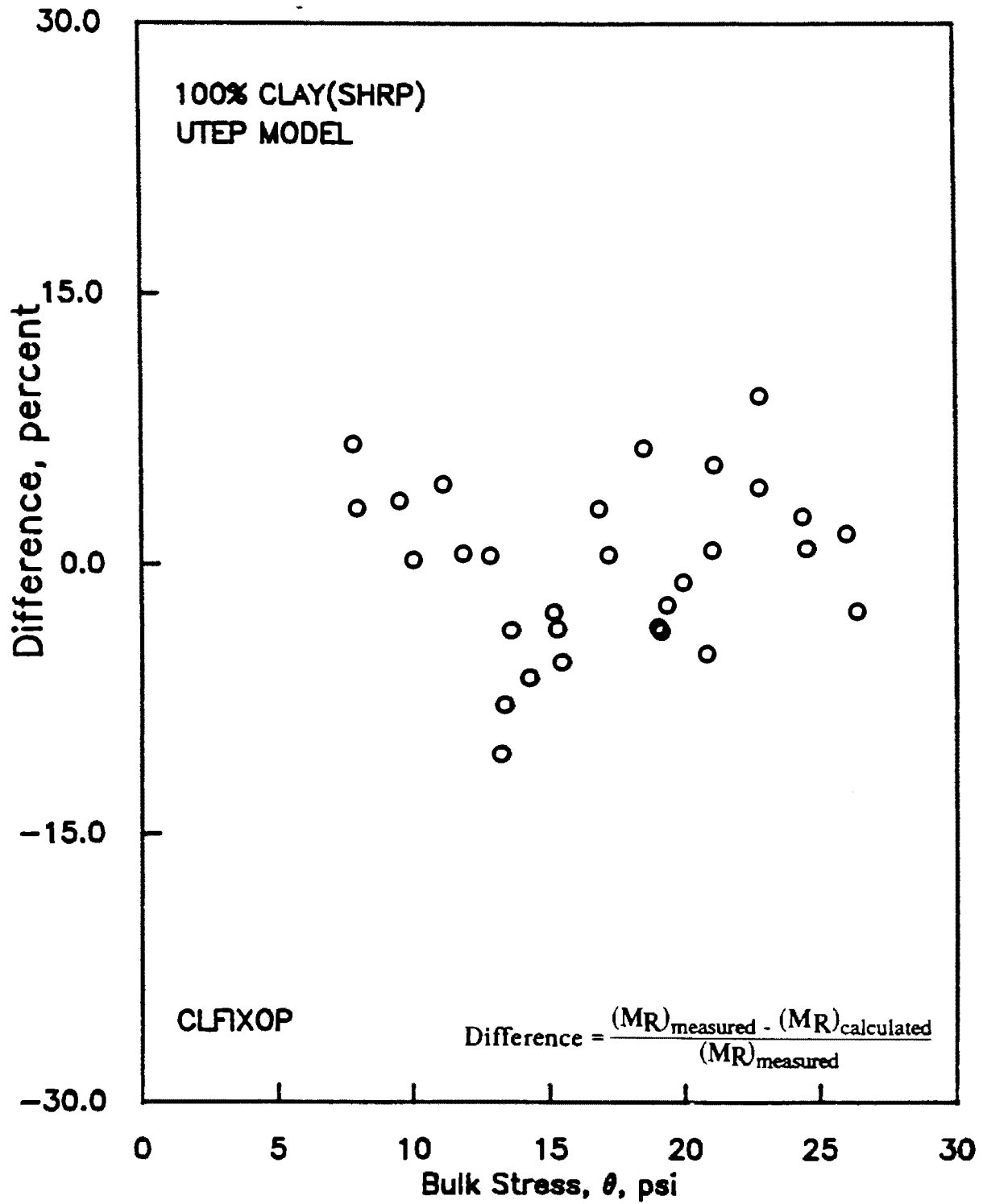


Figure 9.5 - Typical Variation in Percent Difference Between Measured and Modelled Moduli Using Model One on a Clay Specimen.

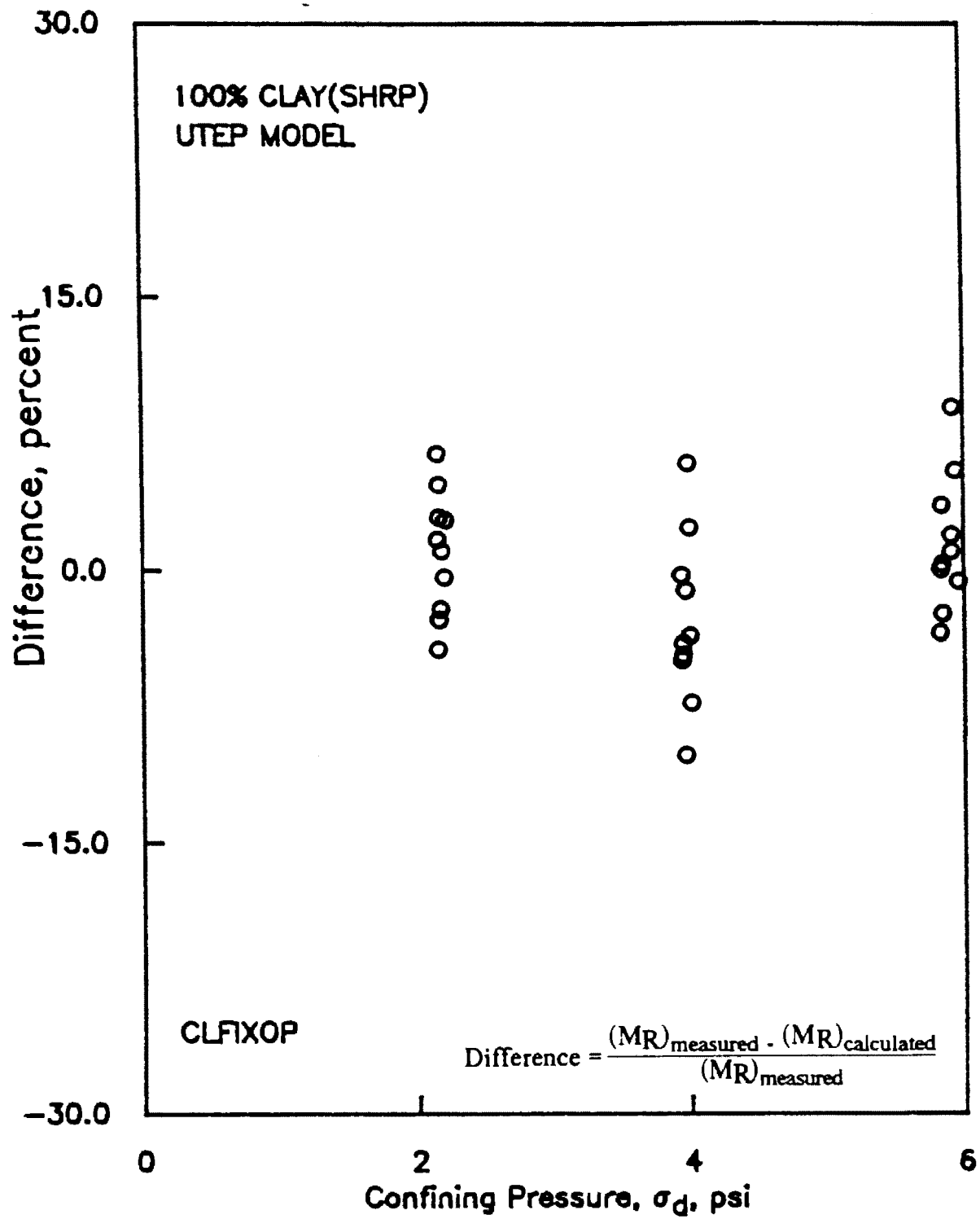


Figure 9.6 - Typical Variation in Percent Difference Between Measured and Modelled Moduli Using Model Two on a Clay Specimen.

## 9.4. Effects of Clay Content

In this section, it has been attempted to develop simplified relationships for determining the constants associated with the constitutive models as a function of clay content. Two constants associated with the AASHTO/SHRP models (or three constants associated with the UTEP models) are related to the clay content.

In all cases, a second degree polynomial in the form of:

$$k_i = A_1 + A_2c + A_3c^2 \quad (9.5)$$

was used. In the equation,  $k_i$  corresponds to either  $k_1$  or  $k_2$  or (if applicable)  $k_3$ . The parameter  $c$  denotes clay content (in percent by weight).

### 9.4.1 AASHTO/SHRP Cohesive Model

Shown in Figures 9.7 through 9.9 are the variations in constant  $k_1$  with clay content for the cohesive soils tested at the optimum water content, two percent wet of optimum and two percent dry of optimum, respectively. For each soil, the constant  $k_1$  was determined following AASHTO/SHRP model (see Equation 9.2). The open circles represent the results from three different tests. The solid symbols correspond to the average values. The least-squares best-fit polynomials are also presented. The equations of the curves are reflected on the figures and are summarized in Table 9.1. For the specimens prepared at the optimum water content or dry of optimum, parameter  $k_1$  is more or less constant; whereas  $k_1$  associated with the wet specimens has a minimum clay content of about 60 percent. At each water content, the amount of scatter in data is small corresponding to the repeatability of the results.

The variation in parameter  $k_2$  with clay content for the samples at optimum water content, wet of optimum and dry of optimum is shown in Figure 9.10 through 9.12, respectively. The scatter in data is relatively larger than for  $k_1$ . Once again, the best-fit curves are reflected on the figures and their values are summarized in Table 9.1.

An inspection of Figure 9.10 reveals that the best-fit polynomial does not describe the data well. This can be partially due to the scatter in data and partially due to the model selected. Given the level of scatter in data, selection of a more sophisticated model may not be justified. For the cases where tests were conducted at wet of optimum, the model is well representative of the data, especially that the scatter in the slopes is quite small. Significant scatter is apparent in the case when  $k_2$  had to be determined from the empirical model described in Equation 9.5. Even though the scatter in data is small, the model cannot adequately describe the data. Once again, given the extent of data, the use of a more sophisticated model may not be appropriate.

### 9.4.2 AASHTO/SHRP Granular Model

Similar to the cohesive soils, relationships were developed between resilient modulus constants and the clay content for the granular (Type 1) materials. Values of  $k_1$  from three tests and the

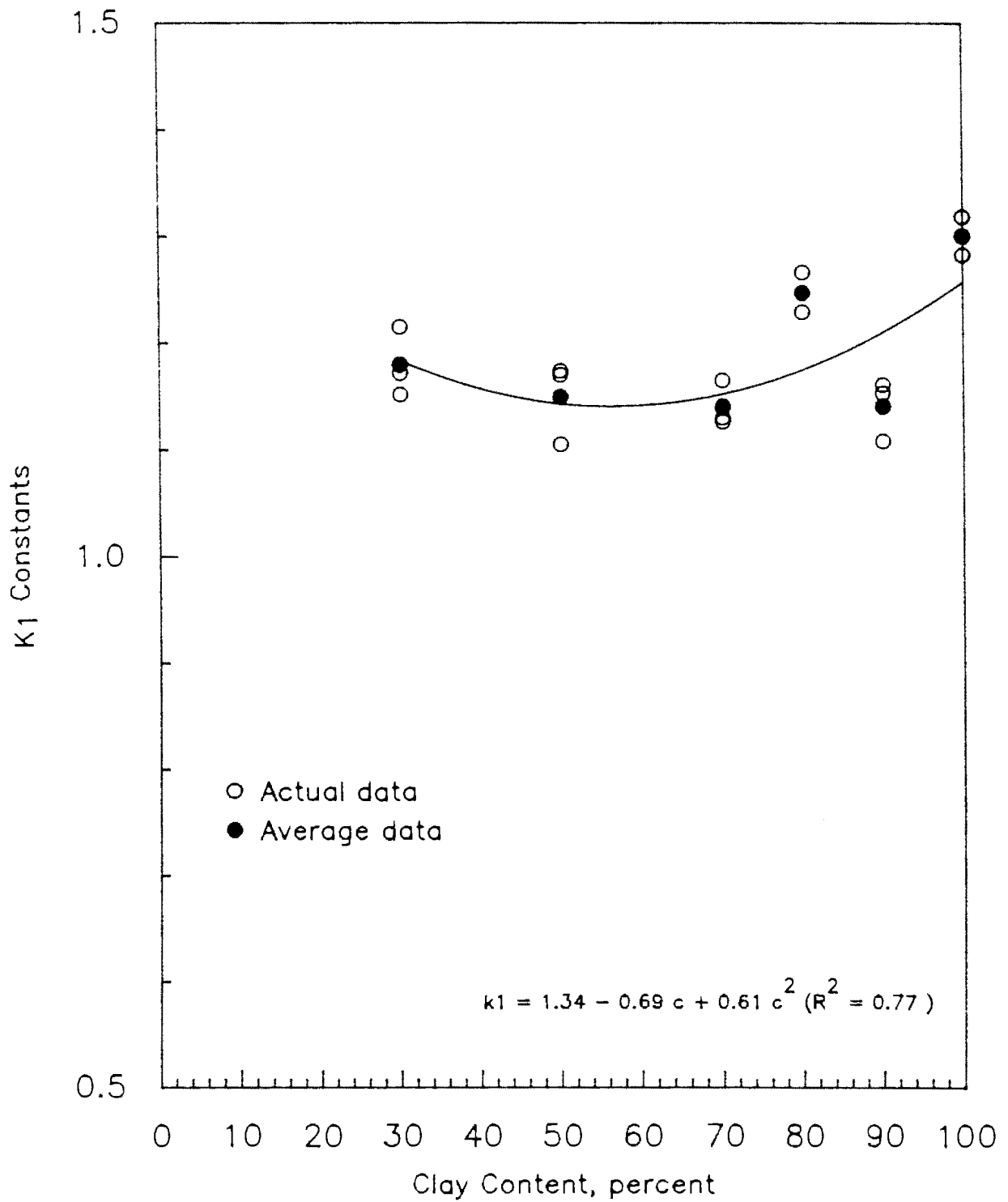


Figure 9.7 - Variation in Constant  $k_1$  from AASHTO/SHRP Model with Clay Content at Optimum Water Content for Cohesive Soil.

Table 9.1 Regression Constants for AASHTO/SHRP Models for Cohesive (Type 2) Soils

| MOISTURE CONTENT | REGRESSION* CONSTANT | A1     | A2     | A3    | R <sup>2</sup> |
|------------------|----------------------|--------|--------|-------|----------------|
| OPTIMUM          | k <sub>1</sub>       | 1.25   | -0.29  | 0.21  | 0.94           |
|                  | k <sub>2</sub>       | .276   | -2.38  | 2.23  | 0.86           |
| DRY              | k <sub>1</sub>       | 1.353  | 0.025  | -0.24 | 0.76           |
|                  | k <sub>2</sub>       | -0.375 | -0.006 | 0.38  | 0.85           |
| WET              | k <sub>1</sub>       | 1.897  | -3.21  | 2.62  | 0.91           |
|                  | k <sub>2</sub>       | 0.138  | -1.80  | 1.19  | 0.97           |

$$* M_R = 10^{k_1} \sigma_d^{k_2}$$

1 - 2 percent dry of optimum

2 - 2 percent wet of optimum

Table 9.2 Regression Constants for AASHTO/SHRP Models for Granular (Type 1) Soils

| MOISTURE CONTENT | REGRESSION* CONSTANT | A1     | A2     | A3      | R <sup>2</sup> |
|------------------|----------------------|--------|--------|---------|----------------|
| OPTIMUM          | k <sub>1</sub>       | 0.0844 | 8.35   | -49.34  | 0.85           |
|                  | k <sub>2</sub>       | 0.700  | -3.38  | 22.63   | 0.91           |
| DRY <sup>1</sup> | k <sub>1</sub>       | 0.214  | 5.24   | -33.21  | 0.86           |
|                  | k <sub>2</sub>       | 0.702  | -2.69  | 16.43   | 0.57           |
| WET <sup>2</sup> | k <sub>1</sub>       | -0.386 | 19.25  | -100.45 | 0.94           |
|                  | k <sub>2</sub>       | 1.12   | -12.94 | 65.66   | 0.86           |

$$* M_R = 10^{k_1} \theta^{k_2}$$

1 - 2 percent dry of optimum

2 - 2 percent wet of optimum

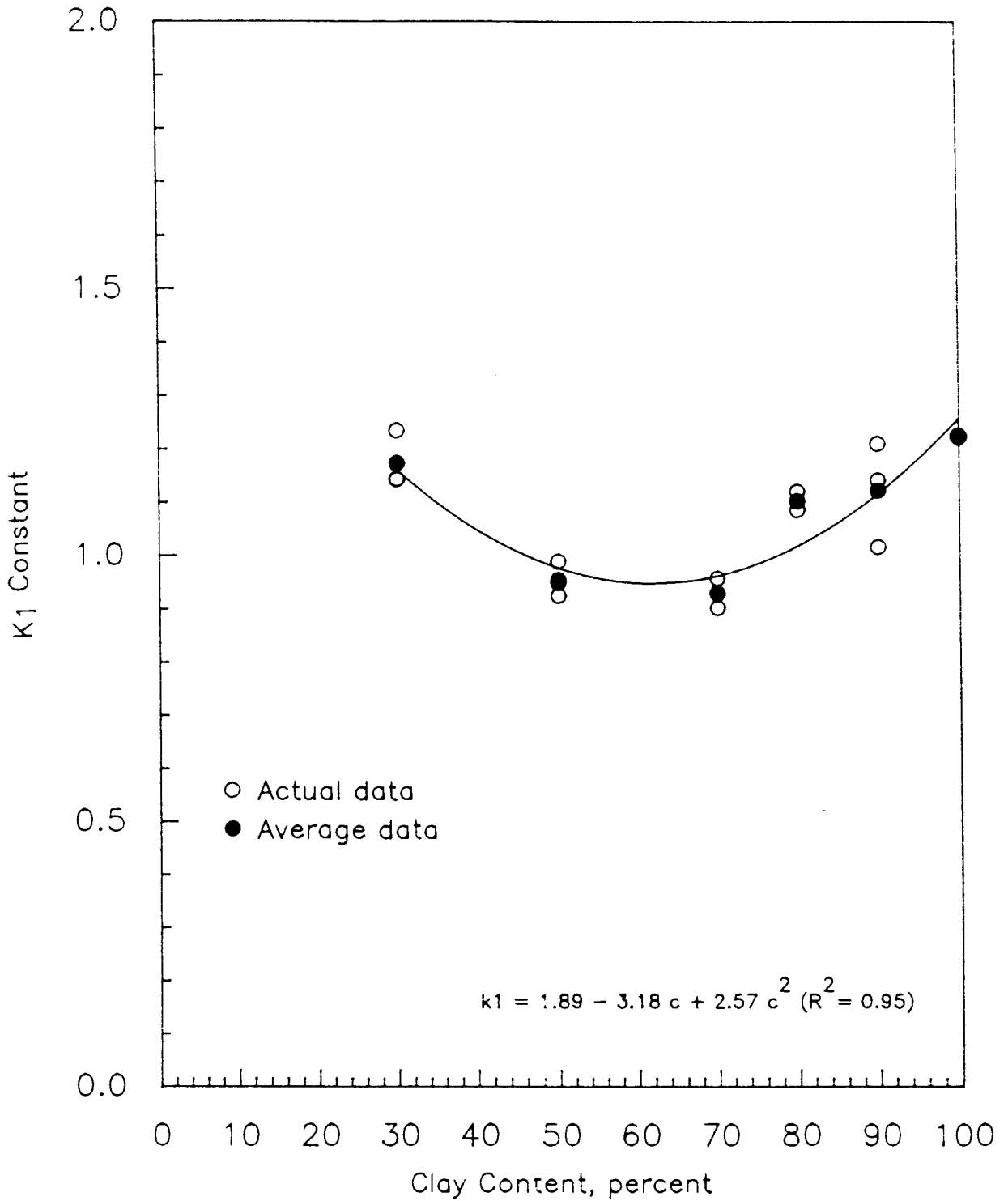
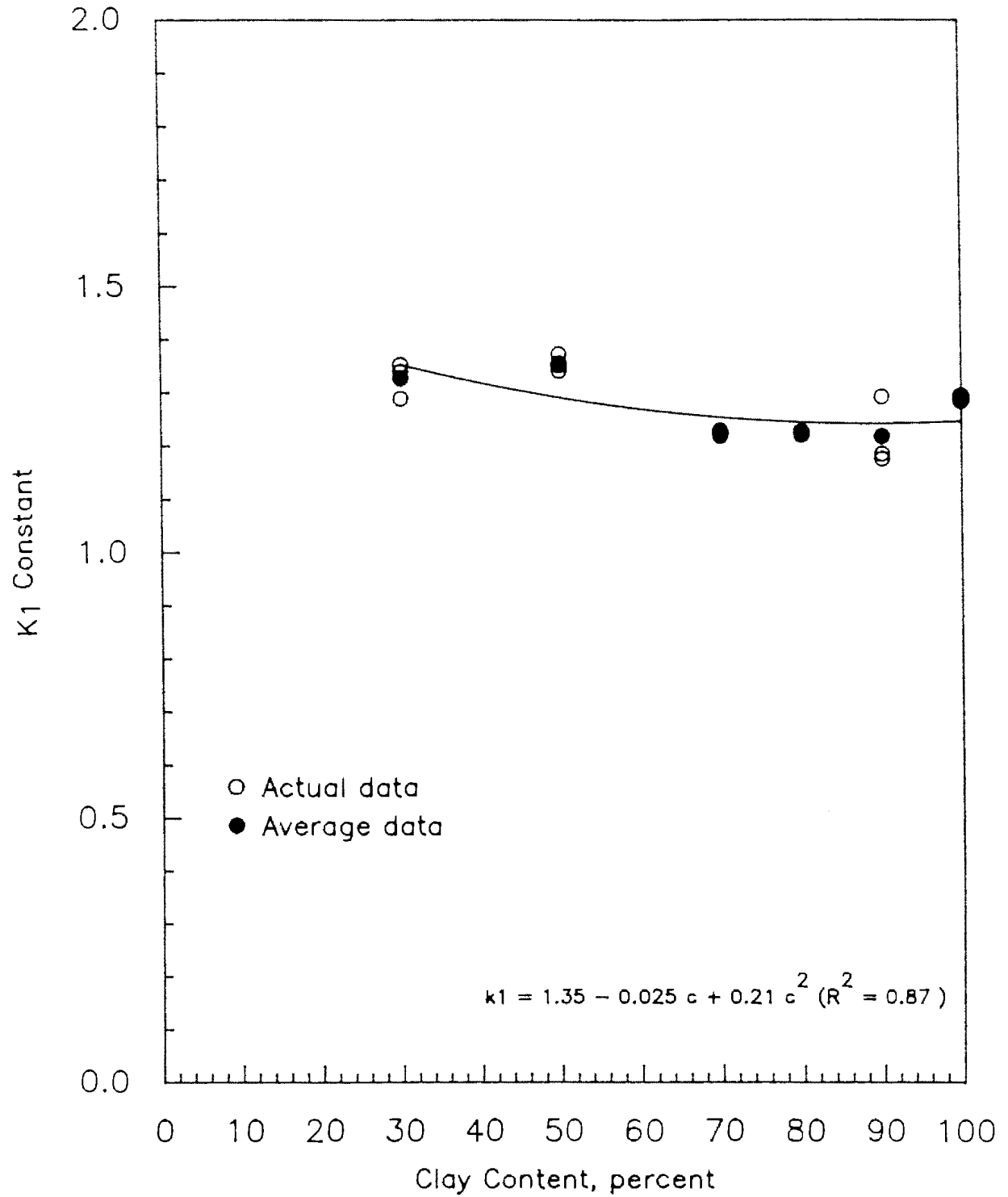


Figure 9.8 - Variation in Constant  $k_1$  from AASHTO/SHRP Model with Clay Content at Wet of Optimum Water Content for Cohesive Soil.



**Figure 9.9 - Variation in Constant  $k_1$  from AASHTO/SHRP Model with Clay Content at Dry of Optimum Water Content for Cohesive Soil.**

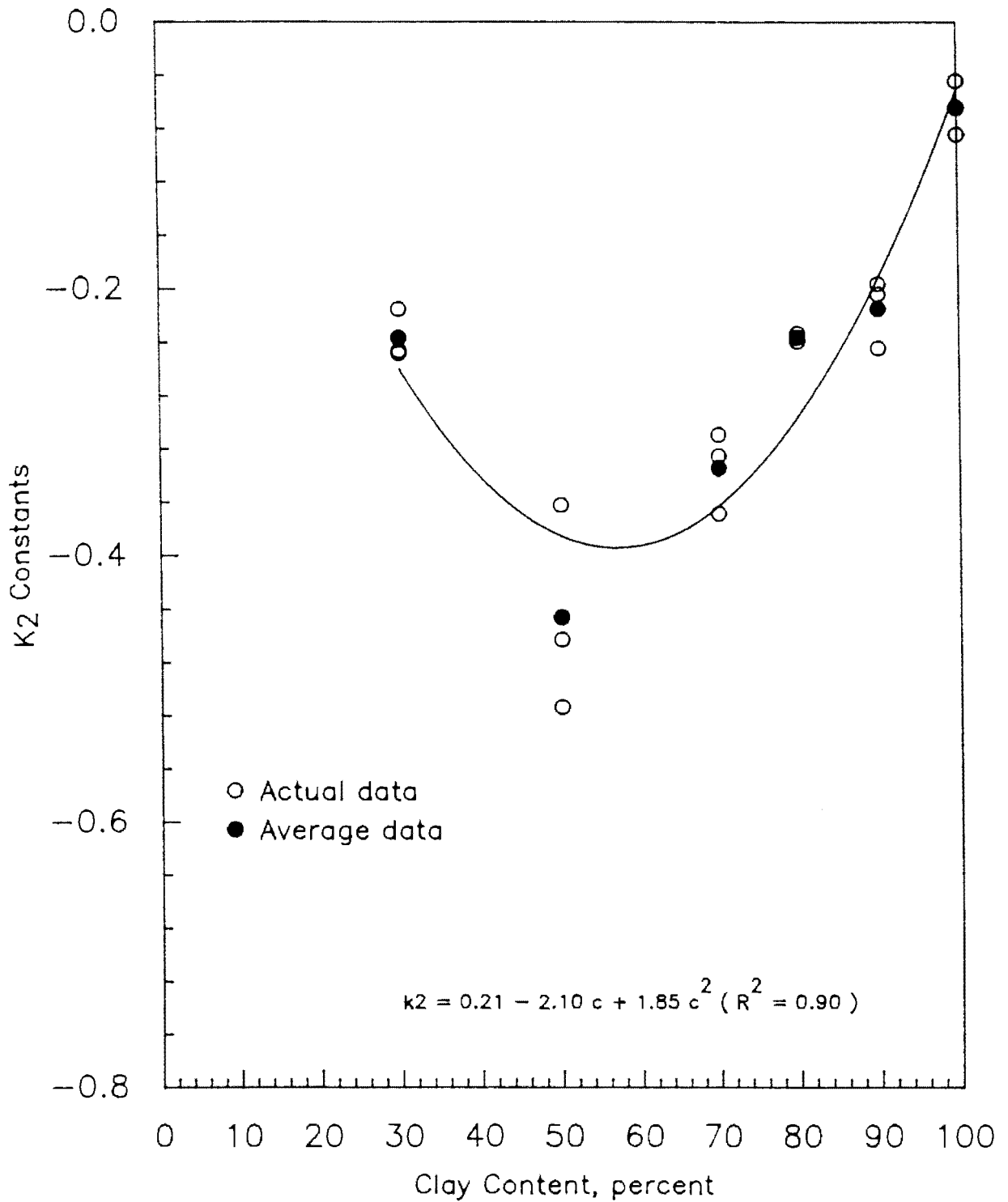


Figure 9.10 - Variation in Constant  $k_2$  from AASHTO/SHRP Model with Clay Content at Optimum Water Content for Cohesive Soil.

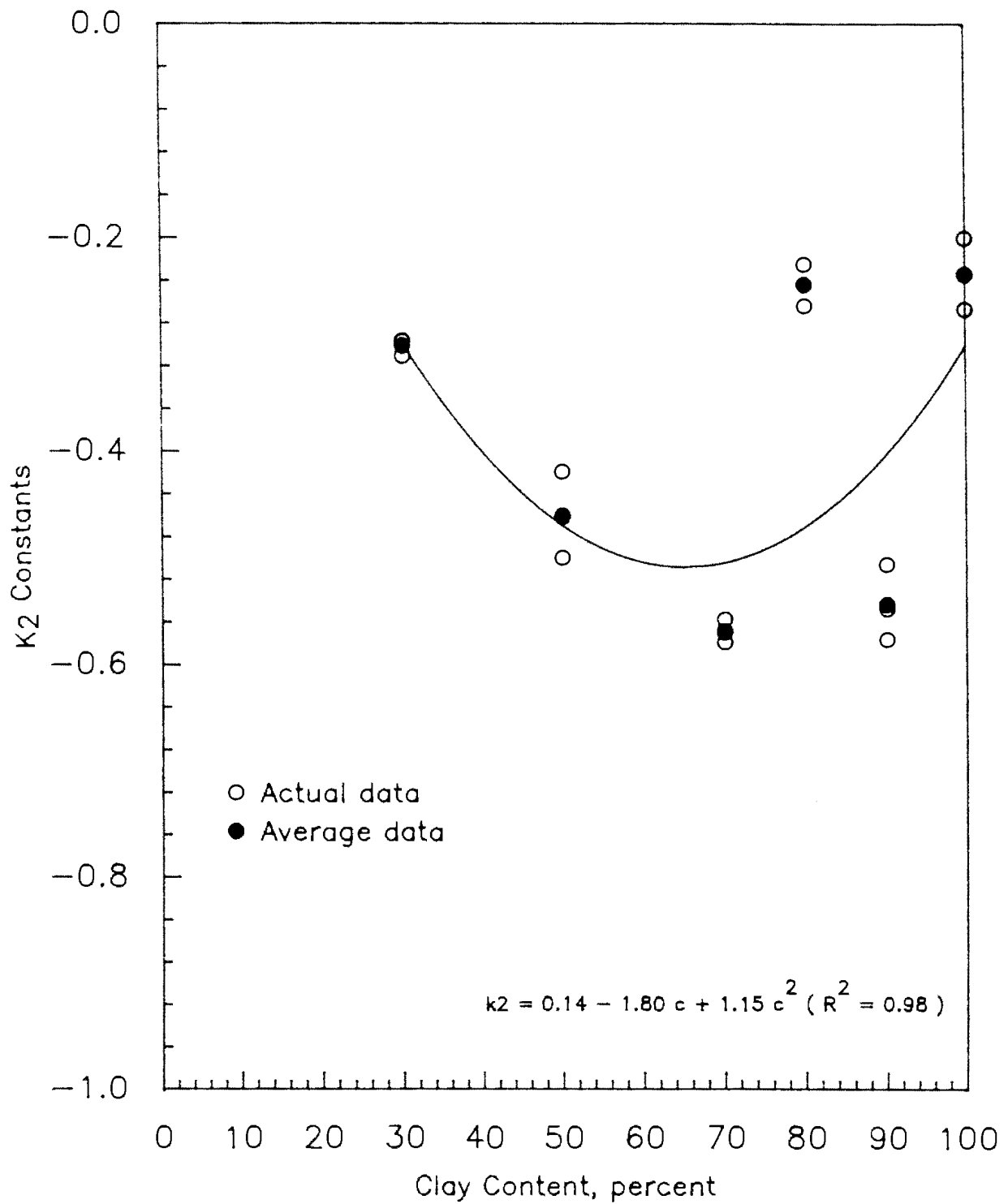


Figure 9.11 - Variation in Constant  $k_2$  from AASHTO/SHRP Model with Clay Content at Wet of Optimum Water Content for Cohesive Soil.

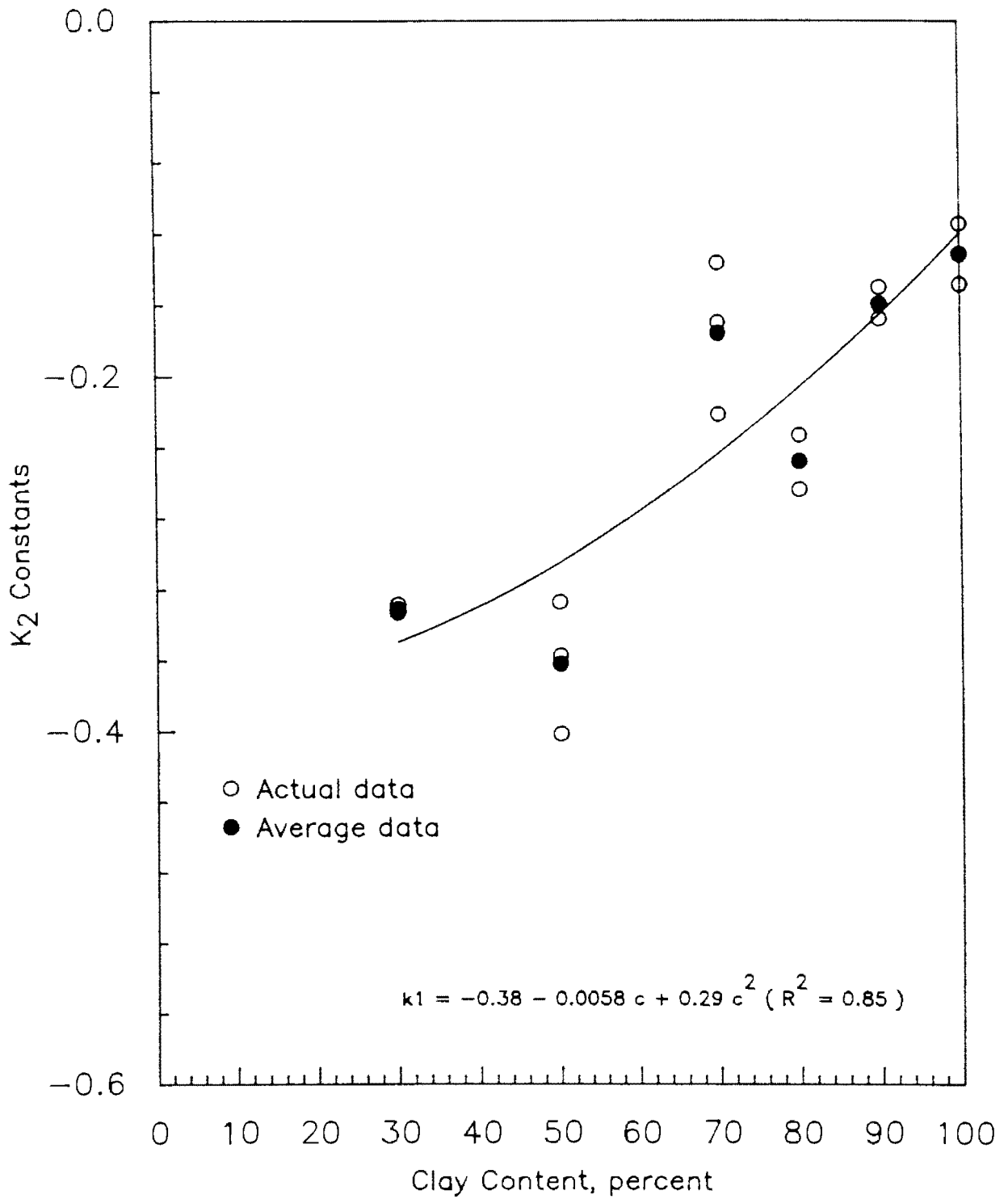


Figure 9.12 - Variation in Constant  $k_2$  from AASHTO/SHRP Model with Clay Content at Dry of Optimum Water Content for Granular Soil.

average values of  $k_1$  are shown in Figures 9.13 through 9.15 for samples tested at optimum water content, two percent wet of optimum and two percent dry of optimum, respectively. The clay content is limited to 15 percent as per SHRP protocol. For each case, the best-fit curve is also shown. The constants for this relationship are summarized in Table 9.2. Given the amount of scatter in data, the best-fit polynomials represent the average  $k_1$  data well. The slopes of the curves from the three water contents are quite similar with a maximum at a water content of 10 percent.

Similarly, the values of  $k_2$  as a function of clay content can be found in Figures 9.16 through 9.18 and the constants of the relationship can be seen in Table 9.2. The values obtained for  $k_2$  exhibit a larger scatter than that for  $k_1$ . Given the large scatter, the model describes the  $k_2$  - clay content relationship satisfactorily.

### 9.4.3 UTEP Models

Similarly, constants  $k_1$ ,  $k_2$  and  $k_3$  for the two UTEP models for both the granular and cohesive materials are determined and summarized in Tables 9.3 and 9.4. The data and fitted curves are included in Appendix F.

Typically, the average values of  $k_1$ ,  $k_2$  and  $k_3$  are well represented by Equation 9.5 utilizing the regression constants reported in Table 9.3 and Table 9.4. However, some scatter exists in the data. At optimum water content, the constants of Equation 9.4 for granular materials (less than 20 percent sand) exhibit large scatter at 5 percent clay content. However, for the other clay contents, the scatter is less evident. The scatter for the dry and wet specimens are almost as much.

For clay specimen described by Equation 9.4, the amount of scatter is much less but still substantial. In contrast, Equation 9.5 represents the relationship between  $k_1$ ,  $k_2$  and  $k_3$ , and clay content moderately well for specimens tested dry of and at optimum water content.

Equation 9.5 yields similar results for the model represented by Equation 9.3. For granular materials tested at optimum water content, the specimens tested at 5 percent clay content exhibit large scatter. Once again, the average  $k_1$ ,  $k_2$  and  $k_3$  are represented well by Equation 9.5. The samples tested dry exhibit large scatter, but once again the average values are well represented. In contrast, the specimens tested wet of optimum water content do not exhibit large scatter and are in good agreement with Equation 9.5.

For clayey materials described with Equation 9.3, Equation 9.5 does not yield representation  $k_1$ ,  $k_2$  and  $k_3$  values suitable for optimum water content. However, the specimens tested wet and dry of optimum water content are well represented.

## 9.5 Evaluation of Accuracy of Models

To evaluate the accuracy of the models proposed, the modulus values obtained from laboratory testing was compared with those obtained from the models. As examples, the results from the

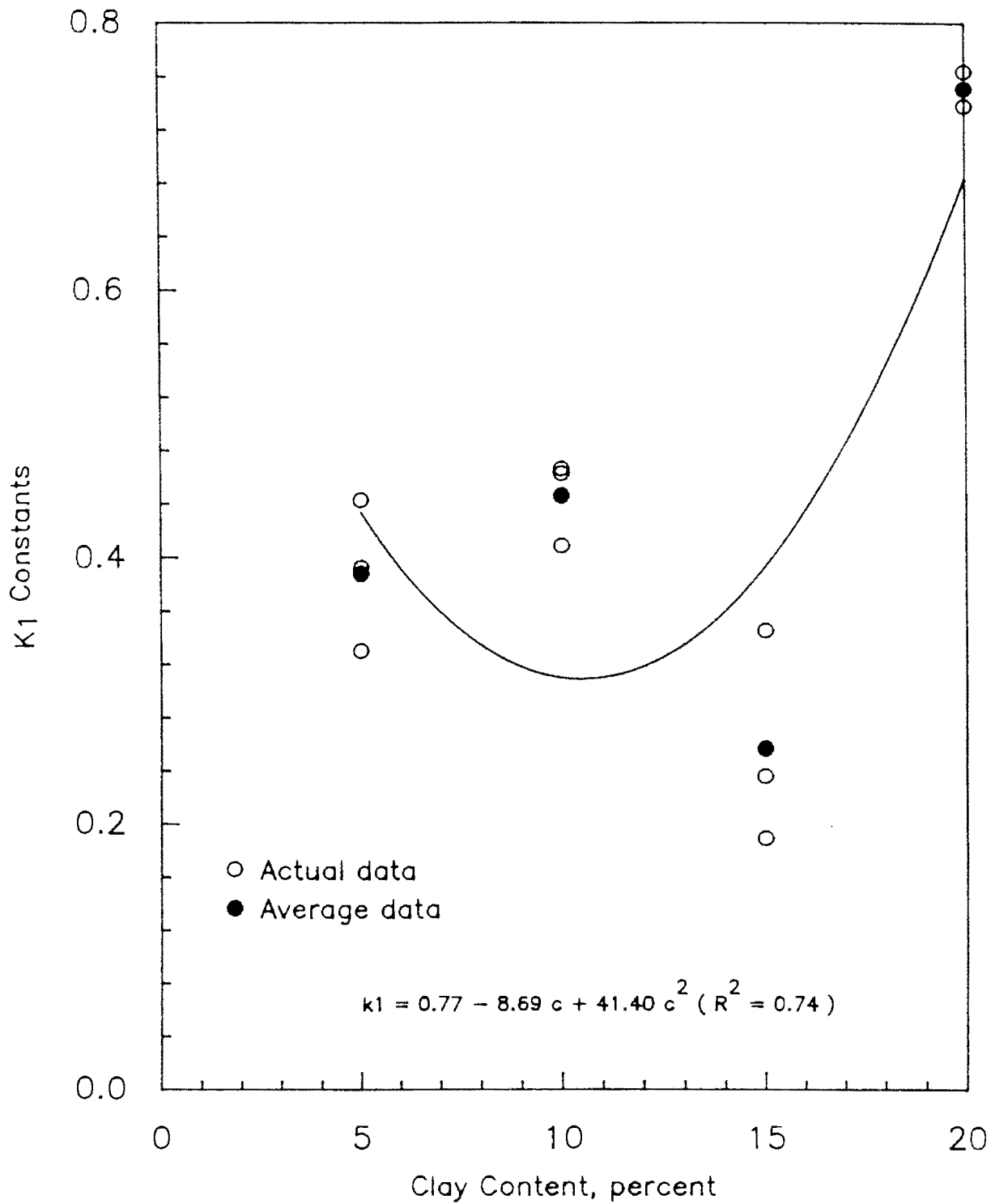


Figure 9.13 - Variation in Constant  $k_1$  from AASHTO/SHRP Model with Clay Content at Optimum Water Content for Granular Soil.

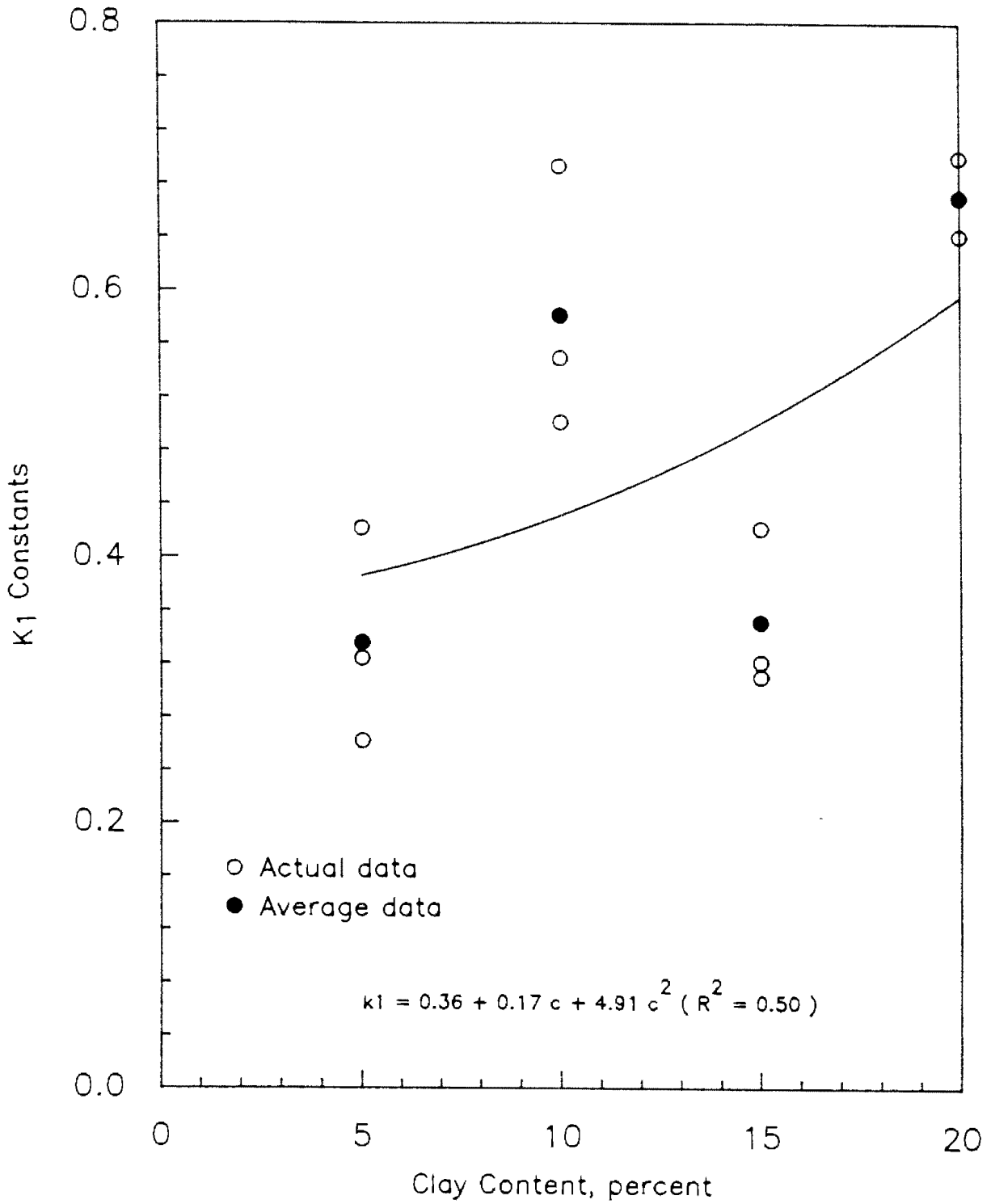


Figure 9.14 - Variation in Constant  $k_1$  from AASHTO/SHRP Model with Clay Content at Wet of Optimum Water Content for Granular Soil.

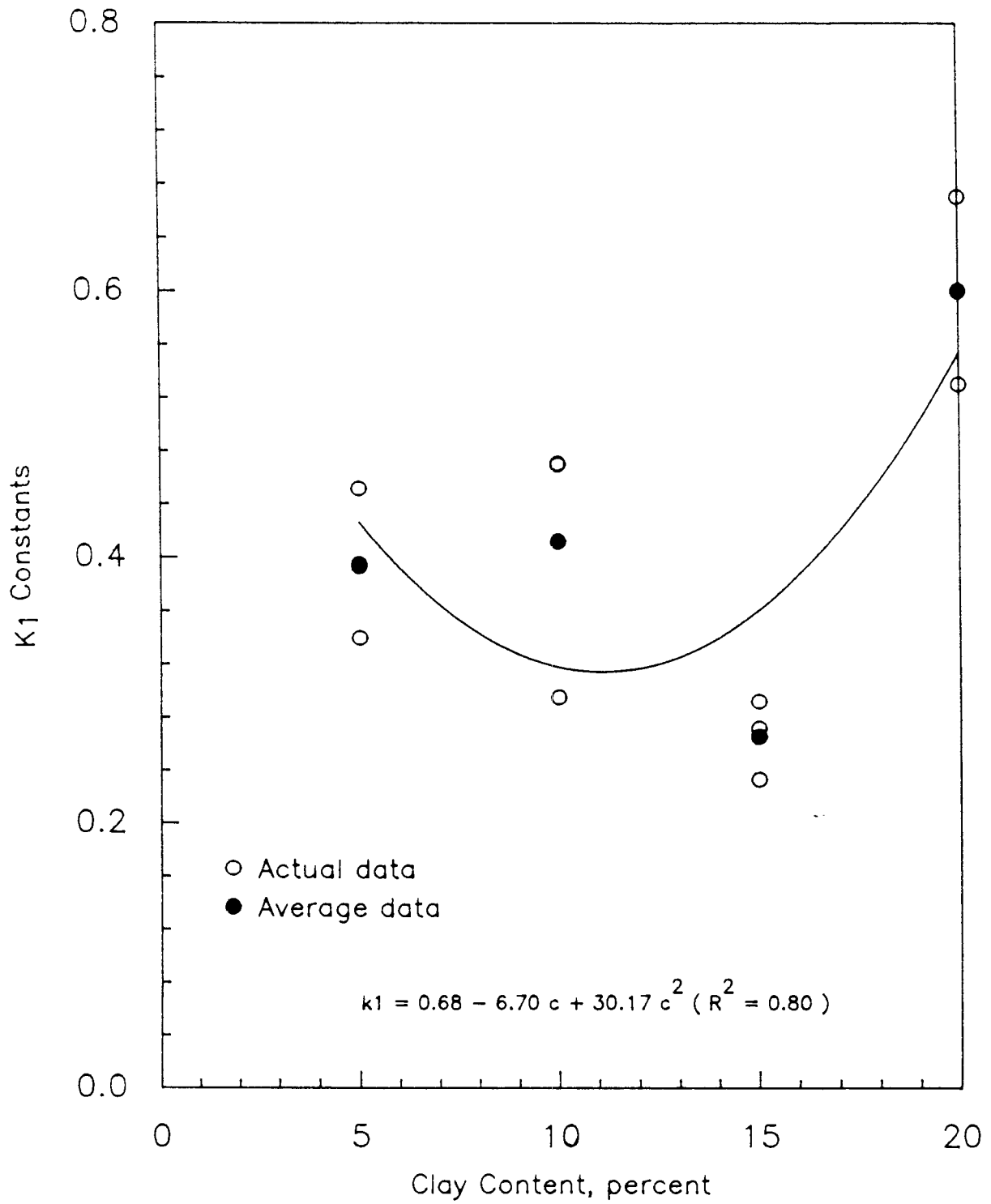


Figure 9.15 - Variation in Constant  $k_1$  from AASHTO/SHRP Model with Clay Content at Dry of Optimum Water Content for Granular Soil.

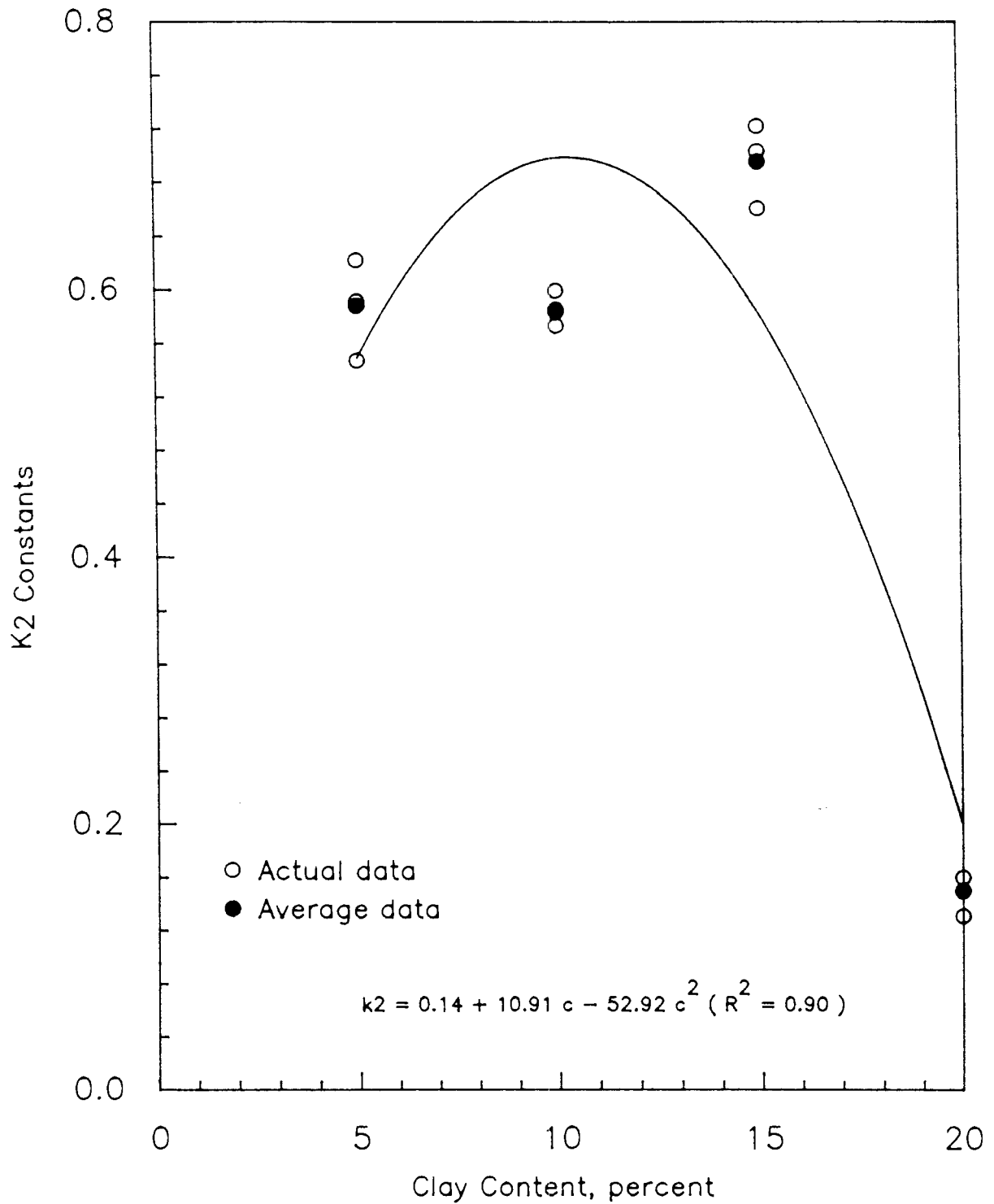


Figure 9.16 - Variation in Constant  $k_2$  from AASHTO/SHRP Model with Clay Content at Optimum Water Content for Granular Soil.

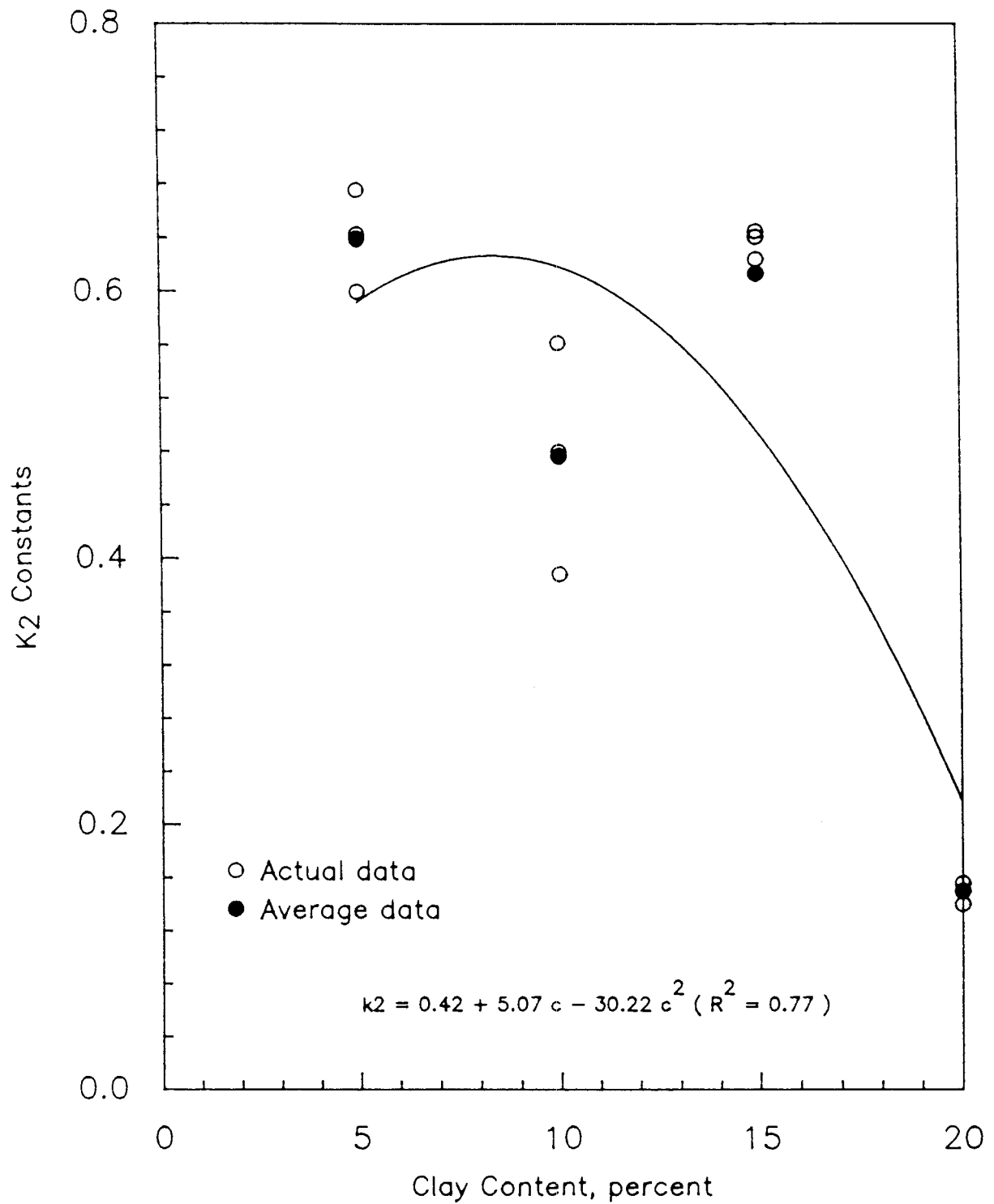


Figure 9.17 - Variation in Constant  $k_2$  from AASHTO/SHRP Model with Clay Content at Wet of Optimum Water Content for Granular Soil.

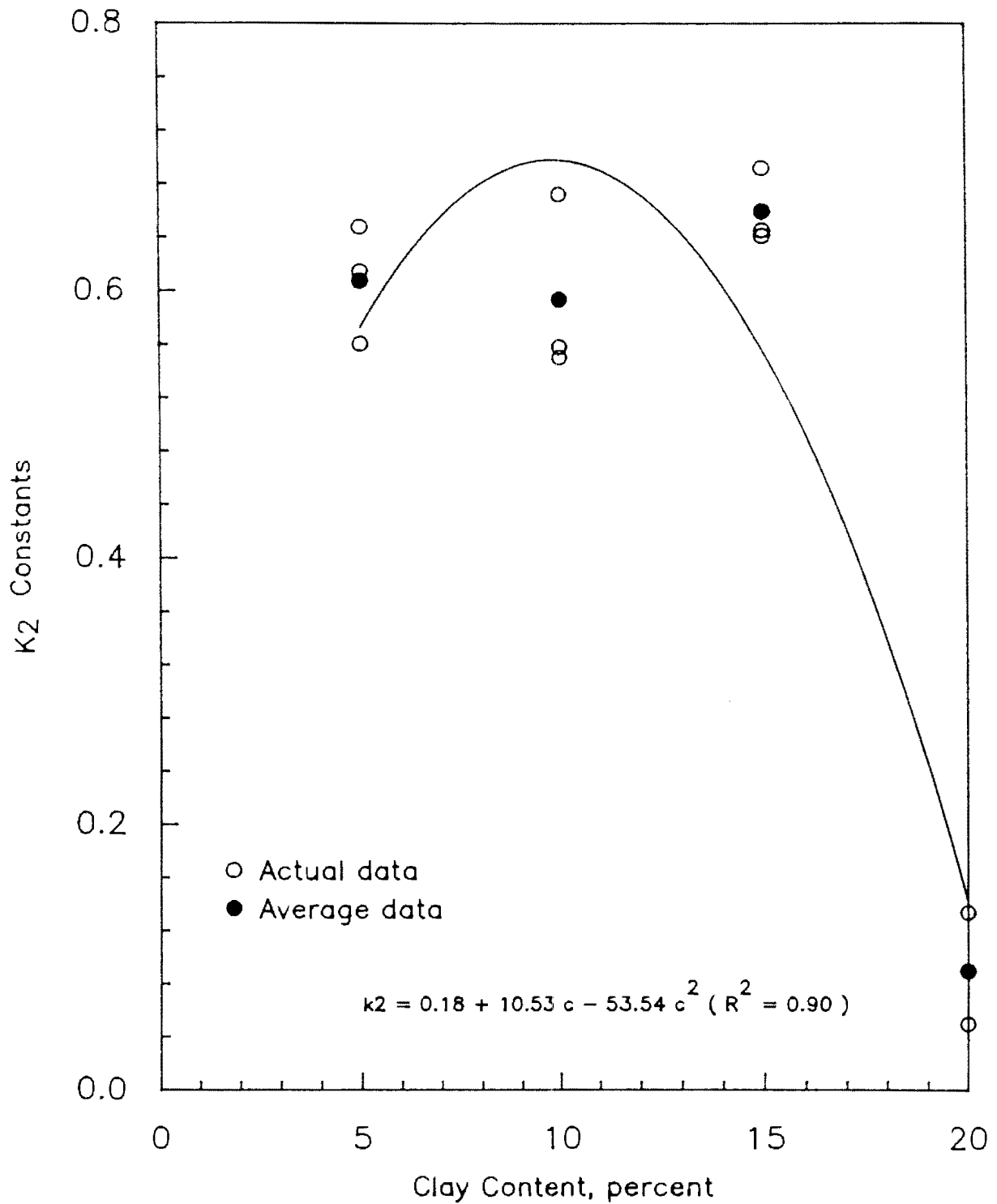


Figure 9.18 - Variation in Constant  $k_2$  from AASHTO/SHRP Model with Clay Content at Dry of Optimum Water Content for Granular Soil.

Table 9.3 Regression Constants for UTEP Model One

a) Granular (Type 1) Soils

| MOISTURE CONTENT | REGRESSION* CONSTANT | A <sub>1</sub> | A <sub>2</sub> | A <sub>3</sub> | R <sup>2</sup> |
|------------------|----------------------|----------------|----------------|----------------|----------------|
| OPTIMUM          | k <sub>1</sub>       | -0.473         | 10.21          | -73.68         | 0.92           |
|                  | k <sub>2</sub>       | 0.504          | -2.39          | -1.75          | 0.56           |
|                  | k <sub>3</sub>       | -0.179         | 0.81           | -11.68         | 0.88           |
| DRY <sup>1</sup> | k <sub>1</sub>       | -0.807         | 10.7           | -65.57         | 0.66           |
|                  | k <sub>2</sub>       | 0.401          | 1.53           | -7.36          | 0.29           |
|                  | k <sub>3</sub>       | -0.405         | 3.27           | -18.91         | 0.56           |
| WET <sup>2</sup> | k <sub>1</sub>       | -1.441         | 22.83          | -110.23        | 0.94           |
|                  | k <sub>2</sub>       | 0.669          | -5.08          | 35.28          | 0.42           |
|                  | k <sub>3</sub>       | -0.533         | 5.66           | 27.23          | 0.88           |

b) Cohesive (Type 2) Soils

| MOISTURE CONTENT | REGRESSION* CONSTANT | A <sub>1</sub> | A <sub>2</sub> | A <sub>3</sub> | R <sup>2</sup> |
|------------------|----------------------|----------------|----------------|----------------|----------------|
| OPTIMUM          | k <sub>1</sub>       | 1.600          | -7.26          | 6.52           | 0.70           |
|                  | k <sub>2</sub>       | 0.009          | 0.80           | -0.85          | 0.43           |
|                  | k <sub>3</sub>       | 0.0946         | -1.51          | -1.35          | 0.81           |
| DRY <sup>1</sup> | k <sub>1</sub>       | -0.341         | 0.60           | 0.21           | 0.91           |
|                  | k <sub>2</sub>       | 0.241          | -0.30          | 0.27           | 0.51           |
|                  | k <sub>3</sub>       | -0.168         | -0.57          | 0.65           | 0.90           |
| WET <sup>2</sup> | k <sub>1</sub>       | -0.784         | -4.22          | 2.83           | 0.93           |
|                  | k <sub>2</sub>       | 0.372          | -0.69          | 0.62           | 0.60           |
|                  | k <sub>3</sub>       | -0.128         | -0.60          | 0.35           | 0.94           |

$$M_R = 10^{k_1} \theta^{k_2} \epsilon^{k_3}$$

1 - 2 percent dry of optimum

2 - 2 percent wet of optimum

Table 9.4 Regression Constants for UTEP Model Two

a) Granular (Type 1) Soils

| MOISTURE CONTENT | REGRESSION* CONSTANT | A <sub>1</sub> | A <sub>2</sub> | A <sub>3</sub> | R <sup>2</sup> |
|------------------|----------------------|----------------|----------------|----------------|----------------|
| OPTIMUM          | k <sub>1</sub>       | -0.0854        | 15.45          | -102.28        | 0.90           |
|                  | k <sub>2</sub>       | 0.478          | -1.25          | -6.55          | 0.30           |
|                  | k <sub>3</sub>       | -0.278         | 4.64           | -30.64         | 0.87           |
| DRY <sup>1</sup> | k <sub>1</sub>       | -0.520         | 16.71          | -100.13        | 0.67           |
|                  | k <sub>2</sub>       | 0.395          | 0.08           | 0.22           | 0.56           |
|                  | k <sub>3</sub>       | -0.459         | 6.16           | -33.67         | 0.64           |
| WET <sup>2</sup> | k <sub>1</sub>       | -0.828         | 20.4           | -99.25         | 0.86           |
|                  | k <sub>2</sub>       | 0.395          | -10.05         | 3.42           | 0.43           |
|                  | k <sub>3</sub>       | -0.532         | 7.04           | -34.25         | 0.88           |

b) Cohesive (Type 2) Soils

| MOISTURE CONTENT | REGRESSION* CONSTANT | A <sub>1</sub> | A <sub>2</sub> | A <sub>3</sub> | R <sup>2</sup> |
|------------------|----------------------|----------------|----------------|----------------|----------------|
| OPTIMUM          | k <sub>1</sub>       | 1.728          | -6.55          | 5.75           | 0.85           |
|                  | k <sub>2</sub>       | -0.048         | 0.75           | -0.75          | 0.43           |
|                  | k <sub>3</sub>       | 0.132          | -1.51          | 1.36           | 0.85           |
| DRY <sup>1</sup> | k <sub>1</sub>       | 0.281          | 0.22           | 0.5            | 0.86           |
|                  | k <sub>2</sub>       | 0.131          | 0.10           | 0.07           | 0.26           |
|                  | k <sub>3</sub>       | -0.256         | -0.13          | 0.31           | 0.82           |
| WET <sup>2</sup> | k <sub>1</sub>       | 1.424          | -5.55          | 3.28           | 0.97           |
|                  | k <sub>2</sub>       | 0.225          | -0.44          | 0.44           | 0.70           |
|                  | k <sub>3</sub>       | -0.024         | -0.892         | 0.65           | 0.98           |

$$M_R = 10^{k_1} \sigma_c^{k_2} \epsilon^{k_3}$$

1 - 2 percent dry of optimum

2 - 2 percent wet of optimum

developed models were compared with those of a predominantly cohesive specimen (i.e. 90 percent and 10 percent sand mixture as demonstrated in Figure 8.4) and a predominantly granular specimen (i.e. 10 percent and 90 percent as demonstrated in Figure 8.5). In each case, the difference between the modulus values obtained in the laboratory and those predicted with the proposed models was determined and plotted. To calculate the predicted modulus, Equation 9.5 was first utilized to determine the constants  $k_1$ ,  $k_2$ , and  $k_3$  as a function of clay content. The constants of Equation 9.5 were selected from Tables 9.3 and 9.4. Knowing parameter  $k_1$ ,  $k_2$  and  $k_3$ , the modulus was then estimated using one of the four constitutive models (Equation 9.1 through 9.4).

The difference between the calculated and measured moduli, from the simplified procedure described above, is exhibited in Figure 9.19 for the AASHTO/SHRP model. The difference between the calculated and measured values is as high as 50 percent but typically within 30 percent. The general trend is that the results are slightly underestimated.

The same procedure followed for the AASHTO/SHRP model was applied to the UTEP model. The differences are depicted in Figure 9.20. In all cases, this model overpredicted the modulus by a minimum of 25 percent. This may result in the underdesign of the pavement. Also, the variations are not randomly distributed. The higher the bulk stress, the larger the variation between the measured and calculated moduli will be.

The deviation between the measured and calculated moduli at each confining pressure and deviatoric stress for Model Two is shown in Figure 9.21. In this case, the level of scatter is smaller than those of the previous two models. From small and medium confining pressures, the variation between the calculated and measured moduli are within 15 percent. At higher confining pressures, the modulus is typically overestimated by 10 to 30 percent.

A similar example is presented for the cohesive specimen. The difference in the calculated and measured moduli using the simplified procedure and AASHTO/SHRP model is shown in Figure 9.22. The deviation is rather small and is limited to 20 percent. The errors are randomly distributed.

The results from UTEP's Model One and Model Two are presented in Figures 9.23 and 9.24, respectively. Once again, Model One overpredicts the modulus values. In this case, the second model yields moduli that are always measured less than ones. For both results, the scatter in data is more pronounced than the scatter from the AASHTO/SHRP model.

To evaluate the models more comprehensively, the typical percent differences between the calculated and measured moduli are summarized in Table 9.5 for granular materials. A comparison of the differences from the three methods reveals that probably the AASHTO/SHRP relationship should be used for this simplified methodology. As reflected in Table 9.5a, from AASHTO/SHRP model, the modulus values are predicted within 30 to 40 percent. In most cases, the other two models yield similar results. But, the differences are not randomly distributed. It, therefore, seems practical and reasonable to use the AASHTO/SHRP model with the simplified model described here.

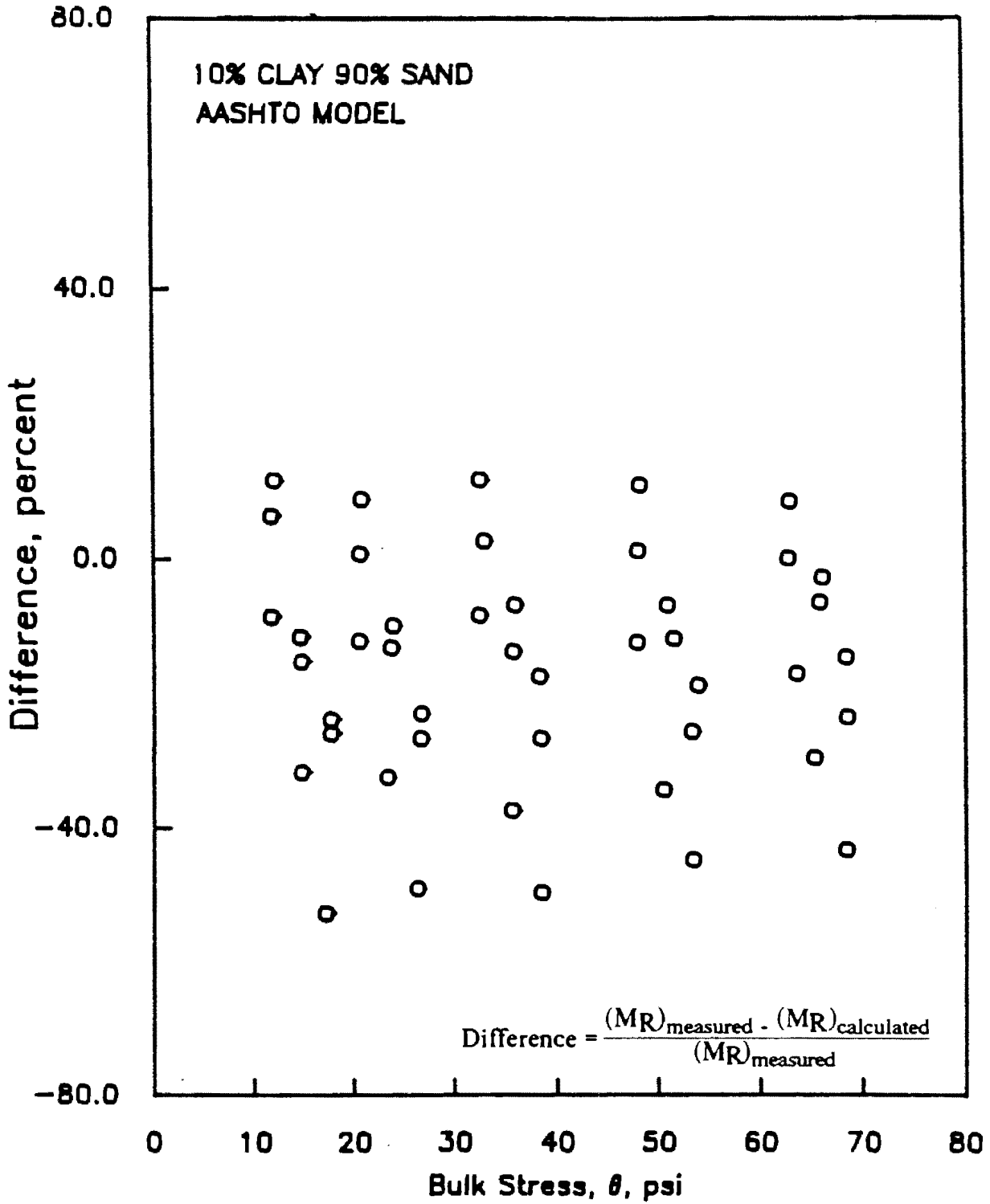


Figure 9.19 - Typical Variation in Percent Difference Between Measured and Modelled Moduli Using Simplified Relationship for Regression Constants of AASHTO/SHRP Model.

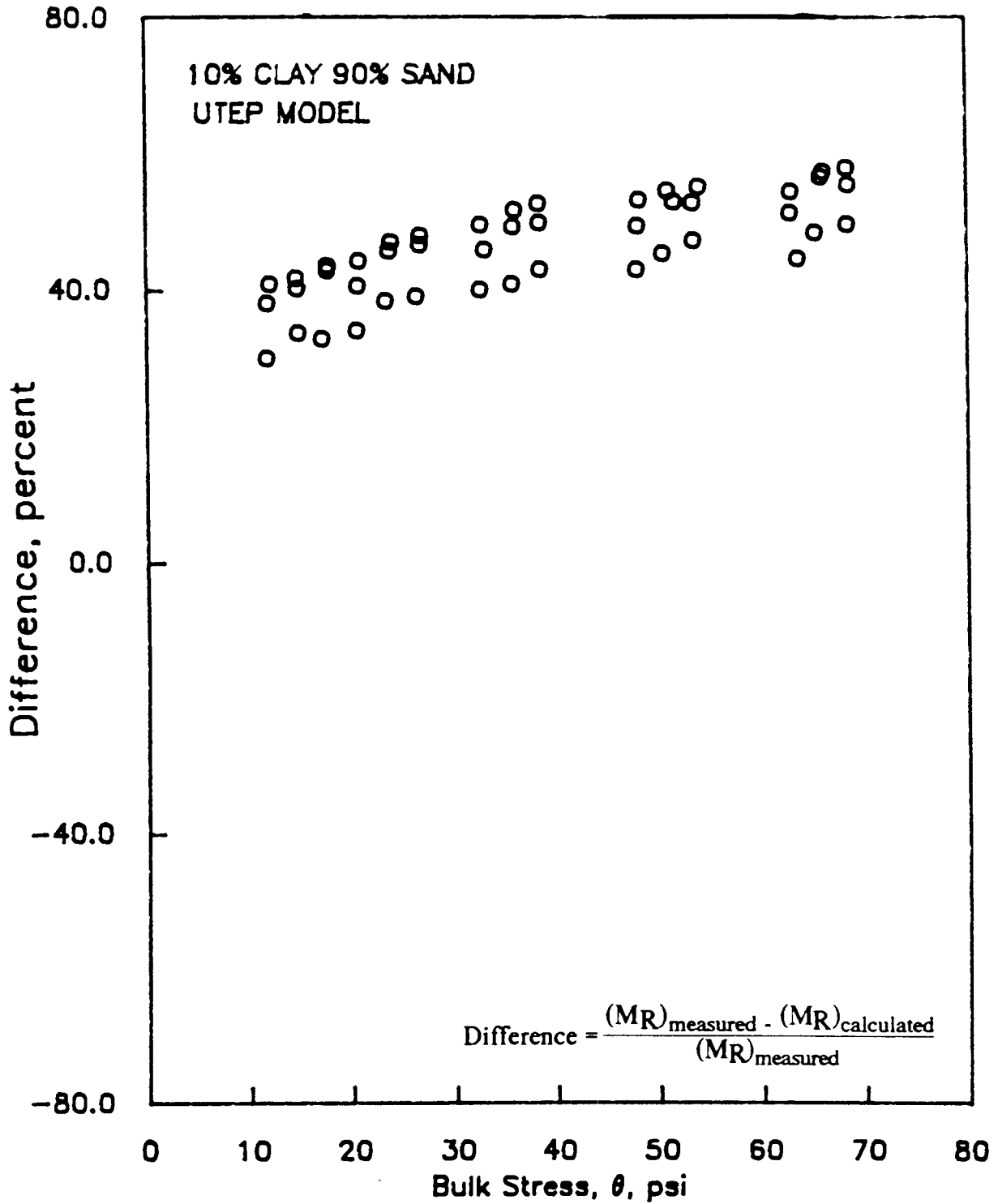


Figure 9.20 - Typical Variation in Percent Difference Between Measured and Modelled Moduli Using Simplified Relationship for Regression Constants of Model One.

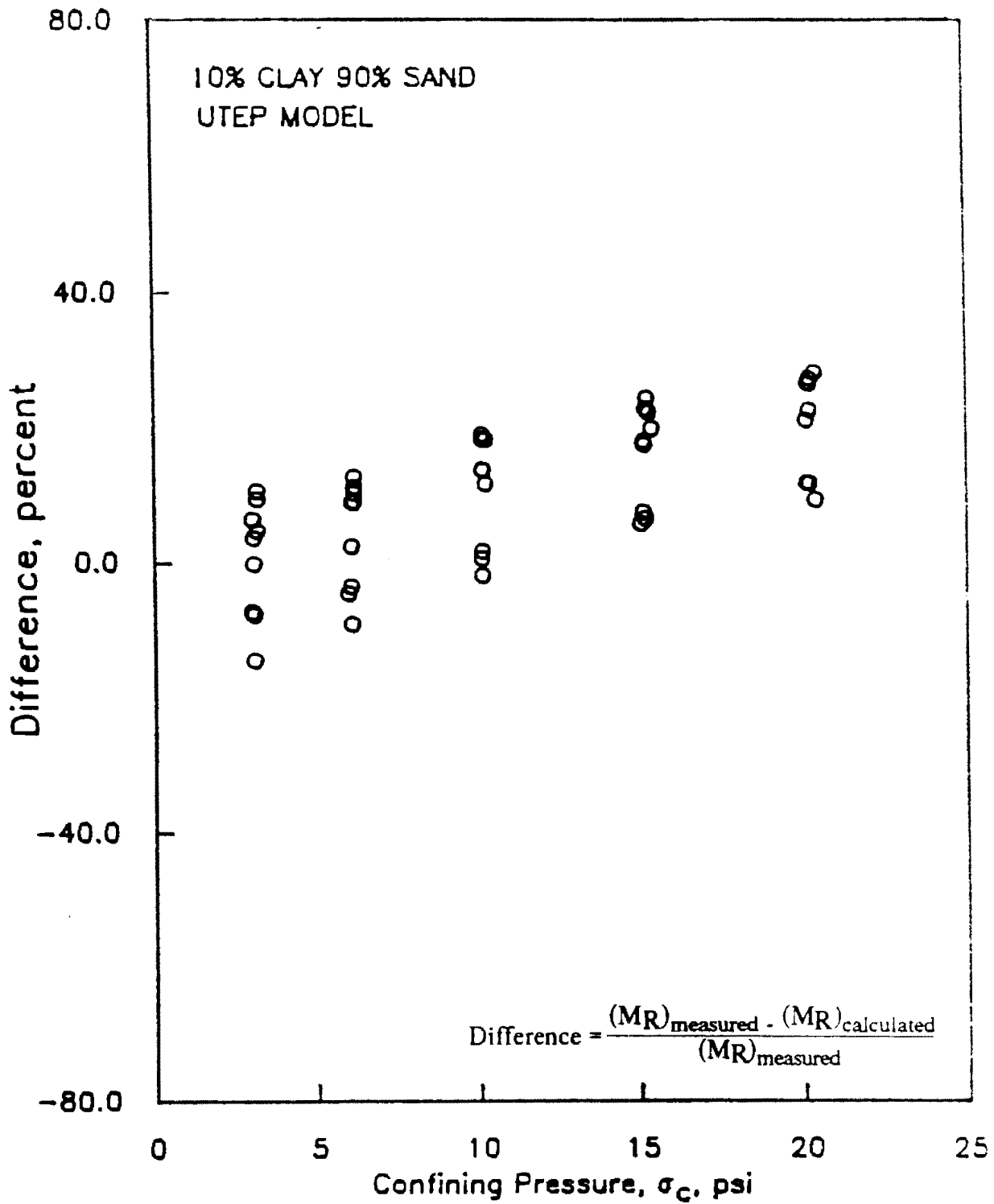


Figure 9.21 - Typical Variation in Percent Difference Between Measured and Modelled Moduli Using Simplified Relationship for Regression Constants of Model Two.

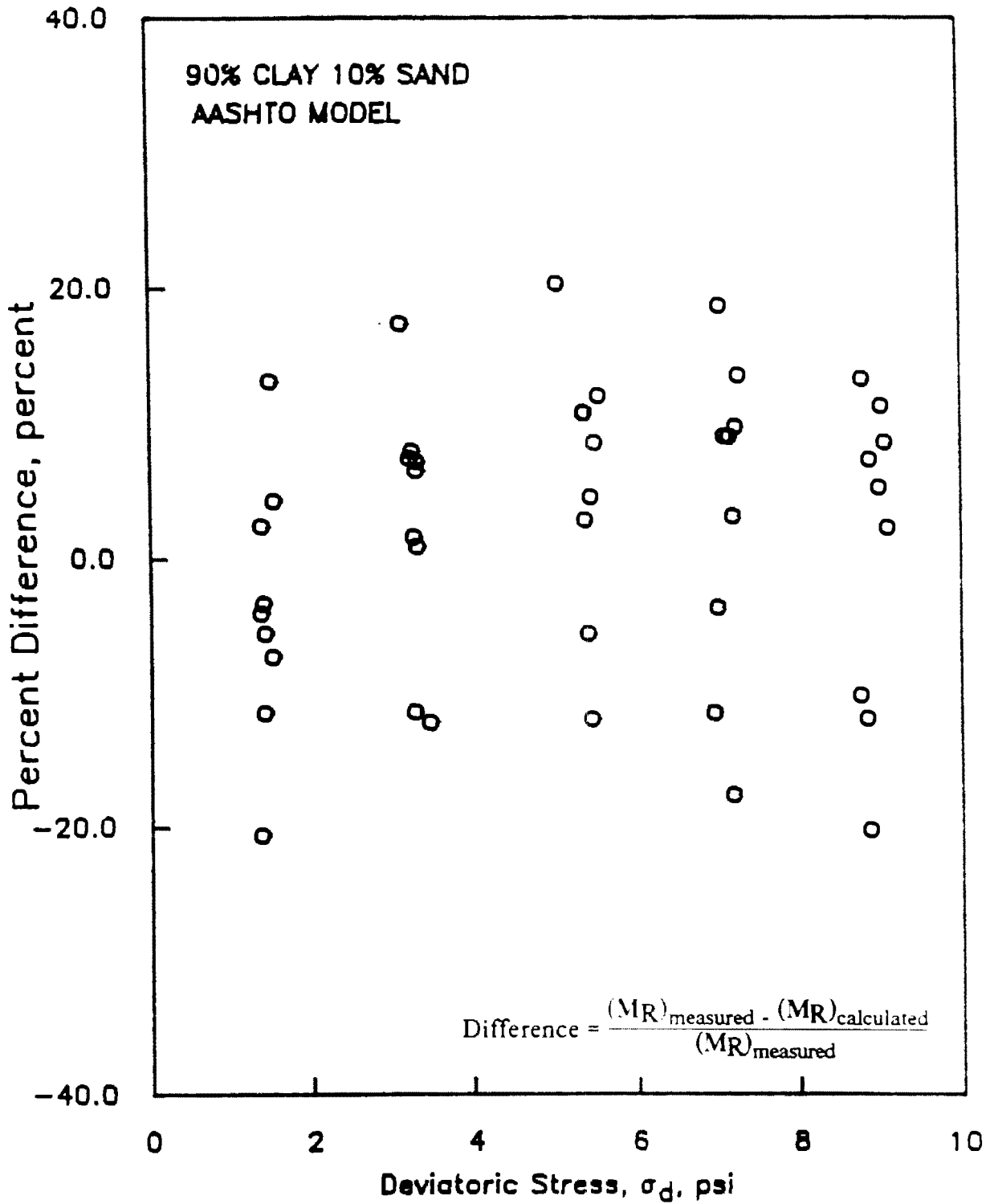


Figure 9.22 - Typical Variation in Percent Difference Between Measured and Modelled Moduli Using Simplified Relationship for Regression Constants of AASHTO/SHRP Model.

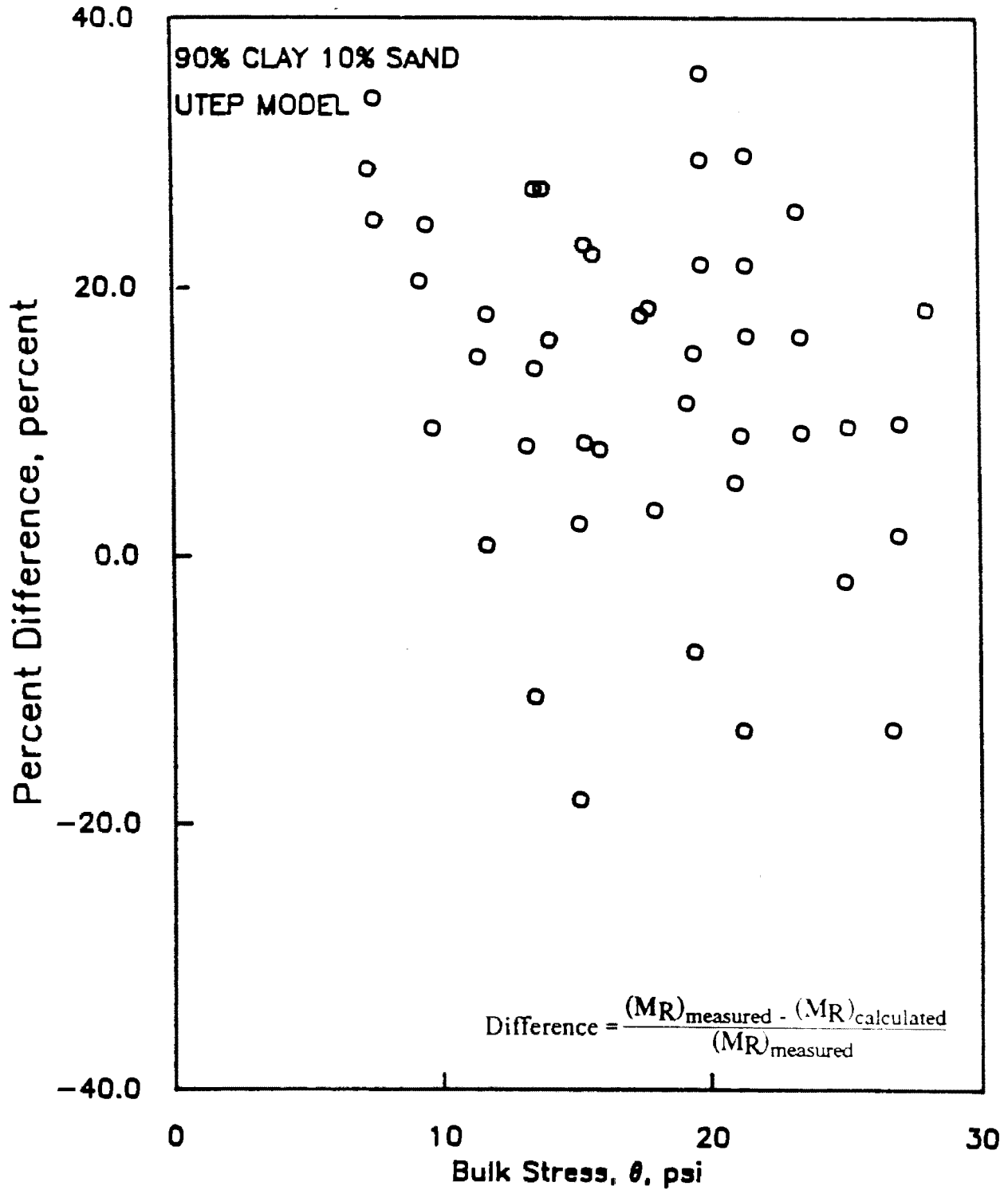


Figure 9.23 - Typical Variation in Percent Difference Between Measured and Modelled Moduli Using Simplified Relationship for Regression Constants of Model One.

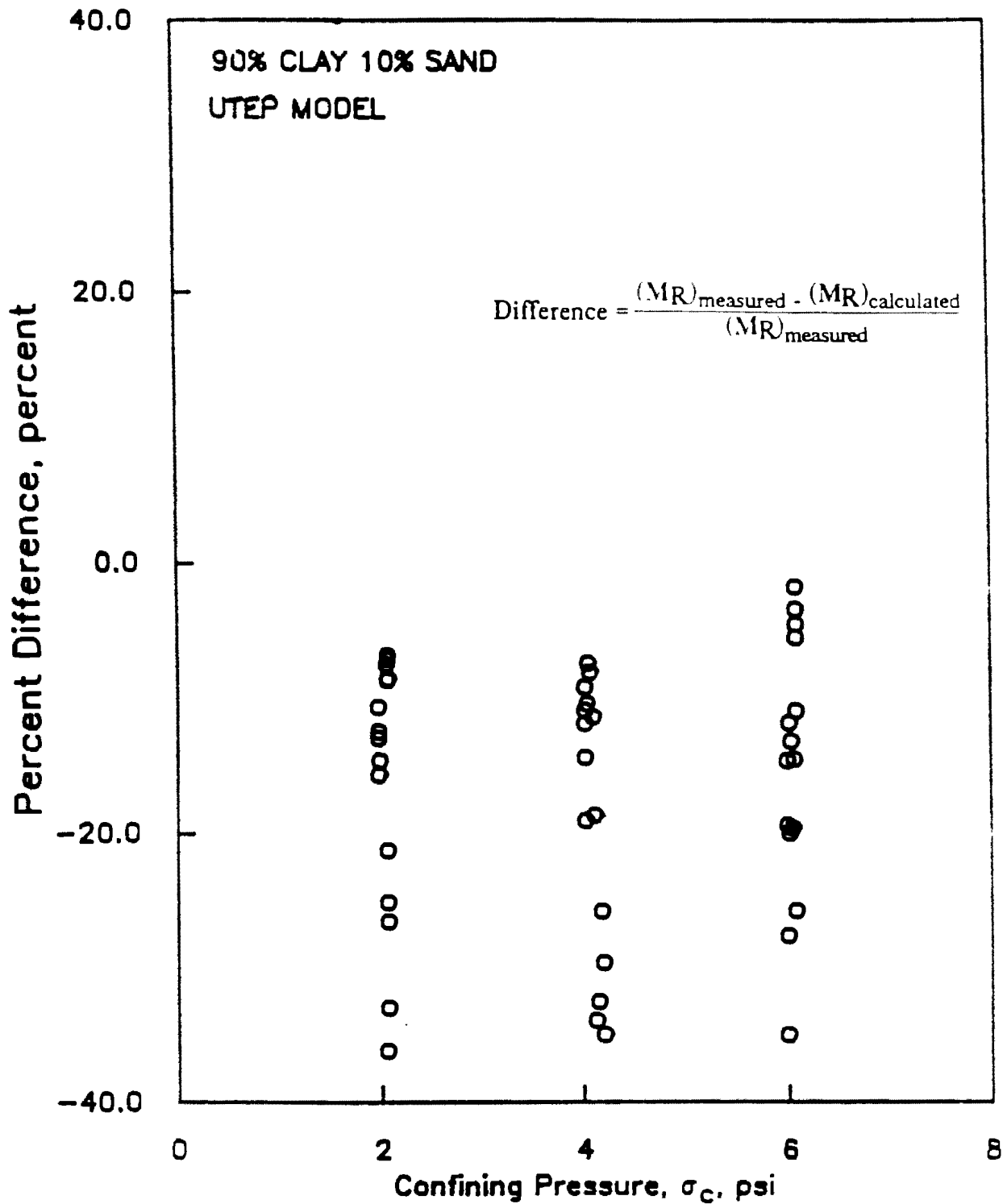


Figure 9.24 - Typical Variation in Percent Difference Between Measured and Modelled Moduli Using Simplified Relationship for Regression Constants of Model Two.

Table 9.5 Typical Differences between Measured and Calculated Moduli from Three Models (Granular Soils)

a) AASHTO/SHRP Model ( $MR = 10^{k_1} \theta^{k_2}$ )

| Clay Content | Difference, Percent <sup>1</sup> |                  |                  |
|--------------|----------------------------------|------------------|------------------|
|              | Optimum                          | Dry <sup>2</sup> | Wet <sup>3</sup> |
| 15           | 30                               | 40               | 30               |
| 10           | 30                               | 30               | 30               |
| 5            | 20                               | 10               | 40               |

1 - Difference =  $\frac{(MR)_{\text{measured}} - (MR)_{\text{calculated}}}{(MR)_{\text{measured}}} * 100$

2 - Dry = 2 percent dry of optimum water content

3 - Wet = 2 percent wet of optimum water content

b) UTEP Model One ( $MR = 10^{k_1} \theta^{k_2}$ )

| Clay Content | Difference, Percent <sup>1</sup> |                  |                  |
|--------------|----------------------------------|------------------|------------------|
|              | Optimum                          | Dry <sup>2</sup> | Wet <sup>3</sup> |
| 15           | 75                               | 10               | 50               |
| 10           | 30                               | 25               | 50               |
| 5            | 50                               | 40               | 40               |

1 - Difference =  $\frac{(MR)_{\text{measured}} - (MR)_{\text{calculated}}}{(MR)_{\text{measured}}} * 100$

2 - Dry = 2 percent dry of optimum water content

3 - Wet = 2 percent wet of optimum water content

c) UTEP Model Two ( $MR = 10^{k_1} \sigma_c^{k_2} \epsilon^{k_3}$ )

| Clay Content | Difference, Percent <sup>1</sup> |                  |                  |
|--------------|----------------------------------|------------------|------------------|
|              | Optimum                          | Dry <sup>2</sup> | Wet <sup>3</sup> |
| 15           | 60                               | 30               | 40               |
| 10           | 30                               | 30               | 30               |
| 5            | 50                               | 15               | 30               |

1 - Difference =  $\frac{(MR)_{\text{measured}} - (MR)_{\text{calculated}}}{(MR)_{\text{measured}}} * 100$

2 - Dry = 2 percent dry of optimum water content

3 - Wet = 2 percent wet of optimum water content

Similarly, the differences between the measured and calculated moduli from the three models proposed for cohesive soils are summarized in Table 9.6. Once again, it is reasonable and practical to use the AASHTO/SHRP model for estimating the modulus of a material based on its clay content.

In summary, the two constitutive models proposed by UTEP can describe the experimental data significantly better than those proposed by SHRP. A simplified procedure is proposed for estimating modulus based solely upon the percent clay. For the simplified procedure, the AASHTO/SHRP model is sufficient.

Table 9.6 Typical Differences between Measured and Calculated Moduli from Three Models (Cohesive Soils)

a) AASHTO/SHRP Model ( $M_R = 10^{k_1} \sigma_d^{k_2}$ )

| Clay Content | Difference, Percent <sup>1</sup> |                  |                  |
|--------------|----------------------------------|------------------|------------------|
|              | Optimum                          | Dry <sup>2</sup> | Wet <sup>3</sup> |
| 90           | 20                               | 20               | 40               |
| 70           | 20                               | 15               | 20               |
| 50           | 70                               | 50               | 70               |
| 30           | 20                               | 30               | 30               |

1 - Difference =  $\frac{(M_R)_{\text{measured}} - (M_R)_{\text{calculated}}}{(M_R)_{\text{measured}}} * 100$

2 - Dry = 2 percent dry of optimum water content

3 - Wet = 2 percent wet of optimum water content

b) UTEP Model One ( $M_R = 10^{k_1} \theta^{k_2}$ )

| Clay Content | Difference, Percent <sup>1</sup> |                  |                  |
|--------------|----------------------------------|------------------|------------------|
|              | Optimum                          | Dry <sup>2</sup> | Wet <sup>3</sup> |
| 90           | 40                               | 50               | 50               |
| 70           | 40                               | 60               | 20               |
| 50           | 50                               | 45               | 10               |
| 30           | 40                               | 30               | 15               |

1 - Difference =  $\frac{(M_R)_{\text{measured}} - (M_R)_{\text{calculated}}}{(M_R)_{\text{measured}}} * 100$

2 - Dry = 2 percent dry of optimum water content

3 - Wet = 2 percent wet of optimum water content

c) UTEP Model Two ( $M_R = 10^{k_1} \sigma_c^{k_2} \epsilon^{k_3}$ )

| Clay Content | Difference, Percent <sup>1</sup> |                  |                  |
|--------------|----------------------------------|------------------|------------------|
|              | Optimum                          | Dry <sup>2</sup> | Wet <sup>3</sup> |
| 90           | 30                               | 50               | 35               |
| 70           | 40                               | 50               | 15               |
| 50           | 50                               | 35               | 15               |
| 30           | 20                               | 25               | 20               |

1 - Difference =  $\frac{(M_R)_{\text{measured}} - (M_R)_{\text{calculated}}}{(M_R)_{\text{measured}}} * 100$

2 - Dry = 2 percent dry of optimum water content

3 - Wet = 2 percent wet of optimum water content

# Chapter 10

## Testing of Subgrade Soils

### 10.1 Introduction

Four actual subgrade soils from four different counties were tested. A database is being developed at CTR to incorporate resilient modulus data from typical soils from different counties in Texas. These test results are to be added to that database. More subgrade materials were originally supposed to be tested. The index properties of the subgrade materials were supposed to be provided, unfortunately, due to monetary and time restrictions, this was not possible. Therefore, the number of samples tested was reduced.

The samples tested were from El Paso County (Rojas pit), Midland, Hardeman and Starr counties. The results from the soil obtained from Starr County is included in the CTR report and are not repeated here. The index properties and resilient moduli of the other three materials are reported here.

### 10.2 Index Properties

The index properties of the soils from the three counties are summarized in Table 10.1. The specific gravity, liquid limit, plastic limit and plasticity index for each soil are reported in the table. The grain size distribution curves of the three soils are included in Figures 10.1 through 10.3 and are tabulated in Table 10.3. The soils were classified utilizing the AASHTO and Unified Soil Classification System (USCS). The classifications are contained in Table 10.2. The soil from El Paso County is a silty sand with low plasticity; whereas the soil from Midland County can be categorized as a silty sand. Both these soils are categorized as A-2-6 in

**Table 10.1 Index Properties of Soils from  
El Paso, Midland & Hardman County**

| COUNTY   | SPECIFIC GRAVITY<br>$G_s$ | LIQUID LIMIT | PLASTIC LIMIT | PLASTICITY INDEX |
|----------|---------------------------|--------------|---------------|------------------|
| EL PASO  | 2.65                      | 17.92        | NP            | 17.92            |
| MIDLAND  | 2.50                      | 18.35        | NP            | 18.35            |
| HARDEMAN | 2.53                      | 40.70        | 21.93         | 19.07            |

**Table 10.2 Proctor Density Relation  
and AASHTO/USCS Classification**

| COUNTY   | OMC (%) | DRY DENSITY<br>$\rho_p/\text{ft}^3$ | AASHTO | USCS  |
|----------|---------|-------------------------------------|--------|-------|
| EL PASO  | 13.25   | 110.75                              | A-2-6  | SM-SP |
| MIDLAND  | 10.50   | 120.90                              | A-2-6  | SM    |
| HARDEMAN | 22.50   | 100.00                              | A-7-6  | CH    |

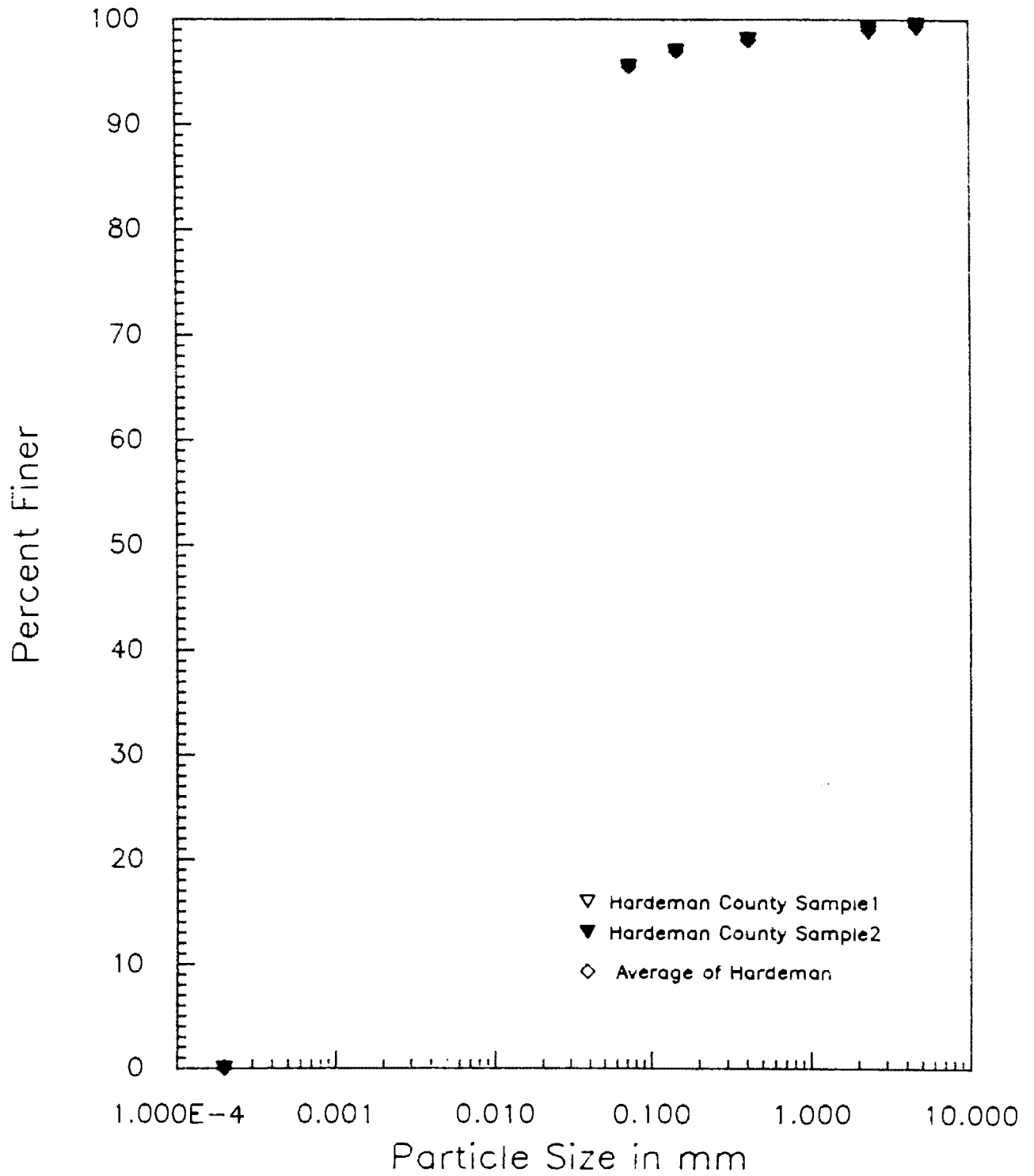


Figure 10.1 - Grain Size Distribution Curve for Hardeman County Soil

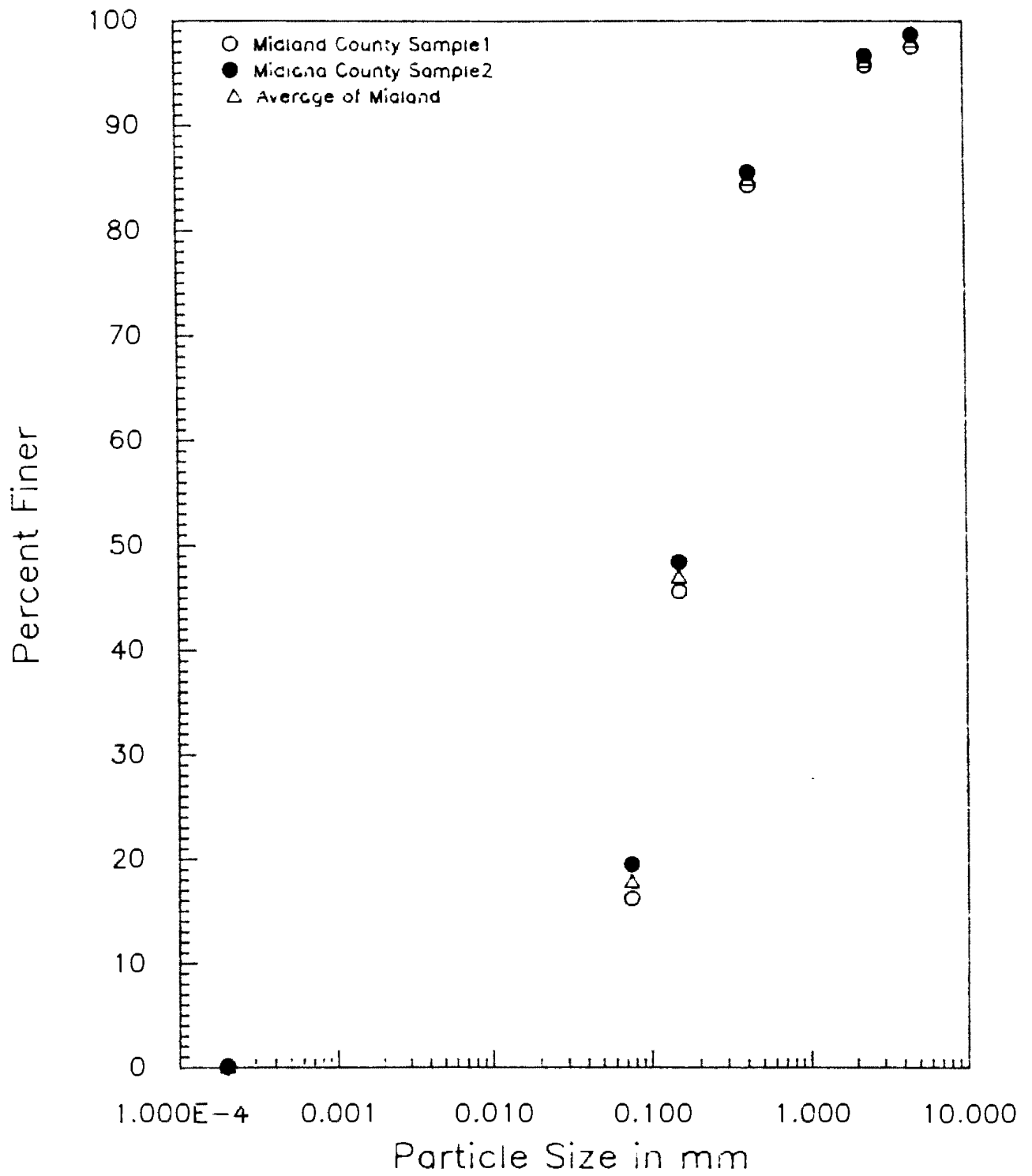


Figure 10.2 - Grain Size Distribution Curve for Midland County Soil

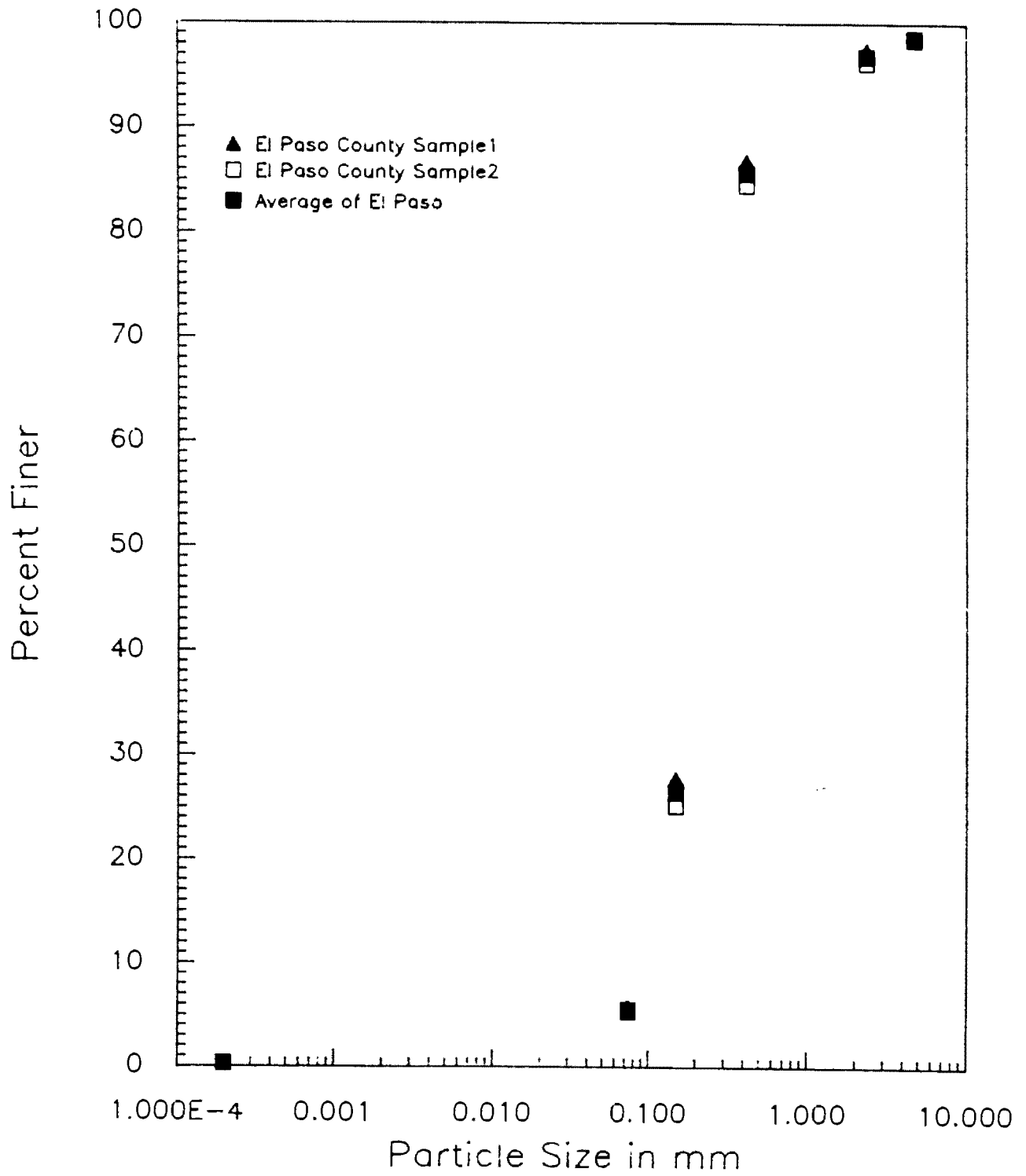


Figure 10.3 - Grain Size Distribution Curve for El Paso County Soil

**Table 10.3. Percent passing for Soils from El Paso, Midland & Hardeman County**

| SIEVE # | SIEVE SIZE (mm) | EL PASO COUNTY |       | MIDLAND COUNTY |       | HARDEMAN COUNTY |       |
|---------|-----------------|----------------|-------|----------------|-------|-----------------|-------|
|         |                 | #1             | #2    | #1             | #2    | #1              | #2    |
| 4       | 4.76            | 98.78          | 98.50 | 97.48          | 98.66 | 99.54           | 99.18 |
| 8       | 2.38            | 97.54          | 96.22 | 95.68          | 96.65 | 99.12           | 98.78 |
| 40      | 0.42            | 86.84          | 84.50 | 84.28          | 85.55 | 98              | 98.08 |
| 100     | 0.149           | 27.74          | 25.10 | 45.58          | 48.39 | 97.06           | 96.96 |
| 200     | 0.074           | 5.74           | 5.30  | 16.18          | 19.45 | 95.58           | 95.50 |
| PAN     | -               | 0.34           | 0.30  | 0.162          | 0.054 | 0               | 0     |

AASHTO soil classification. The third soil from Hardeman County is a highly-plastic clay with very little granular materials.

### **10.3 Testing Matrix**

A total of 18 specimens were tested. The SHRP protocol was followed for the cohesive (Type 2) soils and the UTEP procedure was utilized for the granular (Type 1) soils. Therefore, specimens from El Paso and Midland Counties were tested using UTEP procedure. The SHRP protocol was followed in testing specimens from Hardeman County.

Each subgrade material was tested at three levels of moisture content i.e., Optimum, Optimum plus two percent and Optimum minus two percent. The repeatability of the results was studied by testing two specimens at each moisture content specified.

Each specimen was prepared to the prescribed moisture, placed in a sealed plastic bag, and stored for about three weeks in a humid room before testing. In this manner, equilibrium condition was attained within the specimen, resulting in uniformity in soil properties. Care was taken to remove all twigs and organic matter which was present in high quantities in Midland County soil.

### **10.4 Presentation of Results**

The results from all tests are contained in Figures G.1 through G.18 in Appendix G. In each figure, the constitutive models obtained are also represented. In this section the results are summarized and briefly discussed.

A typical variation in modulus with deviatoric stress for the soil from Hardeman County at optimum moisture content is shown in Figure 10.4. Visually, there is not much scatter in the data at each deviatoric stress. The scatter and closeness can also be judged by inspecting the R-squared values reported for the best-fit curves. As depicted in Figs. G.1 through G.6, this trend generally holds for all other specimens tested from Hardeman County.

A typical variation in modulus with bulk stress for the soil from Midland County at optimum water content is displayed in Figure 10.5. The results are quite logical as described in Chapter 6. The apparent scatter in the results could be mainly attributed to the dependence of the modulus on the confining pressure (see Chapter 6). The results from all tests are presented in Figures G.7 through G.12.

Similarly, a typical variation in modulus with bulk stress for the soil from El Paso County's Rojas Pit at optimum water content is shown in Figure 10.6. The results are once again reasonable; however, some scatter in data is evident. The results from all tests performed on this soil are presented in Figures G.13 through G.18.

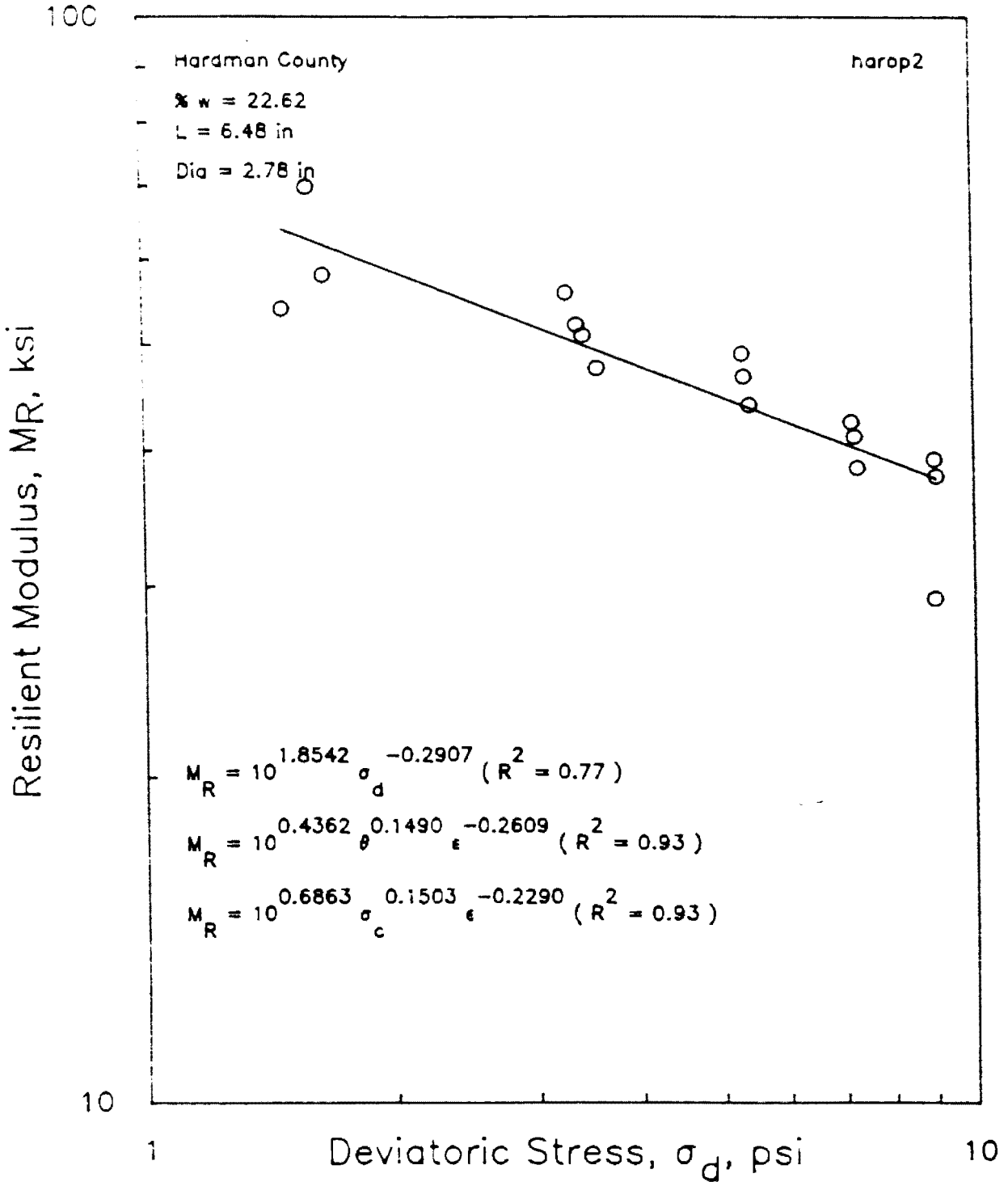


Figure 10.4 - Typical Variation in Resilient Modulus with Deviatoric Stress for Hardman County Specimen at Optimum Water Content

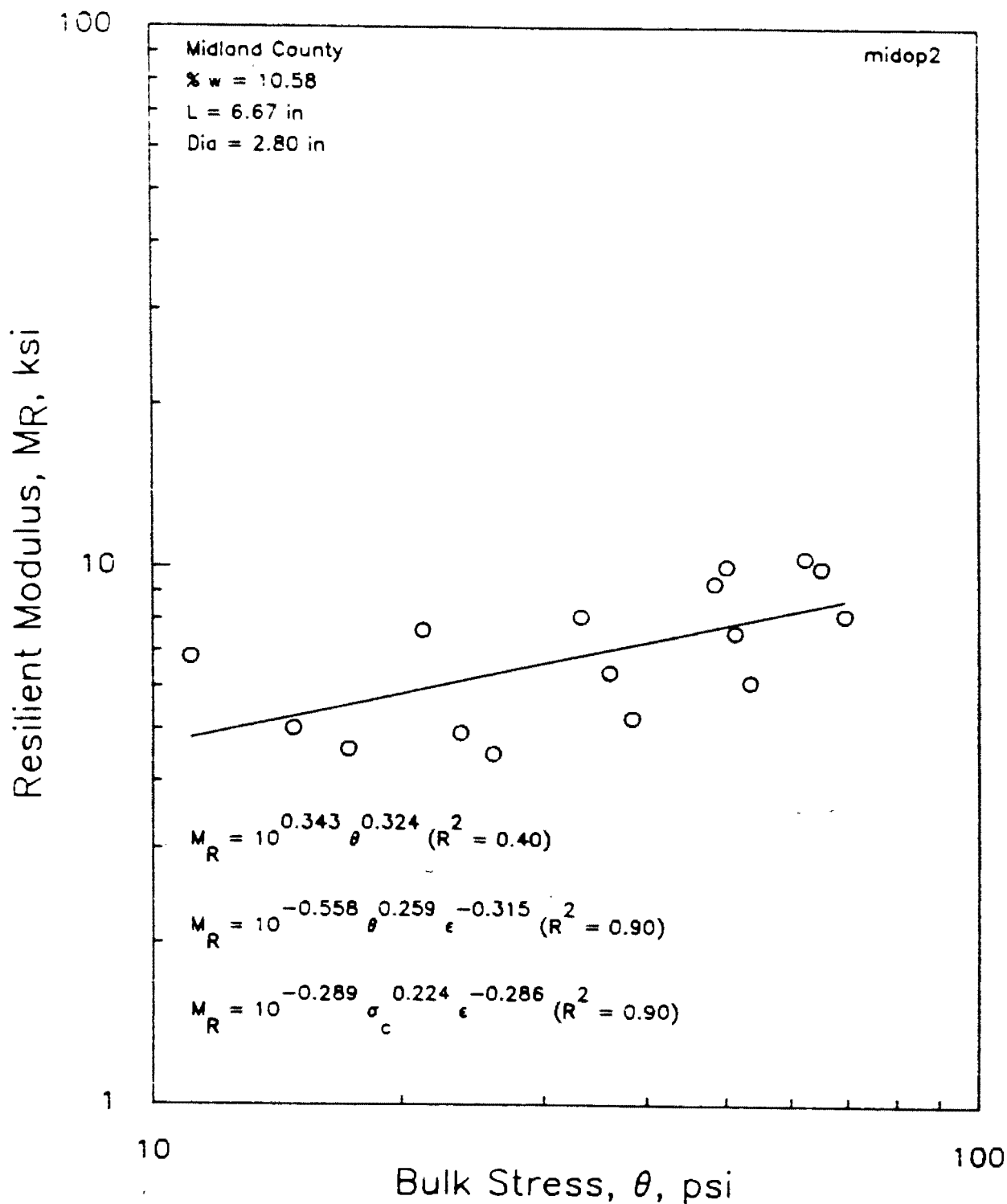


Figure 10.5 - Typical Variation in Resilient Modulus with Bulk Stress for Midland County Specimen at Optimum Water Content

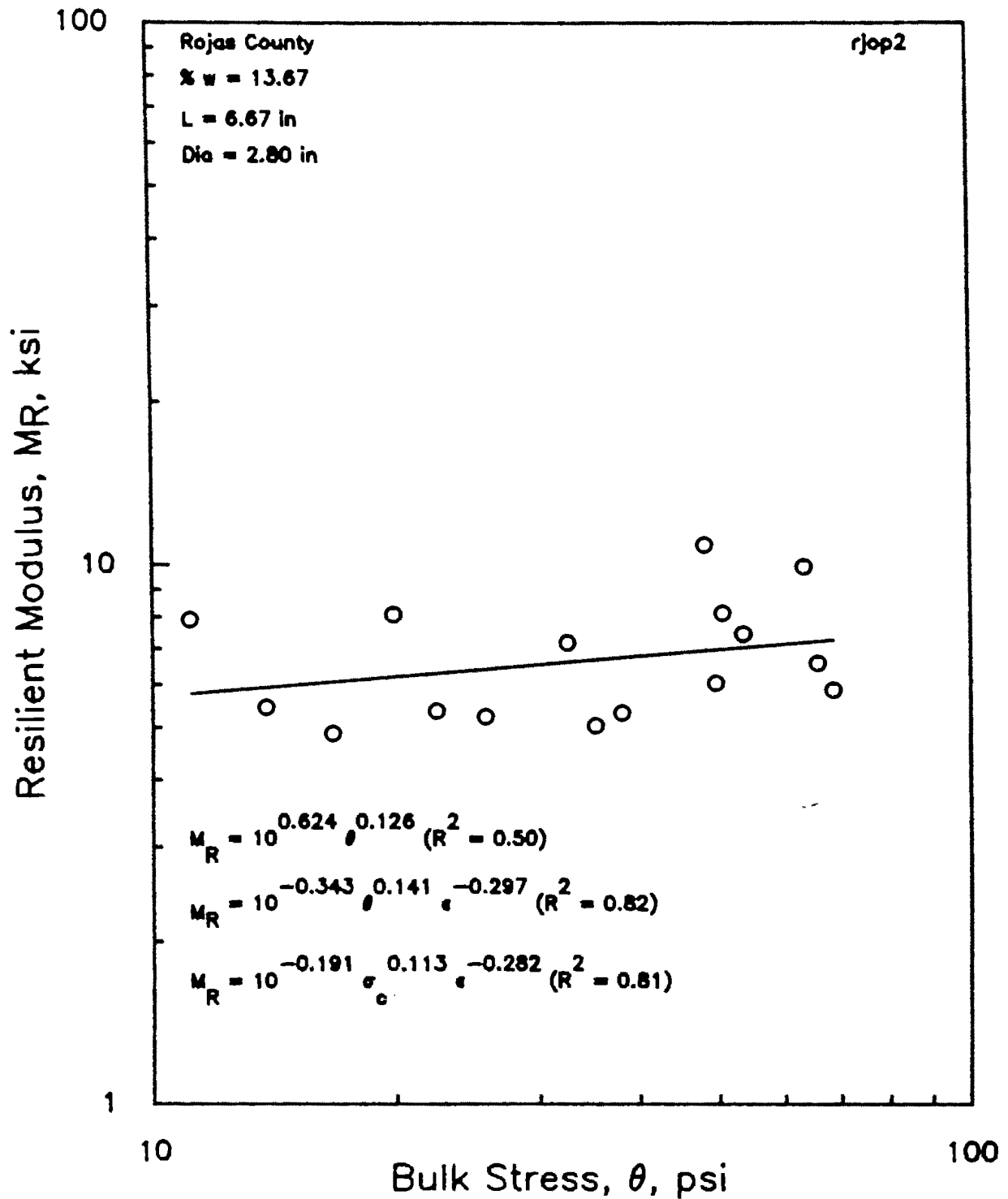


Figure 10.6 - Typical Variation in Resilient Modulus with Bulk Stress for El Paso County Specimen at Optimum Water Content

The results from the three tests are best summarized by inspecting the variation in modulus with moisture content. Such data are presented in Figures 10.7 through 10.9, for the Hardeman, Midland and El Paso Counties, respectively. All moduli are from a confining pressure of 6 psi and a deviatoric stress of 6 psi. As mentioned before, this is the only common deviatoric stress and confining pressure between the SHRP and UTEP procedures.

As seen in Figure 10.7, the subgrade from Hardeman County exhibits the highest modulus at the optimum water content. At this level, the modulus is about 30 percent higher than wet and dry specimens. Also shown in the figure are the modulus obtained from the two specimens at each water content. The variation in modulus is within 10 percent.

The subgrade from the Midland County (see Figure 10.8) exhibits monotonic decrease in modulus with increase in the moisture content. The modulus decreases by a factor of about two from the dry of optimum to the wet of optimum. The variation in modulus between the two specimens tested is quite small, demonstrating the value of UTEP testing procedure.

The soil from El Paso County exhibits similar behavior as the Midland County subgrade. However, the decrease in modulus with water content for this soil is substantially less. The modulus decreases by 25 percent in the range of water contents utilized. This can be attributed to the fact that the percentage of fines in the Midland soil is greater than that of El Paso county. As such, the moisture has a lesser effect on the modulus. The level of scatter for this soil is slightly higher than the other two soils but is limited to about 10 percent of the average.

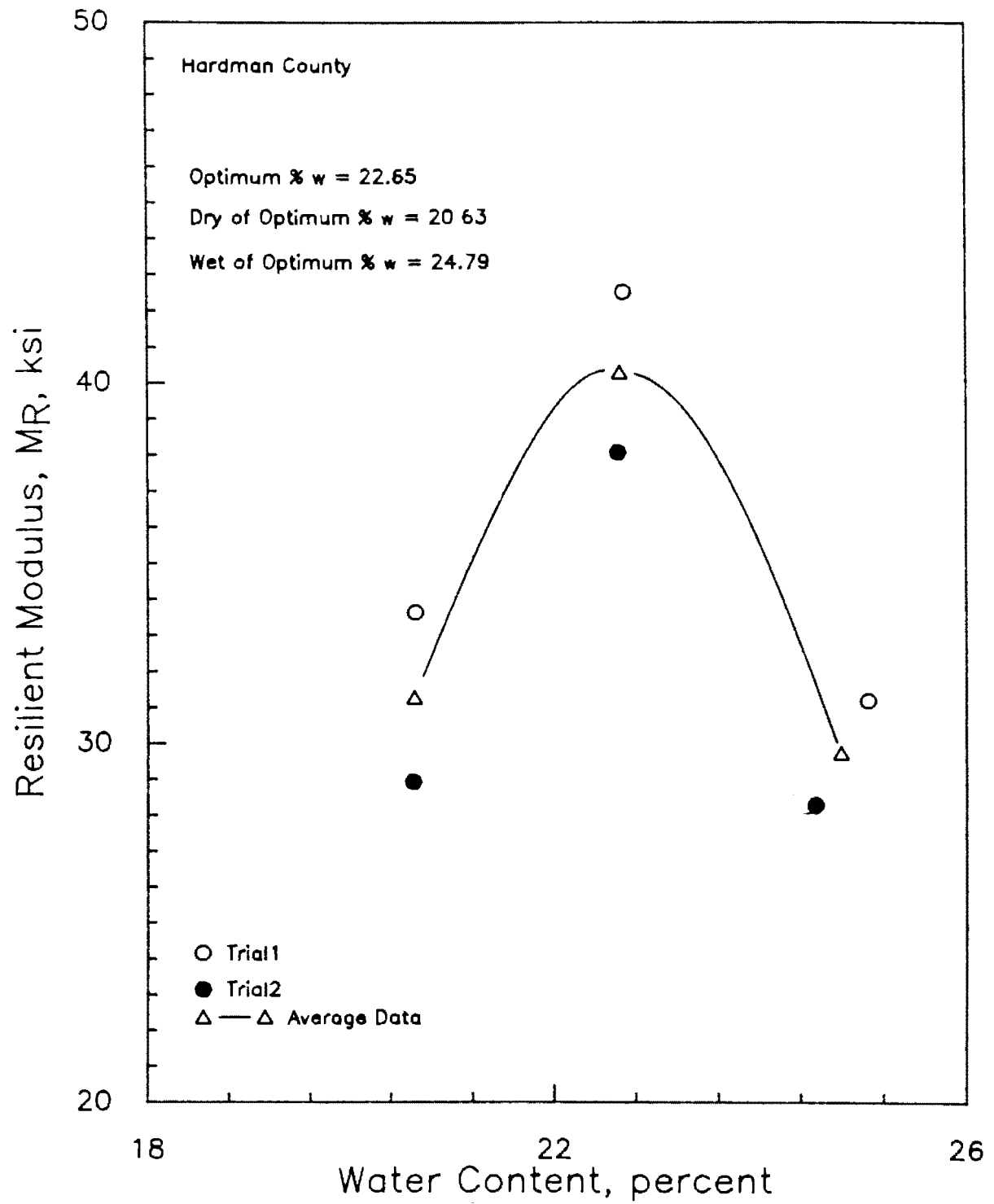


Figure 10.7. Variation in Resilient Modulus with Moisture Content for Hardeman County Soil

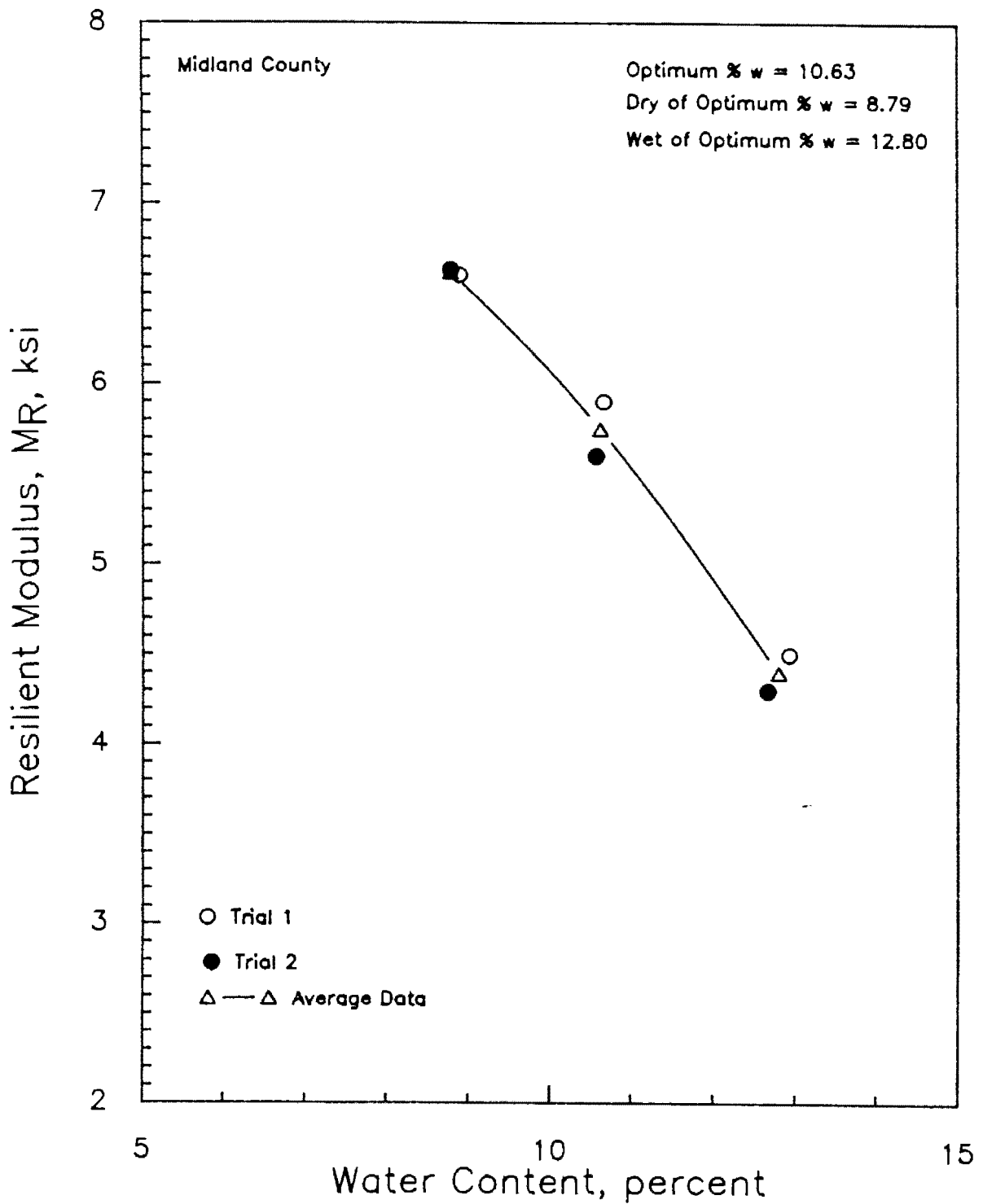


Figure 10.8. Variation in Resilient Modulus with Moisture Content for Midland County Soil

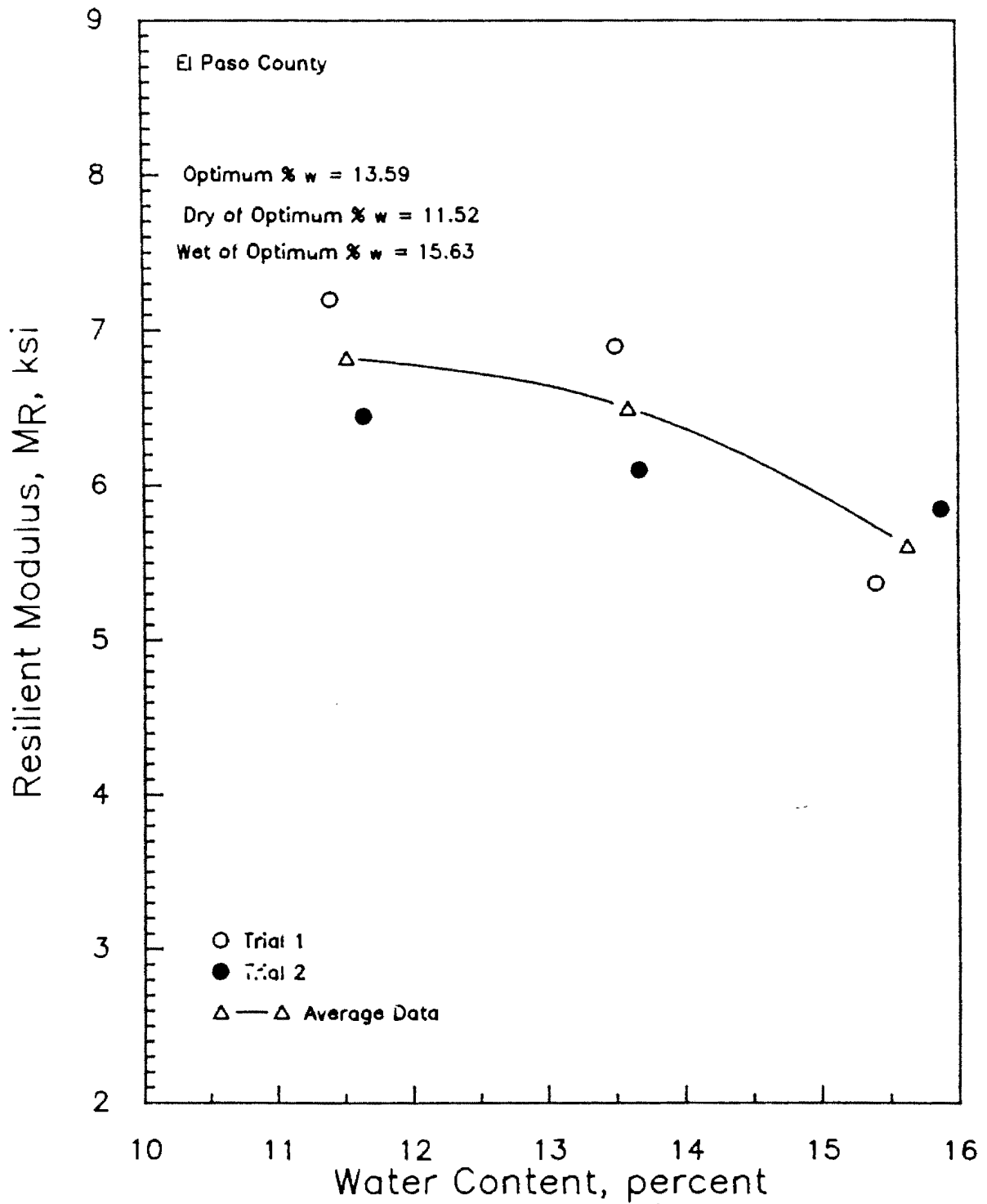


Figure 10.9. Variation in Resilient Modulus with Moisture Content for El Paso County Soil

# Chapter 11

## Conclusions and Recommendations

### 11.1 Summary

This report contains a critical evaluation of the resilient modulus testing procedure. The state-of-the-art for obtaining and interpreting resilient modulus data is reviewed. The initial testing procedure was proposed by AASHTO and then improved by SHRP. These two approaches are evaluated. In addition, a new testing procedure for granular materials is proposed and evaluated.

A sand and a clay native to El Paso, Texas were tested. Mixes with different proportions of the sand and clay were also tested to evaluate the existing and proposed methods. Finally, the models proposed by AASHTO for sands and clays were evaluated. Two alternative models were then proposed. Finally, simplified relationships for determining the constitutive models as a function of clay content and water content were proposed.

### 11.2 Conclusions

Based on this study, the following conclusions can be drawn:

- 1) UTEP system yields reliable and accurate resilient modulus values.
- 2) The AASHTO procedure for resilient modulus testing is inadequate.
- 3) The SHRP protocol for testing cohesive (Type 2) soils is adequate.
- 4) The SHRP protocol for testing granular (Type 1) soils induces sample disturbance during the first level of confining pressure.
- 5) The new procedure proposed here for testing granular materials minimizes sample degradation and disturbance.

- 6) The models proposed by AASHTO may not be adequate for sands or clays.
- 7) Two general constitutive models are more appropriate for describing the behavior of the materials tested. Both models are equally adequate.

# REFERENCES

1. AASHTO, "Standard Method of Test for Resilient Modulus of Subgrade Soils: AASHTO T-274-82", 1986.
2. Allen, D.L., "Resilient Modulus Testing in Kentucky (Present and Future)," In Workshop on Resilient Modulus Testing, Corvallis, Oregon: Oregon State University, 1989.
3. Baladi, G.Y., "Resilient Modulus," In Workshop on Resilient Modulus Testing, Corvallis, Oregon: Oregon State University, 1989.
4. Brickman, A.M., "An Overview of Resilient Modulus Test Systems," In Workshop on Resilient Modulus Testing, Corvallis, Oregon: Oregon State University, 1989.
5. Brown, J.L., "Resilient Modulus and Pavement Design Practice," In Workshop on Resilient Modulus Testing, Corvallis, Oregon: Oregon State University, 1989.
6. Claros, A., et al., "Modifications to the Resilient Modulus Testing Procedure and the Use of Synthetics Samples for Equipment Calibration." A paper presented at 1990 Annual Meeting of the Transportation Research Board, Washington D.C. 1990.
7. Cochran, G.R., "Minnesota Department of Transportation Experience with Laboratory MR Testing," In Workshop on Resilient Modulus Testing, Corvallis, Oregon: Oregon State University, 1989.
8. De Lara Rico, A., "Evaluation of Friction Effects on the Pull-Out Capacity of Horizontal Strip Anchor Plates." submitted in partial fulfillment of the requirements for a M.S. degree, Department of Civil Engineering, The University of Texas at El Paso, 1990.
9. Dhamrait, J.S., "Illinois' Experience with Resilient Modulus," In Workshop on Resilient Modulus Testing, Corvallis, Oregon: Oregon State University, 1989.
10. Drnevich, V.P., "Recent Developments in Resonant Column Testing," Paper Presented at Annual Meeting of the American Society of Civil Engineering, Detroit, Michigan, 1985, pp. 29.
11. Dubby, J. and Mindlin, R.D., "Stress-State Relations of a Granular Medium," Journal of Applied Mechanics, Transactions, American Society of Mechanical Engineers, 1957, pp. 585-593.
12. Dunlap, W.A., "A Report on a Mathematical Model Describing the Deformation Characteristics of Granular Materials," Project 2-8-62-27, Texas Transportation Inst., Tech. Rept. No. 1, 1963.

13. Fager, G. and Valencia, J., "Two Axis Computerized Dynamic Testing System," In Workshop on Resilient Modulus Testing, Corvallis, Oregon: Oregon State University, 1989.
14. Hardin, B.O., "The Nature of Stress-Strain Behavior of Soils," Proceedings, Geotechnical Engineering Division Specially Conference on Earthquake Engineering and Soil Dynamics, Vol. 1, ASCE, Pasadena, CA. 1978, pp. 3-90.
15. Hardin, B.O. and Black, W.L., "Sand Stiffness Under Various Triaxial Stresses," Journal of the Soil Mechanics and Foundation Division, ASCE, Vol. 92, No. SM2. 1966, pp. 27-42.
16. Hardin, B.O. and Black, W.L., "Vibration Modulus of Normally Consolidated Clay," Journal of the Soil Mechanics and Foundation Division, ASCE, Vol. 94, No. SM2. 1968, 353-369.
17. Hardin, B.O. and Drnevich, V.P., "Shear Modulus and Damping in Soils: Measurement and Parameters Effects," Journal of the Soil Mechanics and Foundation Division," ASCE, Vol. 98, No. SM7. 1972, pp. 603-624.
18. Hardin, B.O. and Richart, F.E., Jr., "Elastic Wave Velocities in Granular Soils," Journal of the Soil Mechanics and Foundation Division, ASCE, Vol. 89, No. SM1. 1963, pp. 33-65.
19. Hicks, R.G. and Monismith, C.L., "Factors Influencing the Resilient Response of Granular Materials," HRB, Highway Research Record 345: Washington D. C. pp. 15-31, 1971.
20. Ho, Robert K.H., "Repeated Load Tests on Untreated Soils: A Florida Experience," In Workshop on Resilient Modulus Testing, Corvallis, Oregon: Oregon State University, 1989.
21. Huddleston, Ira J. and Zhou, H., "Round Robin Tests and Use of Test Results in Pavement Design," In Workshop on Resilient Modulus Testing, Corvallis, Oregon: Oregon State University, 1989.
22. Isenhower, W.M., Stokoe, K.H., II, and Allen, J.C., "Instrumentation for Torsional Shear/Resonant Column Measurement Under Anisotropic Stresses," Geotechnical Testing Journal, GTJODJ, Vol. 10, No. 4, Dec. 1987, pp. 183-191.
23. Iwasaki, T. and Tatsuoka, F., "Effects of Grain Size and Grading on Dynamic Shear Modulus of Sands," Soils and Foundations, Vol. 17, No. 3. 1977, pp. 19-35.
24. Jackson, Newton C., "Resilient Modulus of Subgrade Soils," In Workshop on Resilient Modulus Testing, Corvallis, Oregon: Oregon State University, 1989.
25. Kasianchuk, D.A., "Fatigue Consideration in the Design of Asphalt Concrete Pavements," Ph. D. Thesis, University of California, Berkely, August 1968.
26. Kim, Ok-Kee, "Resilient Test in California DOT - Yesterday, Today, and Tomorrow," In Workshop on Resilient Modulus Testing, Corvallis, Oregon: Oregon State University, 1989.
27. Kokusho, T., "Cyclic Triaxial Test of Dynamic Soil Properties for Wide Strain Range," Soils and Foundations, JSSMFE, Vol. 20. 1980, pp. 45-60.
28. Mahoney, Joe P. et al., "Flexible Pavement Design and Rehabilitation Short Course," Developed for Western Direct Federal Division, Federal Highway Administration, 1988.
29. Mahoney, Joe P. and Newcomb, David E., "Elastic Pavement Analysis," In Workshop on Resilient Modulus Testing, Corvallis, Oregon: Oregon State University, 1989.

30. Mitry, F.G., "Determination of the Modulus of Resilient Deformation of Untreated Base Course Material," Ph.D. Thesis, University of California, Berkeley, 1964.
31. Monismith, C.L., "Resilient Modulus Testing: Interpretation of Laboratory Results for Design Purposes," In Workshop on Resilient Modulus Testing, Corvallis, Oregon: Oregon State University, 1989.
32. Moses, T.L., "Alaska DOT/PF Applications of Resilient Modulus Test Results from H&V Equipment," In Workshop on Resilient Modulus Testing, Corvallis, Oregon: Oregon State University, 1989.
33. Murthy, R., "Laboratory Evaluation of Dynamic Properties of Three Soils from the Desert Southwest," submitted in partial fulfillment of the requirements for a M.S. degree. Department of Civil Engineering, The University of Texas at El Paso, 1990, 15-24.
34. Pezo, R.F., et al., "Developing a Reliable Resilient Modulus Testing System," A paper presented at 1991 Annual Meeting of the Transportation Research Board, Washington D.C., 1991.
35. Rada, G. and Witczak, M.W., "Comprehensive Evaluation of Laboratory Resilient Moduli Results for Granular Material," Transportation Research Record No. 810, Transportation Research Board, 1981.
36. Richart, F.E., Jr., "Field and Laboratory Measurement of Dynamic Properties," Proceedings of Dynamic Methods in Soil and Rock Mechanics, Vol. 1. 1977, pp. 3-36.
37. Seim, D.K., "A Comprehensive Study on the Resilient Modulus of Subgrade Soils," In Workshop on Resilient Modulus Testing, Corvallis, Oregon: Oregon State University, 1989.
38. Seed, H.B., Chan, C.K., and Monismith, C.L., "Effects of Repeated Loading on the Strength and Deformation of Compacted Clay," Proceedings, HRB, Vol. 34, 1955, pp 541-558.
39. Seed, H.B., Mitry, F.G., Monismith, C.L. and Chan, C.K., "Prediction of Flexible Pavement Deflection from Laboratory Repeated Load Tests," NCHRP Rept. 35, 1967.
40. SHRP, "Resilient Modulus of Unbound Granular Base, Subbase Materials and Subgrade Soil: Strategic Highway Research Program SHRP Protocol P-46, UG07, SS07," 1989.
41. Silver, M.L., "Laboratory Triaxial Testing Procedure to Determine the Cyclic Strength of Soils," Report NUREG-31, US Nuclear Regulatory Commission, 1976.
42. Stokoe, K.H., II, et al., "In-Situ Testing of Hard-To-Sample Soils," A paper presented in Italy, 1988.
43. Stokoe, K.H., II, et al., "Development of Synthetics Specimens for Calibration and Evaluation of MR Equipment," A paper presented at 1990 Annual Meeting of the Transportation Research Board, Washington D.C., 1990.
44. Thompson, M.R., "Factors Affecting the Resilient Moduli of Soils and Granular Materials," In Workshop on Resilient Modulus Testing, Corvallis, Oregon: Oregon State University, 1989.
45. Thompson, M.R. and Robnett, Q.L., "Resilient Modulus of Subgrade Soils," In Workshop on Resilient Modulus Testing, Corvallis, Oregon: Oregon State University, 1989.
46. Thompson, O.O., "Evaluation of Flexible Pavement Behavior with Emphasis on the Behavior of Granular Layers," Ph.D. Dissertation, University of Illinois, 1969.
47. Vinson, T.S., "Fundamentals of Resilient Modulus Testing," In Workshop on Resilient Modulus Testing, Corvallis, Oregon: Oregon State University, 1989.

48. Uzan, J., "Characterization of Granular Soils," Transportation Research Record No. 1024, Transportation Research Board, 1981.